

STATUS OF THESIS

Title of thesis

MODELING AND SIMULATION OF PMSG WIND ENERGY
CONVERSION SYSTEM USING ACTIVE DISTURBANCE
REJECTION CONTROL.

I SAFWAN SADEQ MAHMOOD ALI

hereby allow my thesis to be placed at the Information Resource Center (IRC) of Universiti Teknologi PETRONAS (UTP) with the following conditions:

1. The thesis becomes the property of UTP
2. The IRC of UTP may make copies of the thesis for academic purposes only.
3. This thesis is classified as

Confidential

Non-confidential

If this thesis is confidential, please state the reason:

The contents of the thesis will remain confidential for _____ years.

Remarks on disclosure:

Endorsed by



Signature of Author

Permanent address:

Block D21-07- one south Serdang

Selangor Malaysia



Signature of Supervisor

Name of Supervisor

DR. Mark Ovinis

Date : 28/05/2022

Date : 28/05/2022

UNIVERSITI TEKNOLOGI PETRONAS

MODELING AND SIMULATION OF PMSG WIND ENERGY CONVERSION SYSTEM
USING ACTIVE DISTURBANCE REJECTION CONTROL

By

SAFWAN SADEQ MAHMOOD ALI

The undersigned certify that they have read and recommend to the Postgraduate Studies Programme for acceptance this thesis for the fulfillment of the requirements for the degree stated.

Signature:


Mark Ovinis
Lecturer
Mechanical Engineering Department
Universiti Teknologi PETRONAS
Bandar Seri Iskandar, 31750 Tringganu
Perak Darul Ridzuan, Malaysia

Main Supervisor:

DR. Mark Ovinis

Signature:


DR. SARAVANAN KARUPPANAN
Associate Professor
Mechanical Engineering Department
Universiti Teknologi PETRONAS
32610 Bandar Seri Iskandar
Perak Darul Ridzuan, Malaysia

Co-Supervisor:

Assoc.Prof.Dr. Saravanan Karuppanan

Signature:


ASSOC. PROF. DR. MASDI BIN MUHAMMAD
Chair
Mechanical Engineering Department
Universiti Teknologi PETRONAS
32610 Seri Iskandar
Perak Darul Ridzuan, Malaysia

Head of Department:

Assoc Prof Dr Masdi B Muhammad

Date:

28/5/2022

MODELING AND SIMULATION OF PMSG WIND ENERGY CONVERSION SYSTEM
USING ACTIVE DISTURBANCE REJECTION CONTROL.

by

SAFWAN SADEQ MAHMOOD ALI

A Thesis

Submitted to the Postgraduate Studies Programme

as a Requirement for the Degree of

MASTER OF SCIENCE

MECHANICAL ENGINEERING

UNIVERSITI TEKNOLOGI PETRONAS

BANDAR SERI ISKANDAR,

PERAK

JUNE 2022

DECLARATION OF THESIS

Title of thesis

MODELING AND SIMULATION OF PMSG WIND ENERGY
CONVERSION SYSTEM USING ACTIVE DISTURBANCE
REJECTION CONTROL.

I SAFWAN SADEQ MAHMOOD ALI

hereby declare that the thesis is based on my original work except for quotations and citations which have been duly acknowledged. I also declare that it has not been previously or concurrently submitted for any other degree at UTP or other institutions.



Signature of Author

Witnessed by


Mark Ovinis
Lecturer
Electrical Engineering Department
Universiti Teknologi PETRONAS
Bandar Seri Iskandar, 31750 Tronoh
Perak Darul Ridzuan, Malaysia

Signature of Supervisor

Permanent address:

Block D-21-07 One south apartment

Serdang Selangor 43300 Malaysia

Name of Supervisor

DR. Mark Ovinis

Date : 28-05-2022

Date : _____

DEDICATION

I would like to dedicate this dissertation to:

My parents. For their endless love, support, and encouragement.

My supervisor, DR. Mark Ovinis – for the guidance, direction, and pearls of wisdom, and offering encouragement precisely when needed and without which it would have been nearly impossible to produce this piece of work.

ACKNOWLEDGEMENTS

Firstly, I would like to give all the praise and glory to the Almighty Allah, the Lord of the Worlds, the Beneficent, and the Merciful. Secondly, I would like to express my deep and sincere appreciation to my supervisor, Dr. Mark Ovinis for his patronage and guidance. Dr. Mark Ovinis was so helpful throughout the research and his contributions enabled me to complete this research in the best possible way. Certainly, without his assistance and guidance, making progress towards the research would have been very difficult. I would also like to extend special thanks and appreciation to my co-supervisor Assoc. Prof. Dr. Saravanan Karuppanan for all the assistance he rendered to me throughout the research. All of you have been tremendous mentors. I am thankful for your positive contributions, encouragement and for allowing me to grow as a researcher. Your advice towards my research and my career will forever remain priceless.

Great thanks to Universiti Teknologi PETRONAS for their generous support during my master's study. I also would like to thank the staff of CGS for facilitating the research work. I also would like to extend my thanks to the members of staff from the mechanical engineering department for their evaluation and guidance during my Symposiums.

In addition, I would like to thank my parents and siblings for the sacrifices that they made on my behalf. Their prayers and spiritual support were what sustained and carried me this far.

Last but not the least, I would like to thank everyone that assisted me in any way to complete my master's journey, without your support, this achievement would not have been possible. Thank you.

ABSTRACT

Electrical power generated from wind turbines inherently fluctuates due to changing wind speeds. Without proper control, disturbances such as changing wind speeds can degrade the power quality factor and robustness of the electrical grid. To ensure good power quality factor, high performance and robustness of the grid against internal and external disturbances, the use of Active Disturbance Rejection Control with an extended state observer ESO for Permanent Magnet Synchronous Generator(PMSG) Wind Energy Conversion System is investigated. The Analysis performances of our system, a conventional PI and the active disturbance rejection control (ADRC) were compared, and the results environment shows that the proposed ADRC methods gives very satisfactory characteristics with good efficiency. It has been established that the Active Disturbance Rejection Control (ADRC) controller not only regulates the wind turbine power, but it also regulates the output voltage at its terminals. The system has been simulated in MATLAB/Simulink at various wind speeds. The obtained simulation results indicate that the controller maintains constant DC voltage at the interface of the generator-side converter and grid-side converters and achieves maximum power. The results also show that the system performance has good stability, precision and rejection of internal disturbances, with an overall system efficiency of 98.65%.

ABSTRAK

Kuasa elektrik yang dijana daripada turbin angin sememangnya turun naik disebabkan oleh perubahan kelajuan angin. tanpa kawalan yang betul, gangguan seperti perubahan kelajuan angin boleh merendahkan faktor kualiti kuasa dan keteguhan grid elektrik. untuk memastikan faktor kualiti kuasa yang baik, prestasi tinggi dan keteguhan grid terhadap gangguan dalaman dan luaran, penggunaan kawalan penolakan gangguan aktif dengan ESO pemerhati keadaan lanjutan untuk sistem penukaran tenaga angin penjana segerak magnet kekal(PMSG) diasasat. Prestasi analisis sistem kami, pi konvensional dan kawalan penolakan gangguan aktif (ADRC) telah dibandingkan, dan persekitaran keputusan menunjukkan bahawa kaedah ADRC yang dicadangkan memberikan ciri yang sangat memuaskan dengan kecekapan yang baik . telah ditetapkan bahawa pengawal kawalan penolakan gangguan aktif (ADRC) bukan sahaja mengawal kuasa turbin angin, tetapi ia juga mengawal voltan keluaran di terminalnya. sistem ini telah disimulasikan dalam MATLAB/SIMULINK pada pelbagai kelajuan angin. keputusan simulasi yang diperoleh menunjukkan bahawa pengawal mengekalkan voltan dc malar pada antara muka penukar sisi penjana dan penukar sisi grid dan mencapai kuasa maksimum. keputusan juga menunjukkan bahawa prestasi sistem mempunyai kestabilan, ketepatan dan penolakan gangguan dalaman yang baik, dengan kecekapan keseluruhan sistem sebanyak 98.65%.

In compliance with the terms of the Copyright Act 1987 and the IP Policy of the university, the copyright of this thesis has been reassigned by the author to the legal entity of the university, Institute of Technology PETRONAS Sdn Bhd.

Due acknowledgement shall always be made of the use of any material contained in, or derived from, this thesis.

© SAFWAN SADEQ MAHMOOD ALI , 2022

Institute of Technology PETRONAS Sdn Bhd

All rights reserved.

TABLE OF CONTENT

DECLARATION OF THESIS	iv
DEDICATION	v
ACKNOWLEDGEMENTS.....	vi
ABSTRACT.....	vii
ABSTRAK.....	viii
COPYRIGHT PAGE.....	ix
TABLE OF CONTENT	x
LIST OF FIGURES	xiv
LIST OF TABLES	xv
CHAPTER 1	1
INTRODUCTION	1
1.1 Introduction	1
1.2 Background	3
1.3 Problem Statement	4
1.4 Research Questions	5
1.5 Research Aim	5
1.6 Research objectives.....	5
1.7 Research scope	5
1.8 Research Significance	6
1.9 Project Block Diagram.....	6
1.10 Thesis Structure.....	6
CHAPTER 2.....	8
Literature Review	8
2.1 Overview of wind energy conversion systems	8
2.1.1 Wind energy conversion system.....	9
2.1.2 Power Transfer in a wind energy conversion system.....	9
2.2 Mechanical Subsystem.....	9
2.2.1 Electrical Subsystem.....	10
2.2.1.1 Squirrel Cage induction generator.....	10

2.2.1.2	Double-fed induction generator.....	11
2.2.1.3	Permanent magnet synchronous generator.....	12
2.2.1.4	Brushless double-fed induction generator.....	13
2.2.2	Power electronic converters.....	13
2.2.2.1	Wind Energy Conversion System with parallel back.....	13
2.2.2.2	Modular multilevel converter.....	14
2.3	Wind Turbine Technologies.....	16
2.3.1	Horizontal axis wind turbine.....	16
2.3.2	Vertical axis wind turbines.....	17
2.3.3	Fixed-Speed Wind Turbine.....	18
2.3.4	Limited Variable-speed Wind Turbines.....	19
2.3.5	Partial-Scale Power Converter.....	19
2.3.6	Full-Scale Power Converter.....	20
2.4	Control of PMSG Wind Turbine.....	21
2.4.1	Traditional three-part control.....	21
2.4.2	Linear control.....	23
2.4.3	Active disturbance rejection control.....	24
2.4.4	Intelligent control.....	25
2.4.5	Non-linear controller.....	28
2.4.5.1	Feedforward control.....	28
2.4.5.2	Adaptive neural network feedforward.....	28
2.4.6	Model predictive control.....	29
2.5	Summary	33
CHAPTER 3		34
Modelling, Design and Simulation		34
3.1	Introduction	34
3.2	Proposed System Architecture	34
3.3	Wind Turbine Model.....	35
3.4	Wind Power.....	36
3.4.1	Wind Turbine Design.....	37
3.4.2	Pitch Angle Controller.....	38
3.4.3	Wind-Turbine Operating Modes.....	39

3.5	Permanent Magnet Synchronous Generator (PMSG).....	40
3.5.1	PMSG Modeling.....	40
3.5.2	Control of the Machine.....	41
3.6	Machine-Side Converter Control.....	42
3.6.1	Design of Generator-Side Converter.....	42
3.6.2	Active Disturbance Rejection Control (ADRC).....	43
3.6.2.1	The selection ADRC design for project.....	44
3.6.2.2	Extended State Observer (ESO).....	45
3.6.2.3	Tuning Method of ARDC.....	46
3.6.2.4	Tuning of Observer Parameters.....	47
3.6.2.5	ADRC Design for the Converter.....	48
3.6.3	Maximum Power Point Tracking Control.....	49
3.6.4	Optimal Tip Speed Ratio.....	50
3.6.5	Tip Speed Ratio (TSR) MPPT.....	51
3.7	Control of Grid Side Converter.....	51
3.8	Analysis testing	55
3.8.1	Test of robustness.....	55
3.9	Validation.....	56
3.10	Summary	56
CHAPTER 4		57
Results and Discussion		57
4.1	Introduction	57
4.2	System Implementation.....	57
4.2.1	Wind Turbine Model Settings.....	57
4.2.1.1	Measurement Inputs Block.....	62
4.2.1.2	Back-to-Back Converter.....	62
4.2.1.3	System load.....	62
4.2.1.4	Speed Regulator and Pitch control.....	63
4.2.1.5	Generator Settings.....	64
4.2.2	Generator Side Converter Settings.....	65
4.2.3	Grid-Side Converter.....	65
4.3	Discussion of Simulation Results.....	66

4.3.1 Performance of Generator-Side Converter.....	66
4.4 Performance of Grid Side Converter	68
4.4.1 Results Summary.....	71
4.5 Research Project Contributions.....	71
CHAPTER	73
Conclusion and Future Recommendations	73
5.1 Conclusion	73
5.2 Future Recommendations	74
References.....	75
LIST OF PUBLICATIONS.....	84
APPENDIX A	85

LIST OF FIGURES

Figure 1.1. A horizontal axis wind turbine.....	2
Figure 1.2. System block diagram for proposed system.	6
Figure 1.3. Thesis Structure.	7
Figure 3.1. Proposed WECS architecture without the control subsystem	35
Figure 3.2. Proposed WECS architecture with the control sub-system.....	35
Figure 3.3. Block of air passing through some region A	36
Figure 3.4. Simulink block diagram for the Pitch angle controller.....	39
Figure 3.5. Wind Turbine Operating Modes	40
Figure 3.6. Rectifier-Fed Boost Converter.....	42
Figure 3.7. ADRC for a 2nd-Order System	45
Figure 3.8. Turbine Power Characteristic with MPPT.....	51
Figure 3.9: Power coefficient as a function of the tip speed ratio	51
Figure 3.10. The machine side converter controller	53
Figure 3.11. Current regulator for the grid side converter controller.....	53
Figure 4.1. Wind turbine model.	58
Figure4.2. Block diagram of the wind turbine system and ADRC controller.....	58
Figure 4.3. Simulink block diagram for the Pitch angle controller	59
Figure 4.4. The machine side converter controller	59
Figure 4.5. Current regulator for the grid side converter controller	60
Figure 4.6. Measurements and transformations block.	61
Figure 4.7. Back-to-Back Converter.	62
Figure 4.8. WECS Load.....	63
Figure 4.9. Speed regulator and pitch Control.....	64
Figure 4.10. Permanent magnet synchronous generator.	65
Figure 4.11. Output voltage and shaft speed of PMSG ADRC and PI.	67
Figure 4.12. Apparent power versus real power output of ADRC controller	68
Figure 4.13. Apparent power versus real power output with PI controller	69
Figure 4.14. Unfiltered 3-phase output voltage and current (pu)	70
Figure 4.15. Filtred 3-phase output voltage and current (pu) with ADRC.....	70
Figure 4.16. System Load voltage and current (pu) with PI controller	71

LIST OF TABLES

Table 2:1. Summary of literature studies	30
Table 3.1. Boost Converter Parameters.....	43
Table 4.1. Comparison table of PI, PD, PID and ADRC.....	71

LIST OF ABBREVIATIONS

AC	Alternating Current
BWEA	British Wind Energy Association
CCM	Continuous Current Mode
CSI	Current Source Inverter
DC	Direct Current
DCM	Discontinuous Current Mode
DES	Distributed Energy Resource
DFIG	Doubly-Fed Induction Generator
DQ	Direct Quadrature
DSP	Digital Signal Processor
DTC	Direct Torque Control
EMF	Electromotive force
FPGA	Field Programmable Gate Array
IGBT	Insulated Gate Bipolar Transistor
LVRT	Low Voltage Ride Through
MCU	Micro Control Unit
MOSFET	Metal-Oxide-Semiconductor Field-Effect Transistor
MPPT	Maximum Power Point Tracking
PFC	Power Factor Correction
PMSG	Permanent Magnet Synchronous Generator
PWM	Pulse Width Modulation
RMS	Root Mean Square
SVPWM	Space Vector Pulse Width Modulation
VSC	Voltage Source Converter
VSI	Voltage Source Inverter
MSC	Machine Side Converter
PCC	Point of Common Coupling
PI	Proportional Integral
SMC	Sliding Mode Control
TSR	Tip Speed Ratio
UPF	Unity Power Factor
WTCS	Wind Turbine Conversion System
ADRC	Active Disturbance Rejection Controller
ESO	Extended state observer
MW	Megawatt

CHAPTER 1

INTRODUCTION

1.1 Introduction

Amidst the rapid global industrial development, the energy deficit is deemed a significant challenge for most countries[1]. On the other hand, the rising emissions of carbon dioxide, increasing cost of fossil fuel-based energy technology with the simultaneous advancement and cost decline of renewable energy technology have necessitated the adoption of renewable energy-based technologies such as wind energy technology[2],[3]. This research study presents the design and control of a wind turbine energy system based on a permanent magnet synchronous generator (PMSG) and active disturbance rejection control (ADRC). The proper justification for using the Active Disturbance Rejection Controller (ADRC) is due to its strong robustness and disturbance rejection, excellent performance, simple design, and convenience compared to the PID controller. The ADRC advantages of the ADRC controller include fast response, robustness, and adaptability. Also, the ADRC controller can deal with uncertainties and large-scale variations under different operating conditions; therefore, ADRC is selected to realize the maximum output power of the generator for different kinds of wind.

Figure 1.1 shows the generic structure for a horizontal axis wind turbine with some major system components: generator, gearbox, nacelle, drive train, rotor, hub and blade[4]. The nacelle contains the electro-mechanical components involved in converting wind energy to electricity.

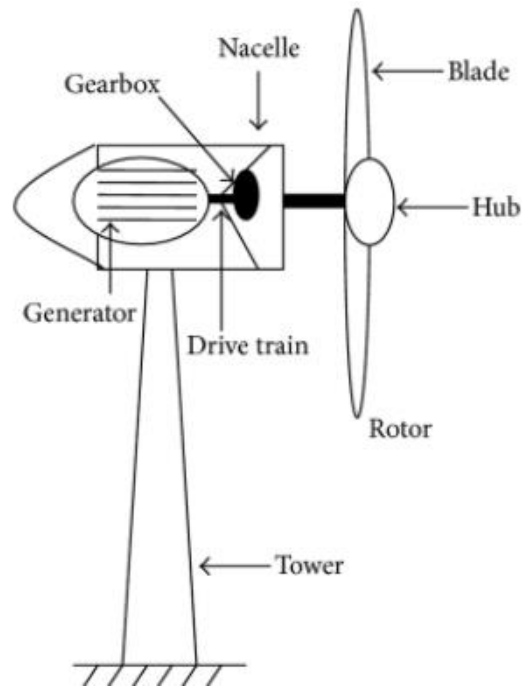


Figure 1.1. A horizontal axis wind turbine [4]

Wind energy is inherently intermittent in nature which results in variations of the output power produced by the wind turbine generator (WTG) [5]. Therefore, a suitable controller and regulator is required for conditioning the WTG output power to match the requirements for utility power grid connection. A WTG extracts energy from the wind by means of a rotor, which drives the generator into motion, thereby, converting the mechanical energy of the turbine into electrical power. There are different types of WTGs which can be classified based on the nature of output power as alternating current (AC) generators or direct current (DC) generators. AC generators can further be classified as single-stage or poly-stage[3]. This research project covers the controller design for a small three-stage AC PMSG. PMSGs have the advantage of low maintenance, this makes them ideal for wind turbine energy conversion systems where the facilities are either remote or difficult to access[6]. Currently, the main types of wind turbines in use are the double-fed induction generators (DFIG) and the synchronous generator permanent magnet (PMSG). The stator windings of the DFIG wind turbine directly link to the power grid. In contrast, its rotor windings are connected to the grid via the power electronics converter (partial power converter), with the wind turbine typically running at 30 % its rated capacity. The key drawbacks of the DFIG are use of rings and poor power management in the event of grid failure[7]. These drawbacks can affect power stability and

make it difficult to meet minimum grid requirements. For PMSG, a full-scale power converter can link the generator's stator winding to the power grid, therefore, all the power produced by the wind turbine can be controlled. Different feedback control strategies have been studied in recent decades for increasing the efficiency and power quality of PMSG-based wind turbines [7].

1.2 Background

Small wind turbines (SWT) are used in some homes and organisations to reduce carbon dioxide emissions and to cut on the electricity bill with the prospect of selling surplus power to the national grid utility[2]. The control of SWTs is considerably less sophisticated compared to that of large wind turbine systems which require complex control systems to track changes in wind direction and speed, and to change turbine orientation, blade pitch, and gearing of generator to keep up with the ideal electrical output [8]. Several wind turbine control schemes with unique dynamic performance for control of the machine side converter (MSC) are presented in literature such as space vector pulse width modulation (SVPWM) control, fuzzy logic control, sliding mode control, PI control, model predictive control and current control [9],[10]. However, these schemes have some drawbacks e.g., PI control schemes fail to track the non-linearity of the wind speed resulting in poor regulation of the turbine output power [9]. While other schemes such as the fuzzy logic scheme may achieve better system performance but tend to be complex as they may require knowledge of the system previous states[11]. A simpler control scheme based on ADRC with an extended observer is presented in [8] as an alternative to complex high-performance schemes. The existing of control design methods that are available in the current work can be categorized into two categories: classical control and modern control [12]. Both strategies are somewhat dependent on the mathematical model of the physical system. Modeling such systems becomes either impossible or highly challenging in the presence of modelling uncertainties and external perturbations. PID control has been extremely popular as a traditional control method and is used in the majority of industrial control application. One of PID control's primary disadvantages is that it is a reactive controller[13] . It is entirely dependent on the system's feedback and has no bearing on the system's internal states. The reactive feature is a basic limitation that has an effect on the PID controller's performance. Due to this constraint, the PID controller performs poorly in the presence of nonlinearities, disturbances, and system uncertainties. Additionally, the controller parameters for the PID control must be determined through trial and error. However, with

recent technological advancements, control tasks have grown increasingly demanding and complex for PID control, necessitating the development of a more capable control system. In the meantime, the industrial engineers continue to choose the PID control despite of its constraints[14]. However, many studies in the current literature have recommended and introduced a new model which is known as an active disturbance rejection controller (ADRC) that is a newly designed practical control mechanism which requires just limited model information and is as straightforward to implement. It requires simply the physical system's relative order and controller gain[15]. As most of the current work results prove that ADRC model is more reliable comparing to other models such as PID due its stability, precision and rejection of disturbances. This study hypothesizes that the proposed ideal ADRC model to improves the current wind turbine power performance.

1.3 Problem Statement

Due to the widespread presence of model uncertainties and external disturbances in industrial control systems, current control theory based on precise models is difficult to implement, and the classical PID control approach continues to dominate the industrial control sector[16]. However, classical PID control has some drawbacks such as overshooting and inability to handle disturbances which affect system performance [17]. Given the latest technological innovations, the control task continues to become more and more challenging and complex for PID control, but other more capable control methods have been identified. PID control is classified as a reactive controller because it only reacts to the feedback of the system, and it is independent of the internal states of the system. The reactive feature is a very fundamental limitation that affects the performance of the PID controller. As a result, PID control may fall short of the performance requirements for complex systems. If the system requirements cannot be precisely estimated or achieved, the designed PID gains may not resist the uncertainties and disturbances, and thus present low robustness. Even though the PID gains can be well-designed, the PID controller still has low robust ability compared with the robust controller when the system encounters multiple challenges from the operating environment of the system, such as temperature, weather, and power surge[14]. In order to overcome the disadvantages of the conventional PI controller which suffers from many limitations, a new control strategy called Active Disruption Rejection Control (ADRC) was selected to remove disturbances affecting the facility. Good system performance can be ensured when the performance of the boost converter is robust to disturbances. Therefore, the converter

controller should actively reject internal or external disturbances as it must not only track the delivery of set-point power, but it must also reject any undesired input. Considering these drawback and constraints, an active disturbance rejection controller (ADRC) was selected due to its strong robustness and disturbance rejection, excellent performance, simple design, and its convenience compared to the PID controller. The ADRC controller advantages include fast response, robustness, and adaptability. Therefore, the ADRC controller is proposed in this study to overcome all the above-mentioned limitations.

1.4 Research Questions

- What method should be used to improve the robust controller?
- Can the proposed model improve the current wind turbine power performance?

1.5 Research Aim

The aim of this research project is to improve the performance and modelling of robust controller for the wind energy conversion system (WECS) based on permanent magnet synchronous generator (PMSG).

1.6 Research objectives

- To improve the performance and modelling of robust controller for the wind energy conversion system (WECS) based on permanent magnet synchronous generator (PMSG).
- To propose a new model for wind turbine power system by integrating control strategies.

1.7 Research scope

- This research study will only focus on improving and modelling the controller performance of the wind turbine model.
- The research study is only based simulation, therefore; no real physical system will be constructed.
- Modelling of the proposed wind turbine system and ADRC controller is carried out in MATLAB/Simulink environment.

1.8 Research Significance

- This research study will produce a wind turbine model with improved controller performance by developing PMSG based WECS with ADRC control.

- The proposed PMSG WECS model will be simulated by using control strategies to establish the most efficiency control strategy.

1.9 Project Block Diagram

Figure 1.2 shows the system block diagram for the proposed system with all the main system components. The diagram shows the energy flow, from the electricity generation point at the wind turbine and to the electricity feed in at the utility grid. The system components include the wind turbine, PMSG, machine side converter, grid side converter, SVPWM, ADRC based MPPT, pitch controller and grid.

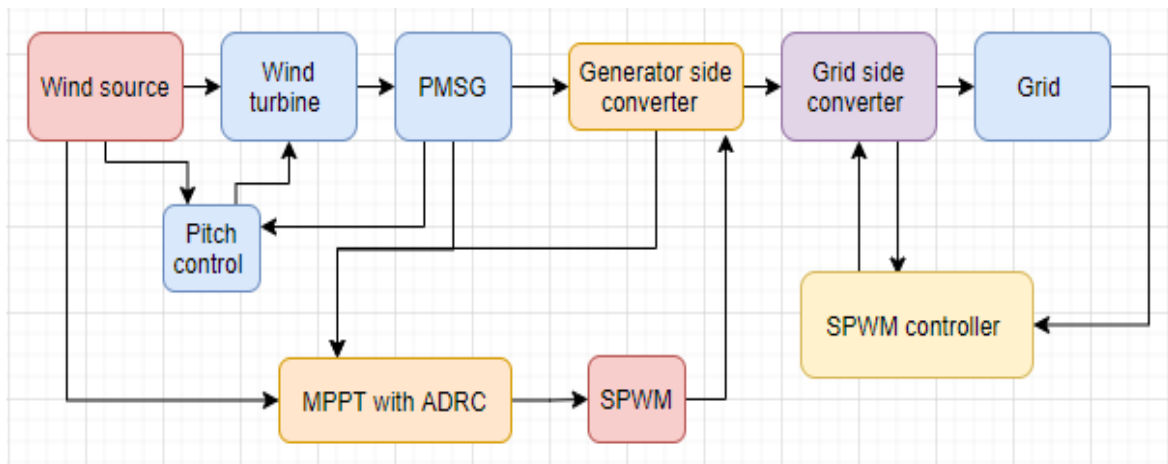


Figure. 1.2. System block diagram for proposed system.

1.10 Thesis Structure

This thesis is organized into five chapters. Figure 1.3 gives a summary of the main headings for the respective chapters which are briefly described below.

- **Chapter 1** presents the thesis introduction and covers an overview of the background of PMSG based wind energy conversion system, characteristics of wind energy and the block diagram for the proposed system showing the system main components.
- **Chapter 2** presents the literature review related to the research work carried out in this research study pertaining to the Control of PMSG Wind Turbines and Wind Turbine Technologies.
- **Chapter 3** presents the architecture for the proposed system, the design, modeling and simulation model.

- **Chapter 4** presents the discussion for the simulation results of the developed MATLAB/Simulink wind turbine energy conversion model. It also covers comparison of obtained results with those of existing models. The simulation results contrasting the performance of two control schemes viz ADRC and PID are also given and indicate the superiority of ADRC over PID.
- **Chapter 5** gives the conclusion for the research work and future work recommendations.

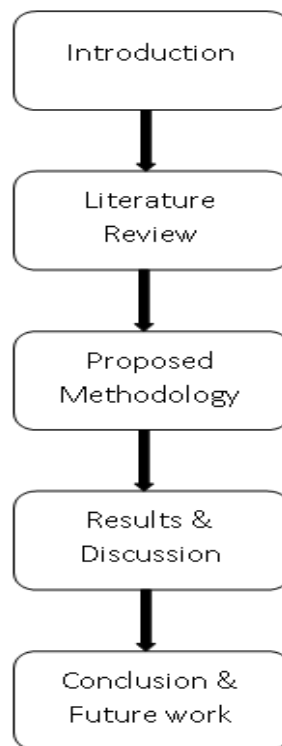


Figure 1.3. Thesis Structure.

CHAPTER 2

Literature Review

2.1 Overview of wind energy conversion systems

In recent years, wind energy has garnered a lot of interest to become one of the most popular renewable energy sources. In addition, the advancement and increased research on wind energy has resulted in increasingly growing number of wind energy conversion systems (WECS) globally. Initially, WECSs were only used for independent off-grid applications, but now they are also used for grid-tied applications to export power to the utility power grid [19]. Figure 2.1 shows Megawatts -WECS configurations.

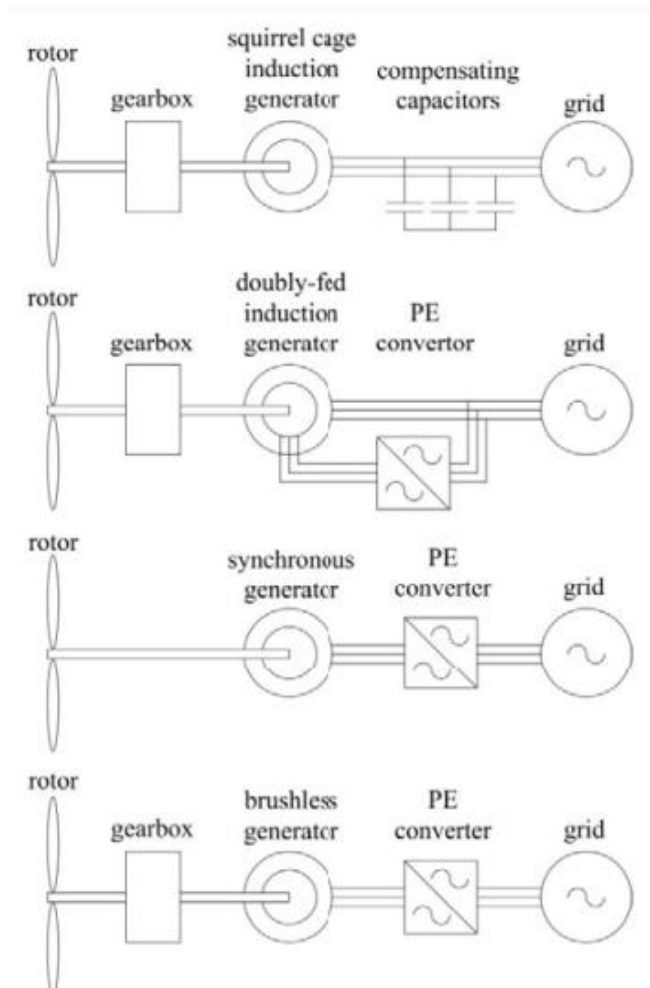


Figure 2.1. Common MW-WECS configurations. [19]

2.1.1 Wind energy conversion system

Figure 2.2 shows the block diagram representation of an WECS consisting of the wind speed as input, wind turbine, electric generator, power electronic interface and Load. The wind turbine converts the kinetic energy of the wind into mechanical rotational energy and the electric generator converts the mechanical rotational energy into electrical energy.

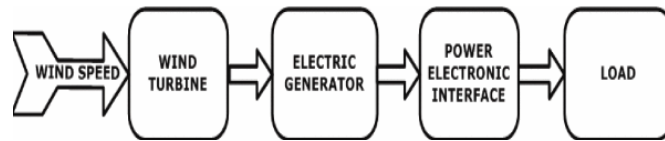


Figure 2.2. Block diagram for a wind energy conversion system. [20]

2.1.2 Power Transfer in a wind energy conversion system

Figure 2.3 shows the power flow within the main subsystems of the WECS namely the mechanical subsystem and the electrical subsystem[20]. As the wind speed changes there is corresponding change in the rotor speed which results in proportional variation of the electric generator output power. So, the power electronic interface is required to control the generator output power[21].

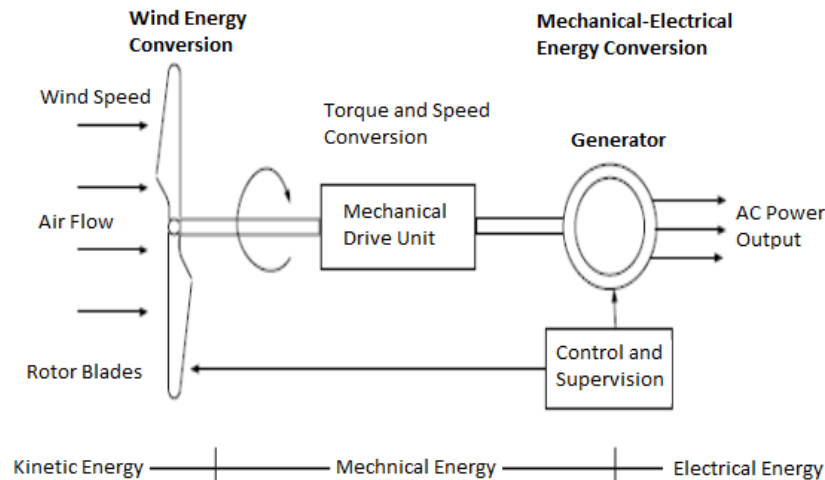


Figure 2.3. Power Transfer in a wind energy conversion system.[21]

2.2 Mechanical Subsystem

The mechanical subsystem comprises the rotor blades, rotor shaft and mechanical drive unit (pitch actuator, gearbox, low and high-speed axis) and converts the kinetic energy of the wind to rotational mass or torque. The rotor blades are connected to the low-speed axis (shaft or rotor)

which links to the gearbox in the mechanical drive unit. On the other hand, the generator is connected to the gearbox through the high-speed shaft. The rotational speed of the low-speed shaft is often lower than the normal generator speed, therefore, the gearing assembly within the gearbox must transform it to high rotational speeds compatible with the generator operating specifications [22]. For an ideal gearbox based on one mass model, the gearing ratio, η , can be described by equation 2.1. Where, Γ_t , is the torque of the turbine, Γ_{load} is the torque of the generator load and, ω_g , is the rotational speed of the high-speed shaft.

$$\omega_g = \eta\omega_t, \quad \Gamma_t = \eta\Gamma_{load} \quad (1)$$

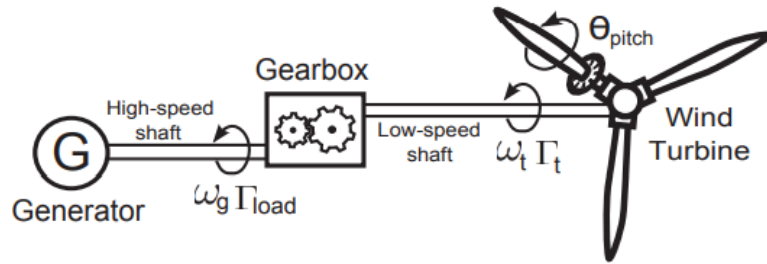


Figure 2.4. Basic Mechanical Subsystem for horizontal axis wind turbine. [22]

2.2.1 Electrical Subsystem

The electrical subsystem consists of the generator, power electronic interface comprising the converter/inverter, output filter, line inductance and the transformer which couples to the grid[20]. The generator converts the mechanical torque of the high speed-shift to unregulated power which is then regulated by the power electronic interface circuitry. The power electronic interface also regulates the electro-mechanical torque of the generator as well as the rotational speed of the rotor when operating in the variable speed region. There are four types of generators that are commonly used in WECSs namely squirrel cage induction generator (SCIG), double-fed induction generator (DFIG), brushless converter with full converter (BG-GFC) and the Permanent Magnet Synchronous Generator (PMSG) (Power Inverter Rectifier 2022).

2.2.1.1 Squirrel Cage induction generator

Generally, squirrel cage induction generators (SCIGs) are constant speed and inexpensive generators that consist of a 3-stage gearbox with a static assembly known as the stator which connects to the electrical network or load [23]. Figure 2.5 shows the diagram for the SCIG and its topological regions. For better performance in terms of noise reduction and improved efficiency

three windings are wound on laminated iron ore to generate magnetic field that rotates at constant speed[23]. The generator speed varies in proportion to the generator torque which reduces wear and tear. Two types of squirrel cage induction generators exist, the pole changing generators and semi-variable speed generators. Pole changing squirrel induction generators have low noise and yield better energy efficiency and have can operate at two fixed speeds, while semi-variable speed generators have wider speed variations with capability to minimize mechanical loads and power quality issues[24],[25].

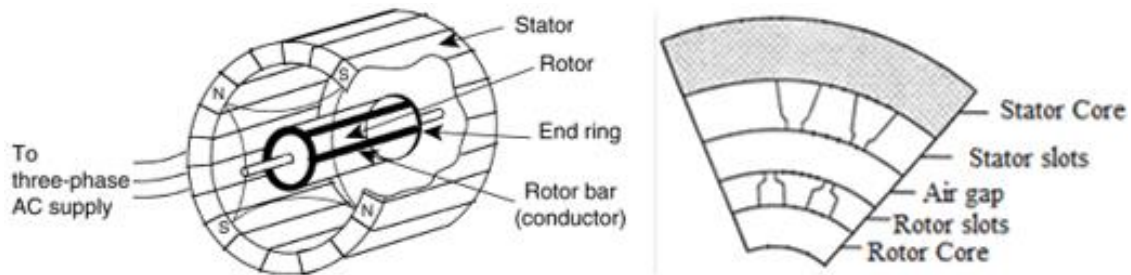


Figure 2.5. Diagram of squirrel-cage induction motor and its topological regions.[25]

2.2.1.2 Double-fed induction generator

Double-fed induction generators (DFIGs) comprise are low-cost generators with a multistage gearbox and partially rated power electronic converter coupled to the rotor winding with pitch control to limit generator output power to the rated generator power for higher wind speeds. DFIGs perform better than constant speed generators in terms of noise, power quality etc., however they have a major deficiency when it comes to grid-fault ride through capabilities[24].

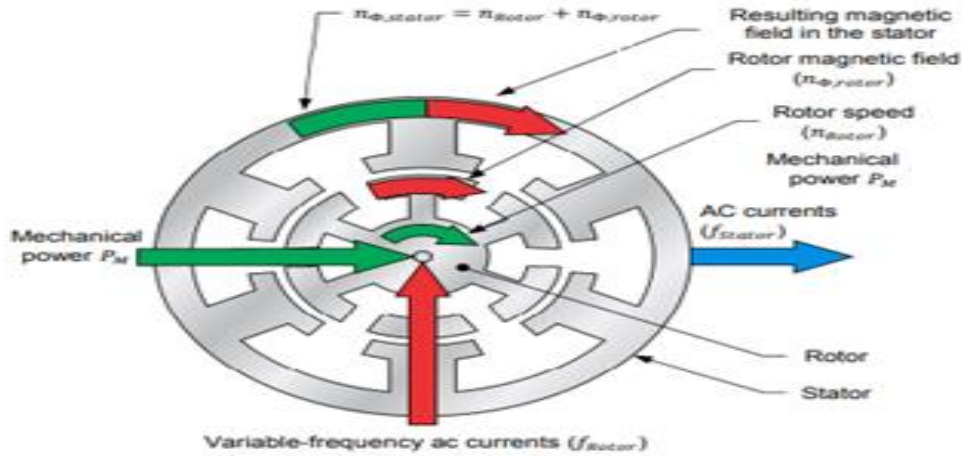


Figure 2.6. Double-fed inductor generator, stator and rotor magnetic field rotating in same direction.

2.2.1.3 Permanent magnet synchronous generator

Similarly, to SCIGs, Permanent magnet synchronous generators (PMSGs) have a stator assembly that directly couples to the electrical network or load, but their rotor have field winding which results in constant speed rotation with the network frequency and stator field and require a full converter for grid connection. PMSGs can operate at wider speed range, are reliable and require less maintenance, however, generator design is complex, expensive, and less efficient due to its bulkiness [23], [26],[27].

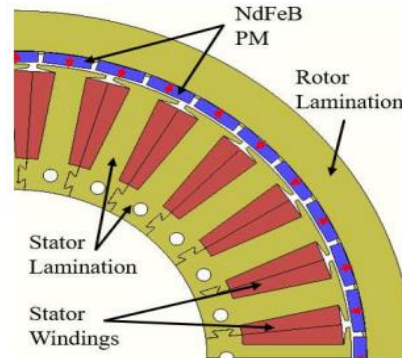


Figure 2.7. Cross-section view of modular PMSG with surface permanent magnet rotor design. [26]

2.2.1.4 Brushless double-fed induction generator

Brushless double-fed induction generators (BDFIGs) consist of two stator windings, one coupled to the grid and the other supplied by the converter and operates under constant ratio between the shaft speed and the stators frequencies[28]. BDFIGs are medium speed systems with low system cost, better efficiency, and reliability[29]. Figure 2.8 shows the different rotor structures for BDFIGs and the cross-section view for the dual-stator BDFIG.

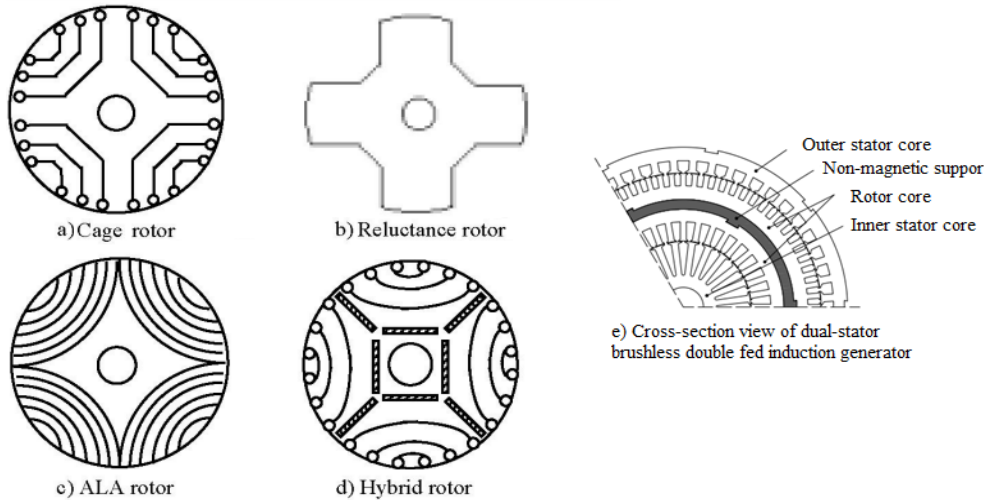


Figure 2.8. Different rotor structures of BDFIGs and cross-section view of the dual-stator BDFIG.[28]

2.2.2 Power electronic converters

2.2.2.1 Wind Energy Conversion System with parallel connected back-to-back

According[29], converters for wind energy systems can be classified into four viz. back-to-back, passive generator side, multiphase generators and converters without dc intermediate link voltages. Back-to-back converters are commonly used for variable speed wind turbine systems[30] and use more than one conversion stage as shown in Figure 2.9 to achieve the fixed frequency and voltage specifications for grid connection. This class of converters can be divided into low voltage and medium voltage and can be used for any generator type due to their bi-directional power flow feature[23]. However, for high power applications requiring high dc link voltage of about 5 kV for 3.3 kV standard grid-side primary voltage, multilevel converters are preferred[31]. According to authors in [32] and [33], in terms of reliability issues, mature traditional multilevel converters are

to be preferred such as the 3-level neutral point clamped multilevel converter topology. Due the high component count of large power conversion systems, it is desirable to minimize system failure and increase system tolerance to faults to achieve system reliability. One of the approaches adopted in industry is to use fault tolerant modular power converters with capability to bypass faulty modules to keep the functional modules operational. Transformer less modular multilevel converters without dc link voltage and that can achieve high ac or dc voltages between 10 kV to 100 kV with capability to connect directly to the utility MVDC or HVDC have been investigated and explored[34].

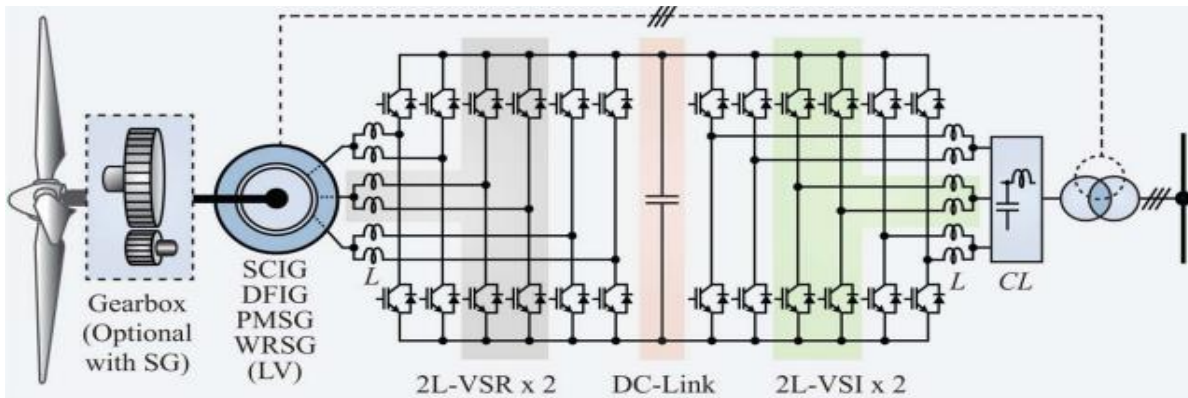


Figure 2.9. Type 3,4 WECS with parallel connected back-to-back 2L-VSCs with dc link voltage[30]

2.2.2.2 Modular multilevel converter

According to Figure 2.10 shows a transformer less modular multilevel converter without dc link voltage. The converter consists of ac/dc converter modules cascaded in series with the generator divided into sections that supply different converter modules to enhance fault tolerance and modularity. This has the advantage of keeping the system operational in case of faulty generator module or converter module. A study by[35], [36] indicates that multilevel converters without dc link voltage require high dc isolation for common mode voltages and have low current density which pose a huge challenge for high voltages.

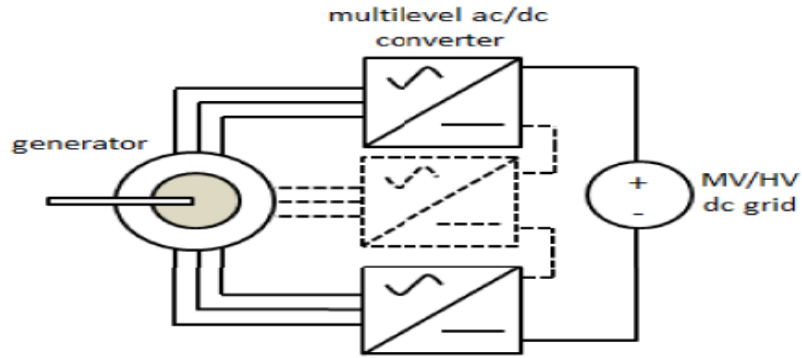


Figure 2.10. Modular multilevel converter[19]

To mitigate for this, an intermediate dc link voltage is introduced between the output stage of the paralleled converter modules and the input of the high step-up modules as shown in Figure 2.11. The step-up modules further increase the dc link voltage to MVDC/HVDC.

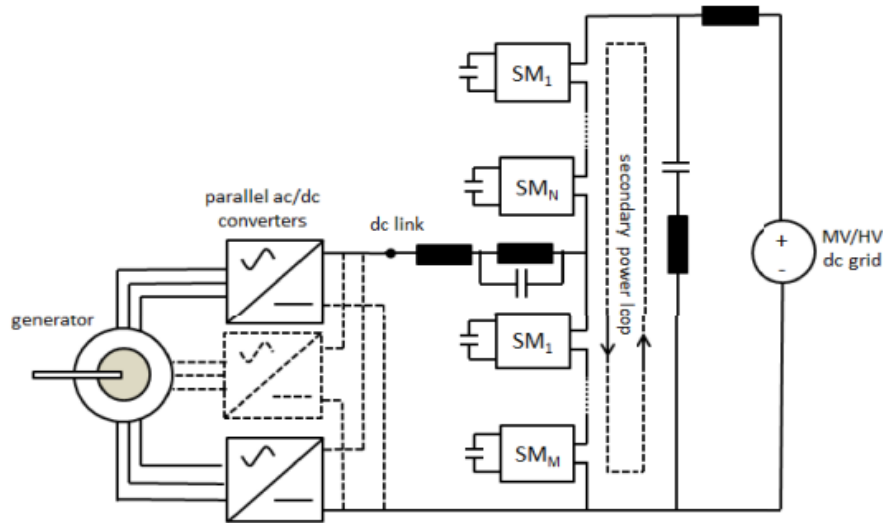


Figure 2.11. Transformer less multilevel converter. [35]

Generators operating at low speeds have higher number of poles which allows them to control reactive power without a gearbox [37]. Figure 2.12 shows configuration of a variable speed PMSG-based WECS. The back-to-back converter consists of the generator side converter and the grid-side converter which connects the synchronous generator to the grid [38]. The converters optimize the generated energy by the generator for different wind speeds, control and distribute active and reactive power to the grid by keeping a constant DC-Link voltage. Several Back-to-

Back converter designs are suggested in literature such as the vector-controlled converter derived from the traditional PI controlled converter [39] ,[40].

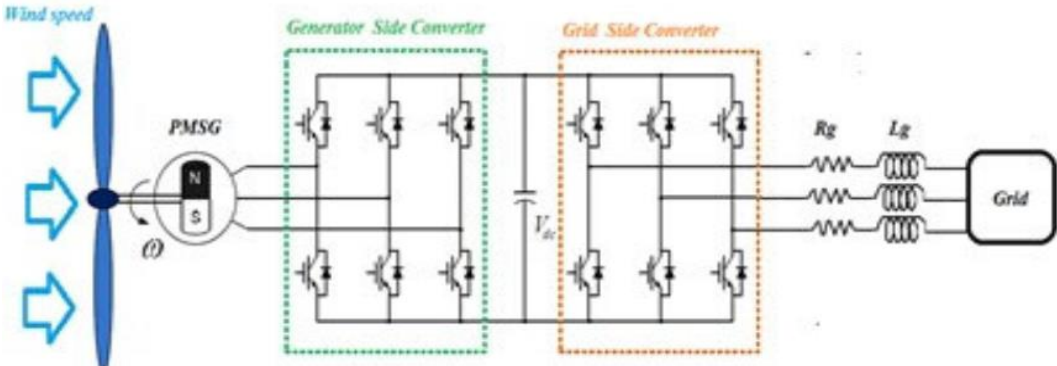


Figure 2.12. Variable Speed PMSG-based Wind Energy Conversion System.[39]

2.3 Wind Turbine Technologies

2.3.1 Horizontal axis wind turbine

Wind turbines can be classified according to turbine generator configuration, physical structure, airflow trajectory to the turbine rotor, turbine size, generator-driving design, power supply mode and installation position. Based on physical structure, wind turbines can be classified into two major groups viz. horizontal axis wind turbines (HAWTs) shown in Figure 2.13 and vertical axis wind turbines (VAWTs)



Figure 2.13. Horizontal axis wind turbine.[41]

2.3.2 Vertical axis wind turbines

Figure 2.14 [41]. However, they can be classified into four major groups based on the electrical subsystem circuitry, rated power capacity and control speed viz. fixed speed wind turbine, limited variable speed wind turbine, variable speed wind turbine with partial-scale power converter and variable speed wind turbine with full-scale power converter. Figure 2.9 shows the basic commonly used generator configurations. HAWTs are mostly for commercial use and can be classified as rotor-upwind design or rotor-downwind design[42]. As the height of the turbine tower increases, there is also a proportional increase in efficiency, output power, turbine noise and size of rotor blades[43]. Rotor-upwind turbines consist of three blades and are widely used due to better performance compared to rotor-downwind turbines which consists of two blades and have poor performance due to flickering and inability to adjust under rapid wind direction change[43], [44]. Key advantages of HAWTs include better efficiency, high generating capacity, tall tower for capturing large amount of wind energy and variable pitch blade capacity [42] , and drawbacks include continuous noise, extensive land use, bird killing, affects radio and TV transmission and radar. VAWTs can be categorised into three based on their mechanical and aerodynamic features namely Savonius-rotor, Darrieus-rotor and H-Darrieus-rotor [44],[41]. The main advantage of VAWTs is accepting wind flow from any direction as crossflow systems, while disadvantages include stalling during gusty winds, blade sensitivity, low initial torque, stability issues and they are restricted to low-speed environments[45].

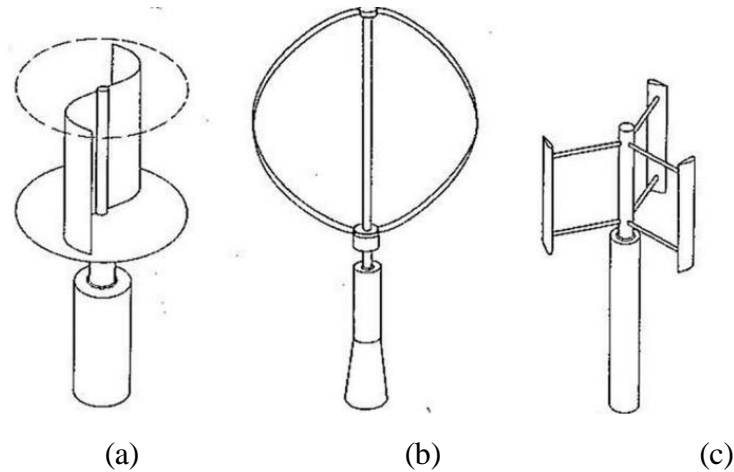


Figure 2.14. Vertical axis wind turbines. (a) Savonius-Rotor. (b) Darrieus-Rotor. (c) H-Darrieus-Rotor

2.3.3 Fixed-Speed Wind Turbine

Fixed-speed wind turbine (FSWT) configuration consists of a multi-stage gearbox and a squirrel cage induction generator (SCIG) coupled directly to utility grid [46] Figure 2.15 shows the design configuration for a fixed-speed wind turbine. FSWT designs are also known as the “Danish concept”, a conventional term coined by Danish wind turbine manufacturers between the 1980s and 1990s[47]. The operating principle of FSWTs assumes that the wind speed fluctuation is transformed into proportional mechanical fluctuations and then subsequently to electrical power fluctuations. FSWTs have limited power quality control, zero reactive power consumption control, and zero aerodynamic speed control [48]. The key benefit of this design is low cost due to its simple off-the-shelf components and two design variants that offer better performance than the traditional design exists viz. pole changing induction generator wind turbine and semi-variable wound rotor induction generator wind turbine[46].

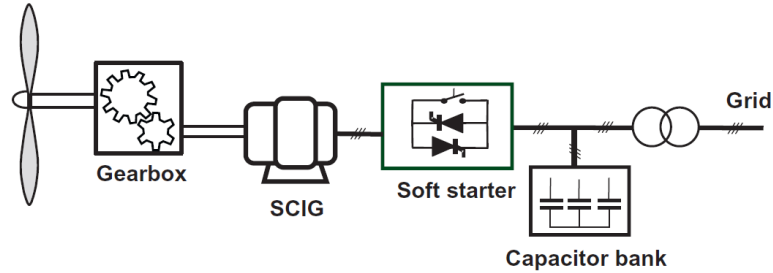


Figure 2.15. Fixed Speed Wind Turbine[47]

2.3.4 Limited Variable-speed Wind Turbines

Limited variable-speed wind turbine (LVSWT) configuration also known as the OptiSlip or FlexiSlip have minimal variable speed control. Danish manufacturer VESTAS marketed this type of wind turbines from the mid-1990s until 2006. LVSWT operate at minimal variable speeds which improves turbine aerodynamic efficiency, although the concept of variable-speed turbines is the most dominant [49].

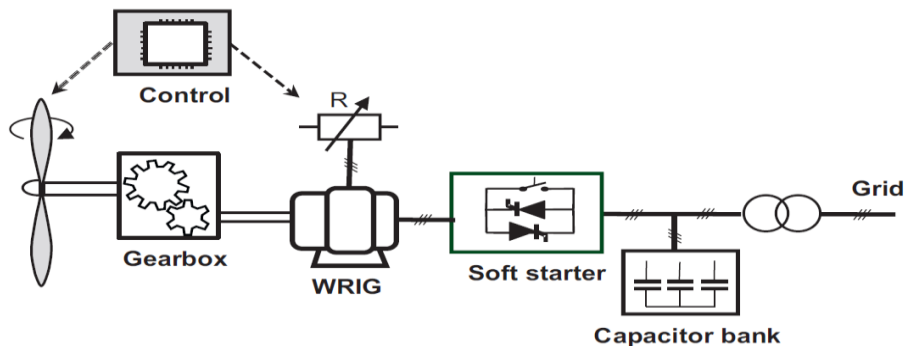


Figure 2.16. Limited Variable-speed Wind Turbine.[47]

2.3.5 Variable-speed Wind Turbine with Partial-Scale Power Converter

Variable-speed wind turbine (VSWT) designs with a partial-scale power converter configuration consists of a multistage gearbox, low-cost double-fed induction generator (DFIG) or rotor wound induction generator (WRIG), controller and partial rated power converter[47]. Figure 2.17 shows the configuration for VSWT design. The partial-scale power converter is a back-to-back converter and connects to the generator rotor usually via slip rings and is responsible for power feed into the utility grid. This configuration offers wide speed range for turbine operation proportional to the size of the power converter [49]. The speed range is determined by the power rating of the partial-scale converter, typically about 30 % the around synchronous speed. Key

advantages for this configuration include flexible match for requirements pertaining to noise, mechanical loads, energy output, power quality; and the main drawbacks include requirement of additional safety mechanism, capability for grid-fault ride through and use of slip rings which require routine maintenance[50].

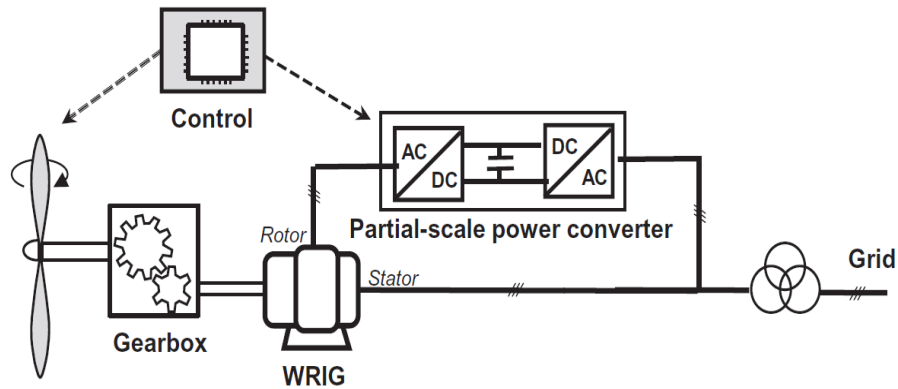


Figure 2.17. VSWT with Partial-Scale Power Converter. [47]

2.3.6 Variable-Speed Wind Turbines with Full-Scale Power Converter

Variable-speed wind turbine (VSWT) with full-scale power converter configuration consists of a variable speed controller with the stator windings, a full-scale power converter and generator. Figure 2.18 shows the configuration for VSWT. Synchronous or induction generators can be used for this configuration. However, a heavier direct driven multipole generator is used for the gearless VSWTs systems. Examples of wind turbine manufacturers using more direct drive systems are Enecom and Siemens Wind Power [50]. Advantages of gearbox-based VSWTs with full-scale power converter over VSWTs with partial-scale power converter include higher generator performance, no slip rings, simpler or no gearbox, maximum controllability of turbine power and speed, higher potential for grid support and less complicated grid-fault ride through capability. While advantages of gearless VSWTs include reduced power losses, reduced costs and improved efficiency due to absence of rotating mechanical parts. The major drawback of full-scaled power converter based VSWTs is high converter costs although converter costs have been steadily decreasing over the last few decades [51].

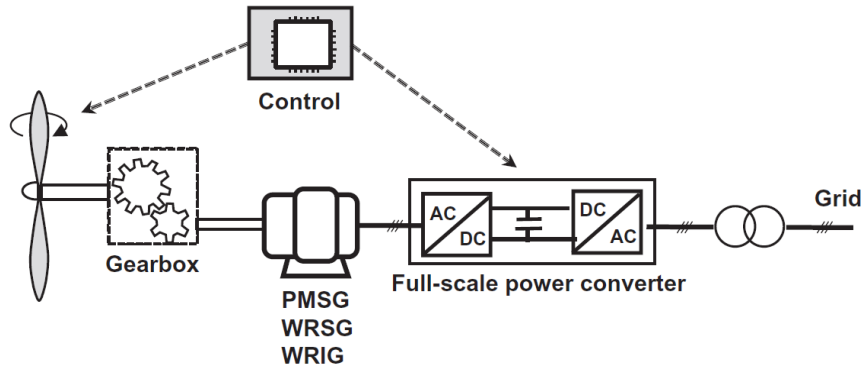


Figure 2.18. VSWT with full-scale Power Converter.[50]

2.4 Control of PMSG Wind Turbine

Generally, the control system for WECS can be classified into three parts viz. speed control, generator-side (machine-side) converter control and grid-side converter control. For traditional WECS with dc link voltage, the dc link voltage influences the stability of the dc distribution network [52]. To ensure stability of the distribution network, the standard control approach is to keep the dc link voltage constant through the power electronic converter. Authors in [53] say most research on wind turbine control systems (WTCS) have sought to improve the ability of control techniques to increase system capacity to supply reactive power and to regulate active power for both grid connected and islanding modes. Other control approaches have aimed at diminishing the generator current, extract maximum power, regulate both DC link voltage and reactive power injected to the grid and reduce harmonic currents at point of common (PCC). PMSG controllers can be grouped into two types as type 1 and type 2. Type 1 controllers use machine-side converters (MSC) for maximum power point tracking (MPPT) and grid-side converter (GSC) for regulating dc link voltage [54], [55]. While type 2 controllers use the GSC for extracting active power from wind turbine and the MSC for regulating dc link voltage [56]. Various control techniques for PMSG WTCSs exist, and the three commonly used control techniques are zero d-axis current (ZDC) control, unity power factor (UPF) control and maximum torque per ampere (MTPA) control [57].

2.4.1 Traditional three-part control

Figure 2.19 illustrates the traditional three-part control strategy for WECS. The main objective for MSC control is to achieve maximum power point tracking, while that for GSC control is to achieve stable dc link voltage and to regulate reactive power [58], [59]. Speed control aims

to achieve maximum output power for the variable speed region by keeping the pitch angle constant and varying the torques accordingly, while for the constant speed region, speed control aims to operate the wind turbine within its safe margin by varying the pitch angle to obtain constant torque setpoints.

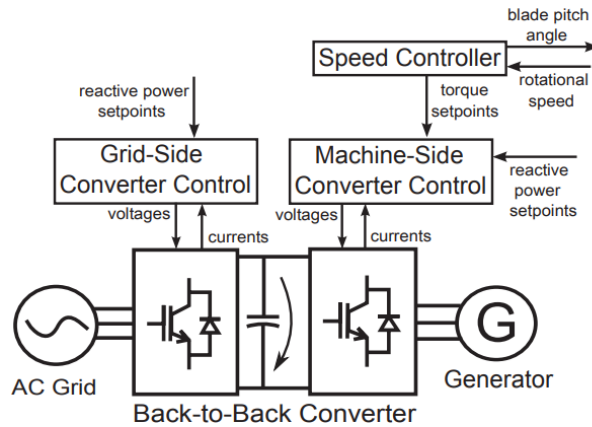


Figure 2.19. Block diagram representation for the traditional three-part control strategy for WECS[59]

The traditional control strategy described above has a major drawback in that during low wind speed fluctuations the dc link voltage also fluctuates, as a result, the slow voltage loop for the controller fails to track the reference d-axis component, i_{gd} , of the grid current [59]

Figure 2.20 shows the structure for the WECS described in[40]. The system consists of a PMSG, speed/power controller, separate MSC and GSC, dc-link voltage, filter, transformer, current and voltage controller. The speed/power controller controls the power, torque and speed of the PMSG. Whereas the configuration of the rectifier and inverter as individual units enable separate control of each power electronic system. The inverter synchronizes the output power of the WECS with the grid's power and keeps the dc voltage link constant. The inverter also adjusts the unit power factor (UPF), reactive and active power deliverable by the WECS to the grid. When the WECS is integrated into an existing electrical network, it needs to meet the IEEE standards and new grid codes under intermittent and grid disruption conditions, as poor power quality of the WECS can pose major challenges for the electricity management strategies.

Modelling and simulation of a variable-speed PMSG-based wind turbine with predetermined wind speed and rotor speed values was carried by Samaria in[60]. Obtained simulation results indicate excellent speed regulation of the rotor speed despite uninterrupted

change in wind speed. A study conducted by Fandi examined a gearless variable speed PMSG-based wind turbine system and developed an equivalent MATLAB/Simulink simulation model for the system [61]. The results from the study are useful in the modelling, simulating and evaluating the effect of wind speed shifts and Q-reference of variable speed PMSG-based wind turbine systems.

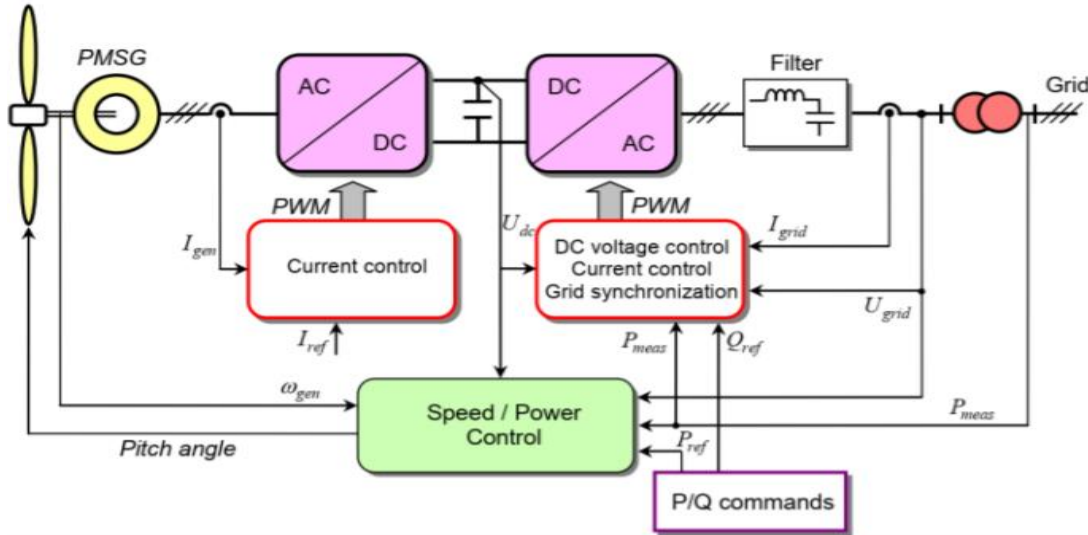


Figure 2.20: Typical structure for WECS connected to an existing electrical Network

2.4.2 Linear control

Various linear control methods have also been used to control grid-connected inverters [54] , [62], however these have major drawbacks such as lack of ability to track sinusoidal trajectory references and cannot reject system disturbances. According to the study by [22], common linear methods such as the PI control technique can only meet some specifications of the desired WTCS requirements. Various research studies have been conducted on nonlinear strategies solutions for controlling grid tied PMSG, but these techniques are sensitive to modelling errors, difficult to implement and require specific PMSG parameters [63]. Several PMSGs are required to have a functional WECS, and these connect direct to the power grid via an offshore step-up transformer and usually mitigation for the system reactive power is achieved by power factor correction implemented by the grid-side control system. Figure 2.21 shows the PMSG based WECS proposed in [53]. The system delivers power to a local load and grid via a grid tied inverter

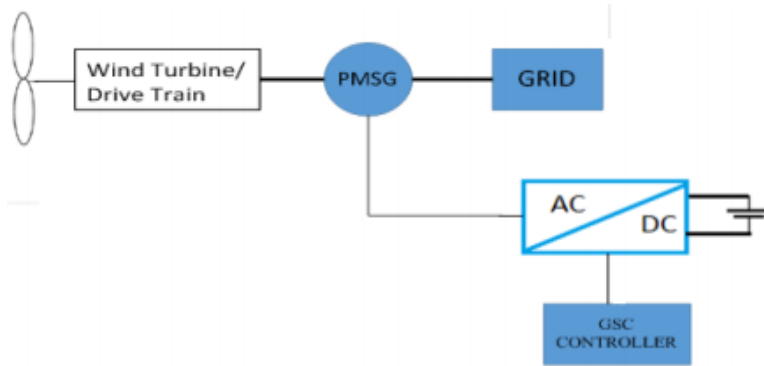


Figure 2.21. Wind Energy Conversion System[53]

2.4.3 Active disturbance rejection control

A study by [37], introduced a new control technique known as active disturbance rejection control (ADRC) for WTCS based on the SCI generator [37]. The aim of the study was to monitor both the MSC and the GSC as well as to control the system and to ensure connection to the power grid. The MSC controls the speed, and the SCI generator facilitates extraction of maximum available power from the wind turbine through the MPPT technique. During high wind speeds, the MSC also maintains extracted power within the acceptable rated value and the pitch actuator system controls the wind turbine pitch angle of the blades. While the GSC monitors the active and reactive power injected into the utility power grid and regulates the dc Link voltage. PMSG wind-turbines require various feedback controllers, this can be challenging for the control mechanism when using controllers such as PI controllers due the presence of various time lapses. The use of an ADRC controller in place of the PI controller can enhance the performance of the wind-turbine system. The ADRC is derived from the extended state observer (ESO). The ESO is a high-gain observer and powerful tool for output feedback control of uncertain non-linear systems, and it can predict the internal and external disturbances of the turbine system including the parameter uncertainties [63]. The unknown uncertainties are directly estimated in a single state without affecting the control functionality of the ADRC. The proposed ADRC controller is investigated, and its performance is compared to the PI controller to prove its fixability and efficiency of the proposed system.

2.4.4 Intelligent control

Intelligent control based on artificial intelligent strategies such as fuzzy logic (FL), artificial neural network (ANN), model predictive control (MPC) etc. can be used to achieve maximum power extraction in WECSs and these have also been implemented with switched-reluctance generators (SRGs) [40]. The controllers can vary the rotational speed of the turbine rotor by setting the rotation angle and by adjusting the blades turning angle. Simulation results based on FL controller indicate improvement in system energy efficiency and accuracy compared to the study conducted by Tan based on MPC[64]. However, the MPC controller proposed by Tan indicates improvement in the system dynamic response and enables parallel generators to operate with more flexibility by eliminating dependency on voltage and frequency synchronization. Researchers in [65] analysed and simulated an FL based variable speed wind turbine controller. An induction-based (IM) wind turbine emulator (WTE) was used to provide a safe testing environment for the WECS. Figure 2.22 shows the design for the proposed WTE in [38] based on an IM field-orientated control system. The WTE was powered by the PMSG, and it was connected to the grid by back-to-back converters. The research objectives included maximum power extraction and feeding of the generated power to the utility grid. FL based MPPTs were used to optimize the generated wind energy at various wind speeds, while a grid-connected inverter with fuzzy adaptive (FA) PI controller facilitated energy transfer to the grid and regulated the dc link voltage. Obtained MATLAB/Simulink simulation results for the system model indicate that FA PI control compared to classical PI control overcomes the nonlinearity of dc link voltage.

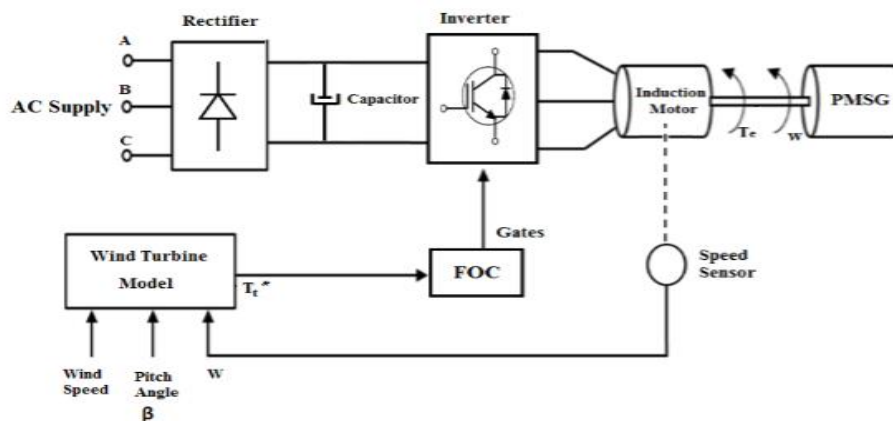


Figure 2.22. Structure for the proposed WTE based on an IM field-oriented control system[38]

WECSs are prone to power grid faults, for instance, when there is a fault in the electrical system the WECS will instantly disconnect itself from the power grid, this is undesirable. Therefore, an appropriate adaptive controller is required to operate the system effectively. One of the most significant adaptive controllers is the neuro controller. Figure 2.23 shows the configuration of the ANN controller. It has two inputs viz. Δe (x) and Δde (y) and one output expressed as $f \in \{x, y\}$. Each input consists of 5 membership functions. The MATLAB model for the ANN based wind generation controller considers five parameters, the PV diode module, a variable speed generator and an MPPT to ensure optimum power extraction from the system. The incremental conductance for the MPPT is set to twenty (20) algorithms. The wind turbine converts the kinetic energy of a moving stream of wind to electricity. But a complete wind turbine model for a standalone system e.g., the trained model considers the mass model and rectifier model, the whole system model associated with the PV model and the wind turbine model. However, based on previous research, the complete model has a major challenge in that it lacks an efficient monitoring system for power generation. In addition, the power electronic conversion circuitry developed for the hybrid system is not effective, which results in power losses and leakages.

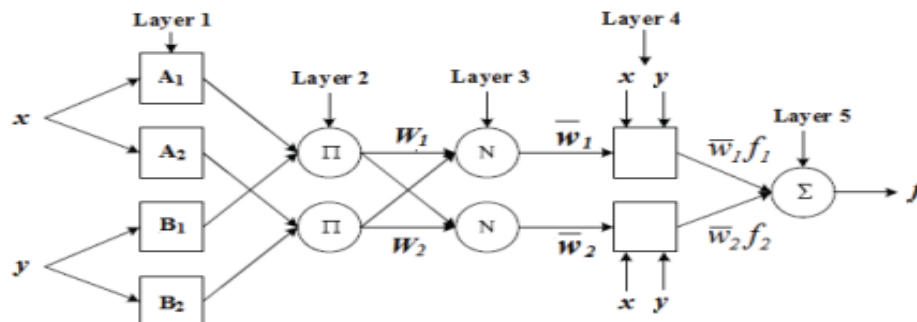


Figure 2.23. Configuration of an ANN controller. [53]

Another control scheme presented in literature is the sliding mode control (SMC) for a PMSG variable speed PMSG based wind farm system (VS-WFS). Variable speed SMC offers the benefits of flexibility because the existing system electronics can be used for the variable speed wind energy converter controller. However, its main disadvantage lies in its ability to increase mechanical stress due to noise, but this can be reduced using different techniques. The overall performance assessment of the PMSG can be augmented using advanced optimization techniques for several control mechanisms to enhance the performance measurement of the generator. But the obtained simulation results in [56] show that the system has low efficiency. The proposed system

focused on developing an effective control strategy for PMSG-based WECS. The WECS model consists of a wind turbine, a PMSG, a PWM rectifier on the generator-side, an intermediate dc circuit and a PWM inverter on the grid-side. The proposed approach to regulate both GSC and MSC of the WECS is based on vector control (VC) theory. The proposed control law therefore combines space vector modulation (SVM) and MPPT control strategy to maximize the generated power under varying wind speed and grid fault conditions[36]. Although, the functionality of the proposed wind turbine simulator scheme has not yet been validated and the effectiveness of the WECS needs to be tested for grid fault conditions by using different control strategies to analyse and then improve the performance of the model. Author [66], proposed a model for a PMSG-based VSWT and control scheme. The developed model describes the mechanical part, the aerodynamic part and the electrical part of the wind turbine. Several issues were identified when using different component models for the WECS which are dependent on the pitch angle and the aerodynamic power was affected by the wind speed [66]

2.4.5 Non-linear controller

2.4.5.1 Feedforward control

In a feedback control system subjected to external disturbance, remedial action is done to eliminate the disturbance's consequences only after the process has been impacted. If the disturbance is measurable, feedforward control can be an effective open-loop control strategy for preventing unwanted responses, as it enables remedial actions to be taken before the disturbance effects the system. Feedforward control is widely employed in industry[67], and this effective way of disturbance rejection has generated substantial study into the integration of feedback and feedforward control systems[68]. According to [69], discrete time feedforward/feedback controllers for broad nonlinear processes with stable zero dynamics are developed, as well as their linkages to model prediction techniques. The resultant controllers are said to be capable of reducing, if not fully eliminating, the effect of quantifiable disturbances and producing a predefined linear response with regard to a reference input. The controllers are designed in a linked way, with the feedforward and feedback controllers achieving their distinct objectives via a single unified control law.

2.4.5.2 Adaptive neural network feedforward

A recent paper[70] introduces an adaptive neural network feedforward compensator for external disturbances impacting a certain class of loop systems. To minimize the impacts of a disturbance on a linear discrete closed-loop system, a nonlinear disturbance model is estimated. For efficient disturbance rejection in this system, the output of the disturbance model must match the compensation signal. Another feedforward control system utilizing artificial neural networks is described in[71], where a nonlinear adaptive feedforward controller is used to compensate for external load disturbances in an automotive engine's idle speed regulation. The feedforward-only strategy is based on approximating specific input-output mappings representing the system using Radial Basis Function networks. The mapping is composed of an optimal control input and a system variable whose control purpose is to minimize a quadratic performance index. Another related work [72] investigates the topic of adaptive feedforward compensation for input-to-state (and locally exponentially) convergent nonlinear systems. The proposed approach successfully suppressed a harmonic disturbance at the nonlinear system class's input. Preliminary results on feedforward control for external disturbance rejection in nonlinear feedback control systems were provided in previous work. Given an asymptotically controllable disturbance-free nonlinear system with feedback control, a decoupled design of feedforward control is achieved for the purpose of removing disturbances and thereby ensuring asymptotic controllability in the presence of disturbances. Before a strategy for monitoring the disturbance and generating appropriate feedforward control signals can be created, it is necessary to get a thorough understanding of the disturbance's impacts on the system. To facilitate comprehension and awareness of the feedforward control objective, the concept of disturbance effect in a nonlinear system subjected to an external disturbance is introduced using Lyapunov stability analysis. As a result, a feedforward control approach may be one that totally eliminates the effect of the disturbance [73]. It is demonstrated that the proposed feedforward controller (to supplement the feedback controller) that senses current disturbance and creates a corrective control signal requires a diminishing control-Lyapunov function to achieve asymptotic controllability.

2.4.6 Model predictive control

Model predictive control is a method for calculating the receding horizon that has been extensively investigated over the last couple of decades. The approach control is particularly useful

since it allows for the handling of time-domain limitations on signals. The method's popularity derives in great part from the fact that the underlying algorithm is simple to comprehend and apply. As a result, practitioners may readily adapt it and it serves as an effective educational tool. The approach control has found application in particular in the process sector[74]. However, MPC has not been used in substitution of popular classical methods such as PID control in the past. Rather than that, it has been used to regulate slow dynamics, for example, by determining set points for low-level controllers that control fast dynamics. Model predictive control involves online calculations, and as a result, was previously insufficient for managing fast dynamics. However, the rising processing capacity of computers and advancements in optimization techniques have expanded the applicability of MPC to applications formerly reserved for offline-designed controllers. The fundamental linear MPC formulation does not account for model uncertainties caused by disturbances, unmodeled dynamics, or nonlinearities. Suboptimal ways to coping with uncertainty in MPC have been addressed in this work [75]. The emphasis has been on finding methods for dealing with uncertainty in MPC without deviating significantly from the main algorithm's online optimization problem.

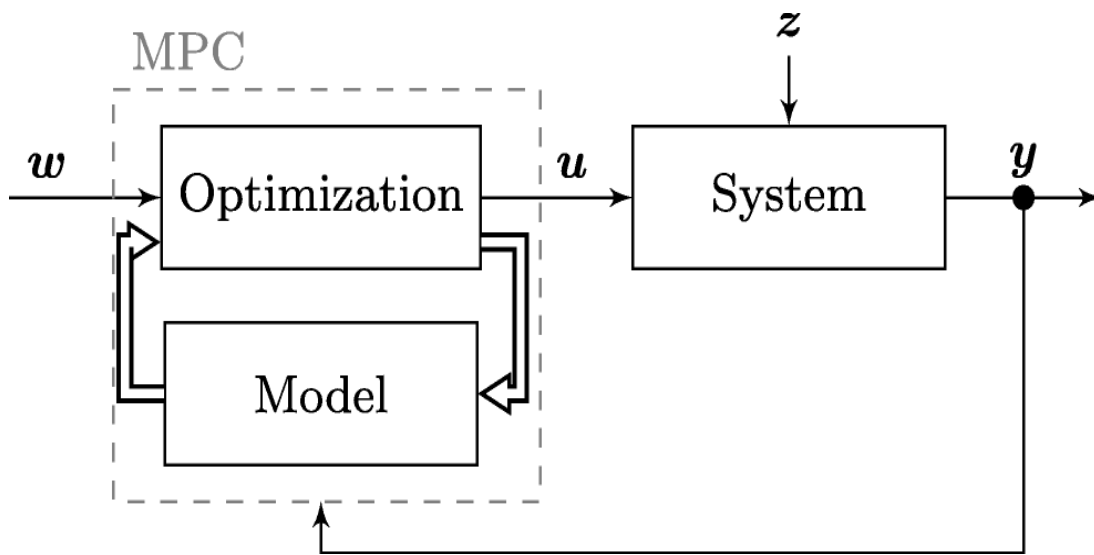


Figure 2.24 Simplified block diagram of a MPC-based control loop

The model predictive control method's anticipatory tendency and ability to incorporate harsh limitations make it extremely valuable for regulating real systems. Model predictive control currently permits the control of systems that were previously inconceivable because to the increase in processing capacity and the increasing availability of models of complex processes for a variety

of diverse systems [75], Model predictive control is based on models from nearly every discipline. This enables the use of this accumulated knowledge and avoids the time-consuming job of explicitly defining a control law – a task often left for control experts. Rather than that, Model predictive control automatically develops the control law via a model-based optimization procedure. This implicit formulation, flexibility, and explicit use of models are the primary benefits of MPC and the grounds for our advocacy in the engineering community. This study summarized the Model predictive control from an application standpoint but will not assert that it is the optimal control technique for any given issue[76]. Model predictive control popularity is due in large part to the fact that, given a proper model, the controller can be simply constructed with a direct physical understanding of the parameters to tune and simple constraint handling. This is truer than ever in the modern era of rapid microprocessor advancements and ubiquitous availability of models. One distinguishing feature of Model predictive control is that the control rule is implicitly determined while solving the restricted optimization problem online. By including physical restrictions in the optimization problem, the effort required to design a controller is shifted away from the controller itself and toward modelling the system to be controlled [77]. Controlling high-level objectives rather than machine tool set points is possible with model-based predictive control (MPC).

Table 2:1 Summary of literature studies

Author	Year	Title	Objectives	Methodology	Gaps
Wu, Chang & Mandal	2019	Grid-connected wind power plants: a survey on the integration requirements in modern grid codes	To compare and summarize the grid codes and the corresponding works about wind power integration around the world.	In a survey paper, more than 30 papers were studied to identify the wind power integration in the literature.	No simulation results were provided; the authors conducted a survey only based on the power wind grid requirements.
Ayodele et al.	2013	Challenges of grid integration of wind power on power system grid integrity: A review	This paper discusses the various challenges of wind power when integrated into the grid and identifies different mitigating strategies for its smooth integration	Secondary data analysis	This study includes only secondary data analysis, and there are no simulations results provided, unlike our study, which simulated a hybrid model and investigated a similar system in the literature.

Sri Anjaneyulu1 et al.	2016	Control of PMSG Wind Turbine Based on PI/ANN Controllers.	To compare a conventional PI controller and Artificial Neural Network (ANN) controller to the Grid side converter of PMSG.	Simulate and verify under two considerations a grid-connected PMSG based wind system under fault analysis and comparison and to compare of Proportional integral (PI) controller and ANN Controller to the PMSG grid-side converter Presents of Nonlinear load.	The proposed ANN-based control strategy obtained poor efficiency. With an overall efficiency equal 84%
Laghrida etal	2019	Comparative analysis between PI and linear-ADRC control of a grid-connected variable speed wind energy conversion system based on a squirrel cage induction generator.	This paper aims at contributing to the modeling and control of a variable speed Wind Energy Conversion System (WEC-System) based on a Squirrel Cage Induction Generator (SCI-Generator).	A new control strategy named the Active Disturbance Rejection Control (ADRC) is proposed and utilized to control the Wind Energy Conversion (WEC) system based on the SCI-Generator.	The restrictive effects of the inaccuracy system model on the ESO function were High. With an overall efficiency equal 88%
Benaouinate et al.	2020	Nonlinear Control Based on Fuzzy Logic for a Wind Energy Conversion System Connected to the Grid	To present, analyze, and Simulation of a variable-speed wind turbine control. Wind turbine emulator (WTE) based on induction motor (IM)	The methods of maximum power point tracking (MPPT) using Fuzzy logic is used to maximize the wind power captured at different wind speeds	The efficiency of this system was poor
Samaria, Sharma & Gidwani[2015	Modeling and Simulation of wind turbine using PMSG.	To model and simulate a variable-speed wind turbine along with permanent magnet synchronous Generator	Simulate a variable-speed Wind turbine along PMSG using MATLAB.	The functionality of the proposed wind turbine simulator scheme is not validating, while in this system, the hybrid model will be validated to analyze the performance of the model. With an overall efficiency equal 83%
Ke Ma et al.	2013	Power Electronics for the Next Generation Wind Turbine System	To evaluate and improve the critical performances of the wind power converter for the next-generation wind turbine system.	Design a wind turbine with a doubly fed induction generator (DFIG) and the ones with a permanent magnet synchronous generator (PMSG)	Failure in stability and are difficult in fulfilling potential grid requirements. With an overall efficiency equal 80%

Y. Mastanamma , & D. Subbarayudu	2019	Permanent Magnet Synchronous Generator for Wind Energy Conversion Systems (WECS)	The paper presents Sliding Mode Control (SMC) Design for Variable Speed Wind Farm Systems (VS-WFS), which is based on and linked to an electrical network using the Permanent Magnet Sync Generator (PMSG).	Simulate of a Variable Speed Wind Farm System (VS-WFS) based grid-connected PMSG	The simulation results obtained show that the system has low efficiency. With an overall efficiency equal 79%
Y. Erramia et al.	2013	Control of a PMSG based wind energy generation system for power maximization and grid fault conditions	This project aims to control the strategy of the PMSG wind energy generation system, and Discusses back-to-back PWM converter control method.	New control strategy for WECS based on the PMSG.	The functionality of the proposed wind turbine simulator scheme is not validating, while in this system, the hybrid model will be validated to analyze the performance of the model. With an overall efficiency equal 89%
Arthur et al	2014	Permanent Magnet Synchronous Generator for a solar- wind power generation system.	This study aimed to design a Solar-wind hybrid system with an energy monitoring system.	Hybrid power storage system consisting of a super capacitor circuit and a battery connected to a Direct Current (DC) bus circuit.	The outcomes of the proposed system show this system obtained low efficiency.
Danapalasingam, La Cour-Harbo and Bisgaard	2009	Disturbance effects in nonlinear control systems and feedforward control strategy	This work focused on development of a feedforward control strategy for measurable disturbance rejection in general nonlinear systems with feedback control.	This study was based on proposing disturbance feedforward control through simulation	The control input constraint is to be included in the formulation and a robust feedforward control method should be investigated to include model uncertainties, inaccurate sensor measurements, etc. In addition, the existence of such a feedforward control solution and methods to obtain them should be studied. With an overall efficiency equal 82%
Achin a nd Georg	2015	On the design and tuning of linear model predictive control for wind turbines	This study on the design of linear model predictive control (MPC) for wind turbines, with a focus on the controller's tuning tradeoffs.	The system approach was proposed and tested via numerical simulations using a nonlinear turbine model.	While model predictive controllers can be effective in the proper situation, they have limitations that are generally not mentioned by the vendors marketing these controllers. Difficulties with operation, high maintenance cost, and lack of flexibility can result in fragile controllers that are not profitable. With an overall efficiency equal 79%

2.5 Summary

Overall, the cited journals and conference papers do relate to my works in wind turbine control research and development that focuses on wind turbine participation in frequency regulation for the utility grid. Many control strategies have been studied with the aim to improve the performance and power quality PMSG based wind turbines. Most of the research used different control to achieve the desire goals of their research. The PID controller was the most widely used controller and has occupied a dominant position in industrial process control systems for over 90 years. However, PID is far from perfect as an engineering solution. As a result, PID control may fall short of the performance requirements for complex systems[14]. If the system requirements cannot be precisely estimated or achieved, the designed PID gains may not resist the uncertainties and disturbances, and thus present low robustness. Due to its strong robustness and disturbance rejection, ADRC has been selected and applied in many fields such as motor systems, robotic systems, and structural vibration among others. However, the employment of ADRC into PMSG-based wind energy conversion systems is rather new. This project proposed ADRC controller to control wind turbine based on an extended state observer ESO. The results showed superior performance of ADRC controller over PI controller in all measures. Based on the summarized table 2.1, Furthermore, authors demonstrated by simulating their project in terms of to increase its ability to supply and regulate active and reactive power in both grid connected and islanding modes , the table summarizes the improvement and development each author produces based on previous discoveries. Even though, some authors achieved the objectives, others left a gap for new researchers to carry on where this project has come across one of the gaps to investigate and to improve an overall system performance .

CHAPTER 3

Modelling, Design and Simulation

3.1 Introduction

This chapter describes the mathematical modelling of the wind turbine and ADRC controller, and design of the simulation models. First, the mathematical equations for various system components of the wind turbine and ADRC controller are derived. The derived mathematical equations are then translated into equivalent state space representation form from which we develop the MATLAB/Simulink Simulation models for the wind turbine system and ADRC controller. The developed models are simulated in MATLAB/Simulink environment to validate the designs for the wind turbine and ADRC models.

3.2 Proposed System Architecture

Figure 3.1 shows the open loop diagram for the proposed system architecture, and Figure 3.2 shows the closed-loop diagram for the system architecture including the control sub-system. The entire system can therefore be divided into two namely the generation control and grid integration. The functionality of both systems is realized by power converters. There are three things that must be controlled in a PMSG based wind turbine system viz. the optimization of power generated by the PMSG at different speed levels, feedback of active and reactive power into the grid, and dc bus voltage for control of the back-to-back converter. The pitch controller driven by the optimal tip speed ratio, λ_{opt} , is responsible for MPP tracking of the turbine output power through control of the PMSG speed to ensure maximum power generation for the given wind speed.

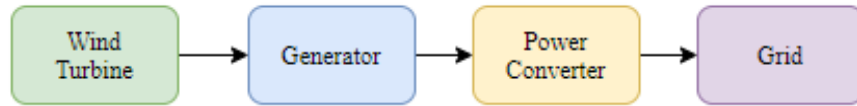


Figure 3.1: Proposed WECS architecture without the control subsystem

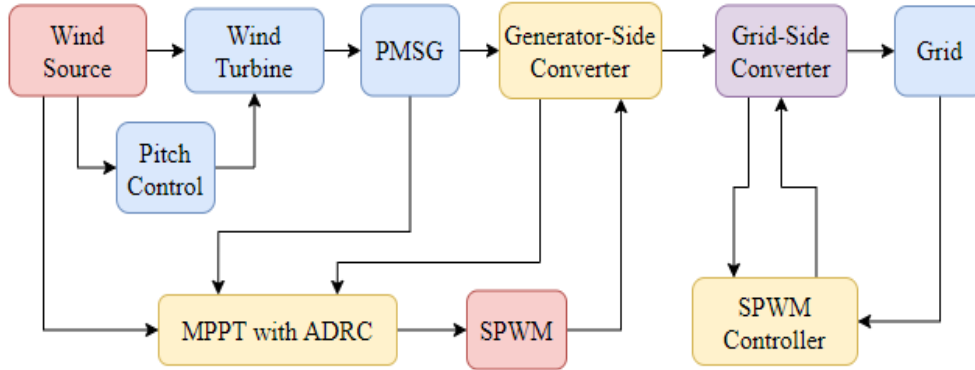


Figure 3.2: Proposed WECS architecture with the control sub-system

A permanent magnet synchronous generator couples to the turbine blades via the servo motor assembly. The turbine blades are driven into angular motion by the kinetic energy of the wind and the resulting momentum is coupled to the servo motors which in turn rotate at an angular velocity proportional to the applied momentum. So, by regulating the angular speed of the servo motors, the motion of the turbine blades and the PMSG can be controlled. The turbine blades have different optimum pitch angles for different wind velocities [78]. The pitch angle can be controlled by the servo mechanism to optimize the turbine output power during steady conditions and to protect the turbine at high wind speeds. When the wind is at cutting speed, the pitch angle of the blade is set to generate maximum energy at the rated wind speed, this ensures that the generator produces the expected electrical power as per rating specifications. The pitch angle increases at higher wind speeds to protect the turbine from damage due to high speeds. For any given wind speeds, the generator produces power with an unregulated voltage that has variable amplitude and frequency. This unregulated output voltage is regulated to pure DC voltage by the generator-side converter also known as machine-side converter (MSC) and the grid-side converter (GSC). Apart from voltage regulation, the GSC controls the active and reactive power injected into the utility electrical grid by the wind turbine system.

3.3 Wind Turbine Model

This section presents a comprehensive overview on wind power, wind-turbines and design thereof and the environmental impact of wind turbines. Wind turbines operating at low wind speeds

require high operational efficiency as opposed to those operating at high wind speeds. This research work focuses on regions with low annual wind speeds of less than 4 m/s such as Malaysia [79]. Malaysia has two weather seasons namely the southwest monsoon from May to September and the northeast monsoon from November to March. The wind speeds vary throughout the year based on the month and region. During the southwest monsoon, wind speeds are often below 7 m/s, but during the northeast monsoon wind speeds can reach up to 15 m/s, particularly in the east coast of the Malaysian peninsula. But in general Malaysia experiences low wind speeds.

3.4 Wind Power

Consider a block of air passing through some region of area A as shown in Figure 3.3, the kinetic energy of the air-packet is given as

$$E_k = \frac{1}{2}mv_w^2 \quad (3.1)$$

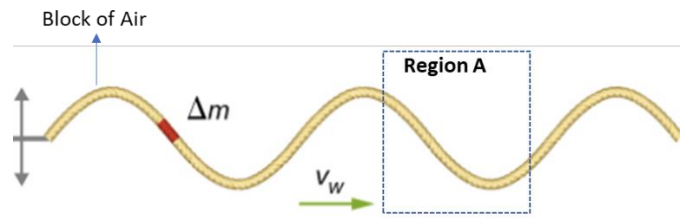


Figure 3.3. Block of air passing through some region A

Where Δm is the mass of the air packet and V_w is the velocity of the air packet. By intuition, the mass of the air packet cannot stay constant, but the wind speed can be assumed constant when it crosses the cross-section area. Wind power can therefore be defined as the rate of energy change over time, and it is given as

$$P_w = \frac{dE_k}{dt} = \frac{1}{2} \left(\frac{dm}{dt} \right) v_w^2 \quad (3.2)$$

Whereas the mass flow rate of wind can be defined as the product of air density, cross-section area and wind speed. Wind power is a function of cross-sectional area, air density and wind speed. At standard condition, assuming constant temperature and pressure wind power can be given as

$$P_w = \frac{1}{2} \rho A v_w^3 \quad (3.3)$$

Wind power is highly affected by the environmental and physical conditions. On the other hand, the environmental conditions affect air density, while physical conditions affect the cross-sectional area and the speed of wind [80]. Based on equation 3.4, air density is affected by ambient temperature and the height of the tower [81]. Where z is the height of the tower from ground level and T is the ambient temperature.

$$\rho = \frac{353.1}{T} \exp\left(-0.0342 \frac{z}{T}\right) \quad (3.4)$$

Wind speed is considerably affected by the height of the tower and the relationship between height of the tower and the wind speed can be expressed as

$$\frac{v_w}{v_0} = \left(\frac{H}{H_0}\right)^\alpha \quad (3.5)$$

Where α is the terrain factor and H_0 is the nominal height from ground-level (usually 10m) and v_0 is the velocity at H_0 . Based on the conducted literature review, the effects of density can be neglected in the design of wind-turbine, while the effect contributed by the height of the tower can be embedded in the design of the tower height.

3.4.1 Wind Turbine Design

Design of the wind turbine involves selection of the tower height and the wind turbine diameter based on the required output power. The relationship described by equation 3.3 gives the ideal quantity of wind power at standard conditions. However, the wind turbine cannot capture all the available power, so its efficiency can be expressed as

$$c_p(\lambda, \beta) = c_1 \left[\frac{c_2}{\lambda_i} - c_3 - c_4 \right] \exp\left(-\frac{c_5}{\lambda_i}\right) c_6 \lambda \quad (3.6)$$

Whereas the inverse of λ_i is given as

$$\frac{1}{\lambda_i} = \frac{1}{\lambda + 0.08\beta} - \frac{0.035}{\beta^3 + 1} \quad (3.7)$$

Thus, from equation 3.3 and equation 3.6 the actual power generated by the wind turbine can expressed as

$$P_w = \frac{1}{2} c_p(\lambda, \beta) \rho A v_w^3 \quad (3.8)$$

Solving for v_w in equation 3.5 and substituting the result into 3.8, assuming $H = D$, where D is the diameter of the wind turbine with $A = \frac{\pi}{4}D^2$, the power captured from the wind by the wind turbine is expressed as

$$P_w = c_p(\lambda, \beta) \frac{\pi}{8H_0^{3\alpha}} \rho v_0^3 D^{(2+3\alpha)} \quad (3.9)$$

Using equation 3.9 and assuming 50% efficiency, for $H_0 = 10m$, $\alpha = 0.245$ and $P_w = 2 \times 10^6W$, the diameter of the wind turbine is calculated and given as 204 m. However, this diameter is smaller in comparison to that of the Halide-X wind turbine, which is regarded as the most powerful offshore wind turbine built in the world today, with a rotor size of 220 m [82]. The Tip ratio speed (TSR) is calculated using the definition of c_p given by equation 3.9 and is given as 8.11. Based on the calculated TSR Value, the rotational speed of the wind turbine is expressed and given as

$$\lambda = \frac{\omega_T \left(\frac{D}{2}\right)}{v_w} = \frac{\omega_T D}{2v_w},$$

$$\omega_T = \frac{2\lambda v_w}{D} = \frac{2 \times 8.11 \times 2.8}{204} = 0.2226 \text{rads}^{-1}.$$

The rotational speed calculated above is quite low, therefore it should be increased. Assuming a gear ratio of 25, the new input speed to the shaft of the generator becomes 5.565rads^{-1} . By design, the PMSG is a synchronous generator with the relationship between its rotational speed and steady-state RMS back-EMF expressed as $V_{GEN} = K_v \omega_{in}$. For this research study, an RMS voltage of 600V is required for the design, therefore, $K_v = V_{GEN} / \omega_{in} = 107.8167V(\text{rads}^{-1})^{-1}$. Such a large value of voltage-constant can be realized by having large number of poles. Thus far, all the component values for the generator-side converter have been calculated. The performance coefficient, c_p , of the wind turbine depends on the mechanical output power of the turbine which is determined by wind power a function of wind speed, rotational speed, and pitch angle.

3.4.2 Pitch Angle Controller

The pitch-angle for the wind turbine blade is controlled using a servo mechanism to augment the turbine output mechanical force during a consistent wind-state and to secure the turbine during high wind speeds. This control mechanism is known as the pitch-angle regulator. At cut-in wind speed, the pitch-angle pitch point is set to generate power, while at low wind speed

it is set to deliver generated output power from the generator. At higher wind speeds, the pitch point increases thus preventing the wind turbine from over-speeding. Figure 3.4 shows the Simulink block diagram for the pitch angle controller. The controller output is a function of the wind-speed and the optimal TSR, $\beta_{opt} = f(v_w, \lambda_{opt})$. The controller input is the measured mechanical power, which represents wind speed. As the turbine power goes higher than its rated power, the pitch controller kicks in to regulate the turbine speed and thus turbine power.

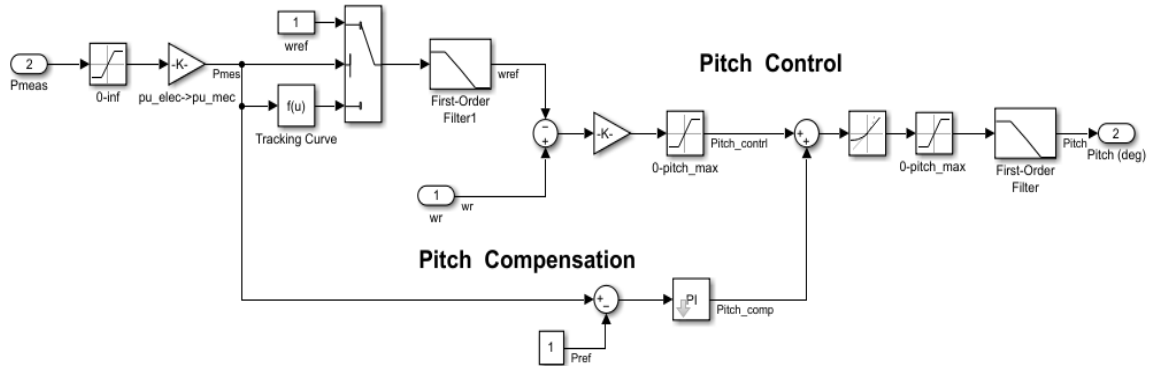


Figure 3.4. Simulink block diagram for the Pitch angle controller.

3.4.3 Wind-Turbine Operating Modes

DD-PMSG based wind turbines can operate over a wide range of speed. But based on the intensity of the wind, the wind turbine generator can be controlled to operate in three different modes as shown in Figure 3.5 viz parking mode, MPPT mode and constant power mode. The parking mode occurs when the wind speed is lower than the cut-in speed, the wind turbine will not rotate by staying in parking status due to the fact that the electrical power generated by the PMSG system is insufficient to compensate for the internal power losses. The wind turbine is kept in parking mode by a mechanical brake. The MPPT mode occurs at wind speeds greater than the cut-in speed when the wind turbine generates sufficient electro-motive force. Since the wind speed is moderately low, the power generated by the wind turbine is below its low value, therefore MPPT control is required to optimize the wind turbine operation. The MPPT mode ends when the wind speed is greater than the low wind speed, which is 12 m/s in this study. The constant Power mode occurs at wind speeds greater than the rated wind speed and when the generated system power becomes greater than the power generated when MPPT control is applied. The constant power mode increases the electrical stress on the PMSG, power converters and increases the risk of

damage arising from overvoltage. As a result, the cutting blade angle of the wind turbine blades should be controlled appropriately in the strong wind reach to keep the system working inside its appraised output condition.

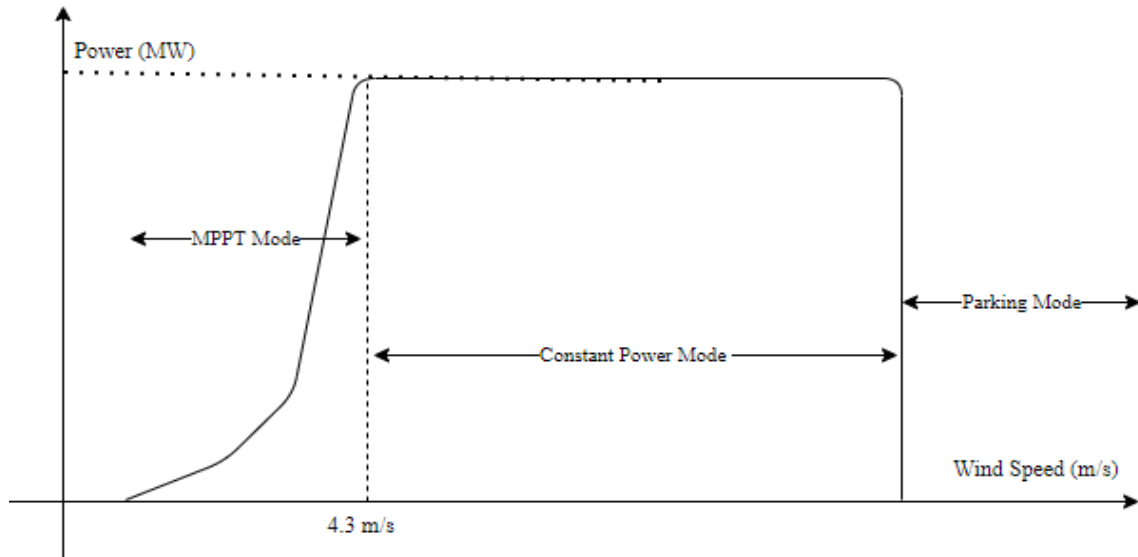


Figure 3.5. Wind Turbine Operating Modes

3.5 Permanent Magnet Synchronous Generator (PMSG)

PMSG defined as a variable speed wind turbine generator with a full-scale power electronic interface which have a super durable magnet to create an electro-magnetic field required for power generation. It does not require an outer power supply for excitation or a controllable rotor circuit. PMSG allows the generator to work at low speed without a gearbox. This decreases the weight and dimensions of nacelle equipment, mechanical losses in process as well as maintenance requirements. Unlike the induction generators, the gearbox demands regular replacement of oil, generates mechanical vibration and as a consequence decreases the overall stability of the system. A PMSG can contribute to the grid voltage support by producing more reactive power since it is interfaced with the power system by a full-scale back-to-back converter. These properties have made PMSGs to become popular, despite the fact that converter losses raise.

3.5.1 PMSG Modeling

The PMSG has 3-phase winding on its stators and approximately sinusoidally distributed magnets in the rotor. The magnetic materials used offer high power and harmonic density, thus,

such machines are finding frequency applications in modern systems. If a prime mover such as a wind turbine rotates the synchronous machine, 3-phase electrical voltages are produced which are given by

$$\begin{bmatrix} v_a \\ v_b \\ v_c \end{bmatrix} = \begin{bmatrix} R_a & 0 & 0 \\ 0 & R_b & 0 \\ 0 & 0 & R_c \end{bmatrix} \begin{bmatrix} i_a \\ i_b \\ i_c \end{bmatrix} + \frac{d}{dt} \begin{bmatrix} \lambda_a \\ \lambda_b \\ \lambda_c \end{bmatrix} \quad (3.10)$$

The parameters R_a , R_b and R_c are the stator phase resistances and the parameters $\lambda_{a,b,c}$ are the respective flux linkages. The flux linkages are defined as

$$\begin{bmatrix} \lambda_a \\ \lambda_b \\ \lambda_c \end{bmatrix} = \begin{bmatrix} L_{aa} & L_{ab} & L_{ac} \\ L_{ba} & L_{bb} & L_{bc} \\ L_{ca} & L_{cb} & L_{cc} \end{bmatrix} \begin{bmatrix} i_a \\ i_b \\ i_c \end{bmatrix} + \begin{bmatrix} \lambda_{am} \\ \lambda_{bm} \\ \lambda_{cm} \end{bmatrix} \quad (3.11)$$

The parameters L_{aa} , L_{bb} and L_{cc} are self-inductances, and the parameters $L_{ab} = L_{ba}$, $L_{bc} = L_{cb}$ and $L_{ca} = L_{ac}$ are the mutual inductances of the state circuit. The terms λ_{am} , λ_{bm} and λ_{cm} are permanent (PM) fluxes linking the stator windings. All the inductance and flux linkage variables are the functions of electrical angles. As the machine rotates their values change. This is the reason, perhaps, Parks transformation from rotatory reference frame to stationary reference frame is revolutionary. Parks transformation converts the above dynamics into more-easily understandable equations expressed as

$$\begin{aligned} u_d &= R_d i_d + L_d \frac{di_d}{dt} - N\omega i_q L_q \\ u_q &= R_q i_q + L_q \frac{di_q}{dt} + N\omega(L_d i_d + \lambda_m) \end{aligned} \quad (3.12)$$

The output torque to/from the machine is defined as

$$T = \frac{3}{2} N [i_q (L_d i_d + \lambda_m) - i_d i_q L_q] \quad (3.13)$$

The synchronous machine is designed to produce a root mean square (RMS) voltage of 600V, while delivering maximum power of 2MW.

3.5.2 Control of the Machine

The machine is coupled to a rectifier-fed boost converter, whose control is sometime dependent on the machine operation, but no specific control of the machine is needed if used in

generation mode. The machine will convert the supplied mechanical power to electrical power with variable-frequency.

3.6 Machine-Side Converter Control

The machine side converter is a cascade of 3-phase diode bridge rectifier and a dc-dc boost converter. Ideally, the diode rectifier produces a pulsating DC voltage waveform which is converted to pure dc voltage by dc-dc converter. The PWM control of the converter is realized by using active disturbance rejection control. This section begins with the description of the proposed research control technology, followed by the converter design and control implementation. The converter design is accompanied by the modeling and dynamic analysis of the controller.

3.6.1 Design of Generator-Side Converter

Figure 3.6 shows the converter circuit used for the design of the generator-side converter. The design of the rectifier involves selection of appropriate diodes such that the selected diodes can handle the expected rectifier current. Since the frequency of the sinusoidal input is not fixed, the diodes must also be capable of rectifying varying frequency AC power. The rectifier and the boost converter are linked by the capacitor which functions as the DC filter. The capacitor value is made high enough to obtain near DC regulated voltage. Practically, the capacitor cannot achieve near DC regulated voltage, so the boost converter is cascaded with it. The design of boost converter includes the selection of switching devices component values for the filtering elements.

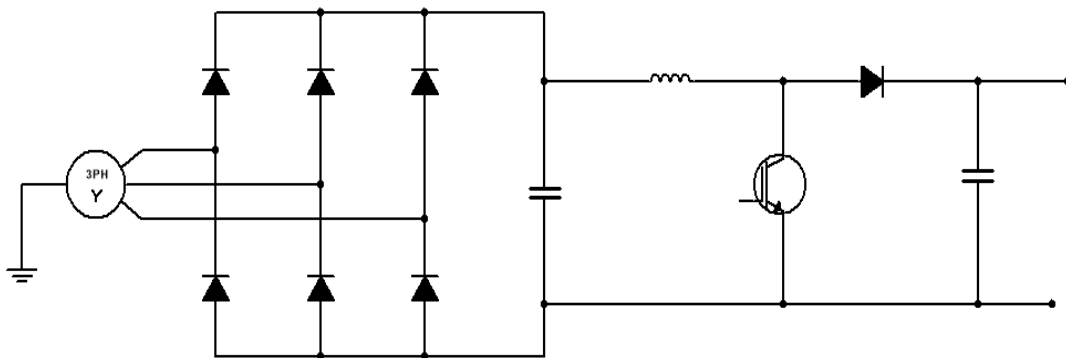


Figure 3.6. Rectifier-Fed Boost Converter

When the converter is operated under continuous-conduction mode, the value of the inductor peak-to-peak ripple current is expressed as

$$\Delta i_L = \frac{DV_{in}}{fL} \quad (3.14)$$

From equation (3.14) the required inductor value can be calculated by simply solving for L. Whereas, the capacitor ripple voltage across the capacitor is given as

$$\Delta v_c = \frac{DI_o}{fC} \quad (3.15)$$

While the average input and output voltages of the converter are defined as

$$V_o = \frac{1}{1-D} V_{in} \quad (3.16)$$

Given the input and out voltage specifications in table 3.1, the duty cycle D is calculated and given as $D = 0.25$. Using equation 3.14 – 3. 17, the respective boost converter parameters are calculated and listed in table 3.1. For the design of the boost converter controller, the control to output voltage transfer function of the boost converter is required. The boost converter transfer function is expressed as

$$\frac{V_o(s)}{d(s)} = \frac{-\frac{V_o}{(1-D)RC} \left(s - \frac{R(1-D)}{L} \right)}{s^2 + \frac{1}{RC}s + \frac{(1-D)^2}{LC}} \quad (3.17)$$

Table 3.1: Boost Converter Parameters

Parameter	Value	Parameter	Value
V_{in}	600V	V_o	800V
D	0.25	f_{sw}	3000 Hz
ΔI_L	25A	ΔV_c	0.8V
C	0.0781 F	L	100 μ H

3.6.2 Active Disturbance Rejection Control (ADRC)

The active disturbance rejection controller (ADRC), a novel control mechanism, was developed by researchers recently. The fundamental idea of ADRC is to use an extended state observer (ESO) to estimate the noise, disturbances, and the anomalies of a system. The ADRC controller directly suppresses this extended state, thus eliminating the control issues. ADRC has been effectively applied in many fields due to its robustness and strong disturbance rejection.

ADRC operating principle is based on error feedback control theory of the traditional PID controller and the advancement of the current control theory. ADRC is less subject to the exactness of the mathematical model of the controlled object and only relies on the order of the system. ADRC has the attributes of quick reaction, robustness, and adaptability. The original ADRC formulation was in the form of non-linear actions. Although the controller itself is very powerful for the generation of required performance, its tuning is extremely complex due to the large number of controller parameters. The tuning is typically dependent on human practices. Artificial intelligence, reasoning methodologies were employed to regularize the ADRC parameters, yet the tuning algorithm were not easily adoptable. Somehow the linear form of ADRC was found on which linear tuning methods such as arbitrary pole-placement, QR/LQG design methods, and optimization algorithms were easily applicable. In these methods, the number of parameters were decreased, which made the tuning process more sensible. Research results indicate that the linear ADRC still attained high performance and great robustness.

3.6.2.1 The selection ADRC design for project

The research project is restricted to the linear version of the ADRC. While tuning the ADRC parameters, the plant system could be non-linear or complex. When a single extended state is unable to predict the unknown behavior, it is suggested that we use the m^{th} - order ESO, while the value of m would still need to be determined. This scenario creates two challenges. Firstly, the order of the system becomes $n + m$, thus a state-feedback controller $n + m$ states is required. Since all the states are to be estimated, so, the computational cost of estimation and feedback control action become huge. Secondly, the value of m is unknown, so it needs to be determined based on the designer's experience and based on the trial-and-error method. These two issues pose a real challenge for the designer. But if the plant is linear with moderate complexity, up-to 2nd-order system, the ADRC's performance will be excellent. Since for such a system single order ESO would be enough. The implementation in this research project is a boost converter and when linearized it is a 2nd-order system. Thus, ADRC can easily be designed for the system.

Figure 3.7 shows the block diagram for the ADRC. ADRC is SISO-controller with input affine nonlinear dynamical system and with a well-defined Full Relative Degree (FRD).

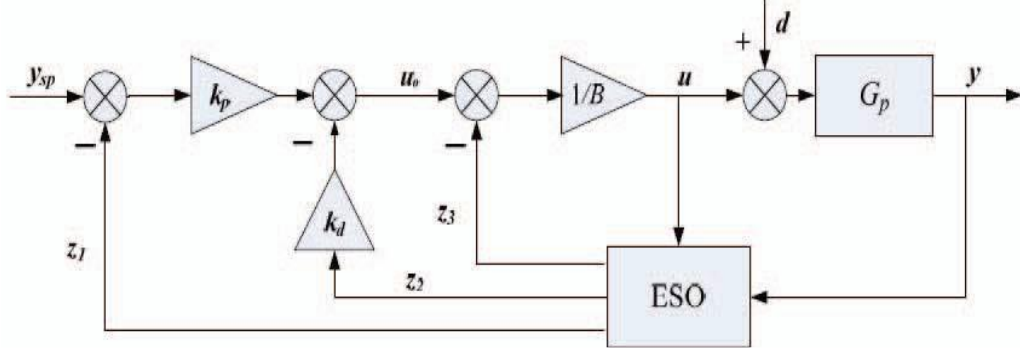


Figure 3.7. ADRC for a 2nd-Order System

The mathematical equation of the plant for the system in Figure 3.7 can be expressed in state-space format as

$$\begin{aligned}
 \dot{x}_1 &= x_2 \\
 \dot{x}_2 &= b_0 u + g(t) \\
 y &= x_1
 \end{aligned} \tag{3.18}$$

3.6.2.2 Extended State Observer (ESO)

The state observers are fundamental in control low design when the controller cannot read all the system states. In ADRC design, a state observer needs to have an extended state, which assesses the external disturbances and nonlinearities of the system. The ESO is considered as a third-order estimator for second-order nonlinear systems. Key to ESO formulation is to assume that a system with a differentiable nonlinear function $g(t)$ can be expressed as an expanded system as

$$\begin{aligned}
 \dot{x}_1 &= x_2 \\
 \dot{x}_2 &= x_3 + b_0 u \\
 \dot{x}_3 &= \dot{g} = D(t) \\
 y &= x_1
 \end{aligned} \tag{3.19}$$

whereas the system's input u is the control signal produced by the ADRC technique, the extended state is $x_3 = g(t)$, and its time-derivative is $D(t) = \frac{dg(t)}{dt}$. The matrix form of the above system is given as

$$\begin{bmatrix} \dot{x}_1 \\ \dot{x}_2 \\ \dot{x}_3 \end{bmatrix} = \begin{bmatrix} 0 & 1 & 0 \\ 0 & 0 & 1 \\ 0 & 0 & 0 \end{bmatrix} \begin{bmatrix} x_1 \\ x_2 \\ x_3 \end{bmatrix} + \begin{bmatrix} 0 \\ b_0 \\ 0 \end{bmatrix} u + \begin{bmatrix} 0 \\ 0 \\ 1 \end{bmatrix} D(t) \tag{3.20}$$

The ESO is expressed by using the extended system given by equation 3.20 and designing a Luenberger-like observer, which is given by

$$\dot{\mathbf{x}} = \mathbf{A}\hat{\mathbf{x}} + \mathbf{B}u + \mathbf{L}(y - \hat{y}) \quad (3.21)$$

The matrix given by equation 3.21 is the matrix of observer gains. It is clear that $\hat{y} = \hat{x}_1$, so the above system can also be written as

$$\dot{\mathbf{x}} = \mathbf{A}\hat{\mathbf{x}} + \mathbf{B}u + \mathbf{L}(y - \hat{x}_1) \quad (3.22)$$

3.6.2.3 Tuning Method of ARDC

If the observer can provide near to exact estimation of the states, then a control input can be defined as

$$u = \frac{1}{b_0} [k_p(r - x_1) - k_d x_2 + f(t)] \quad (3.23)$$

Using the control law in equation 3.20 we obtain

$$\begin{bmatrix} \dot{x}_1 \\ \dot{x}_2 \end{bmatrix} = \begin{bmatrix} 0 & 1 \\ -k_p & -k_d \end{bmatrix} \begin{bmatrix} x_1 \\ x_2 \end{bmatrix} + \begin{bmatrix} 0 \\ k_p \end{bmatrix} r \quad (3.24)$$

Equation 3.24 describes the dynamics of a closed-loop system. The selection of the controller parameters determines the dynamics of the whole system. Thus, the output to control transfer function form of the system can be expressed as

$$\frac{Y(s)}{R(s)} = \frac{k_p}{s^2 + k_d s + k_p} = \frac{\omega_n^2}{s^2 + 2\zeta\omega_n s + \omega_n^2} \quad (3.25)$$

3.6.2.4 Tuning of Control Parameters k_p and k_d

The control parameters are set using the closed-loop transfer function given by equation 3.25 and can be expressed as

$$k_p = \omega_n^2, \quad k_d = 2\zeta\omega_n \quad (3.26)$$

Whereas ω_n represents the control bandwidth, also known as the undamped natural frequency. As the settling time, t_s , and the overshoot are the principle dynamic performance factors. From the above analysis, it can be clearly seen that both k_d and k_p can be selected to design any kind control system with desired dynamics.

3.6.2.5 Tuning of Observer Parameters

For tuning simplicity, the proposed observer gains viz. $\beta_1, \beta_2, \beta_3$, can be expressed as

$$\beta_1 = 3\omega_n, \quad \beta_2 = 3\omega_n^2, \quad \beta_3 = \omega_n^3 \quad (3.27)$$

where ω_n is the observer bandwidth, thus making each of the three observer poles to be located at ω_n . The bigger the ω_n is, the sooner the disturbance is observed by ESO and declined by the controller. But ω_n cannot be excessively huge, or it will lie out of the stable region, particularly once the order of the closed-loop system is higher than two. To make the ESO function with small ω_0 values, it is important to locate a new approach to tune the observer parameters. The resulting transfer function between $z(s)$ and $f(s)$ is given as

$$\frac{z(s)}{f(s)} = \frac{\beta_3}{\beta_3 + \beta_2 s + \beta_1 s^2 + s^3} \quad (3.28)$$

However, the following facts are noteworthy:

- In the real control circumstance, low and middle frequencies are considerably more significant than high frequencies.
- In general, the coefficients of low and middle frequencies (β_3 and β_2) are much greater than the coefficients of high frequencies (β_1)

Only the first two terms in the denominator of equation 3.26 are often sufficient to identify the character that z_3 track f . Thus, we have

$$\frac{z_3(s)}{f(s)} = \frac{k}{s + k} \quad (3.29)$$

Where $k = \frac{\beta_3}{\beta_2}$. Based on the first-order system equation given by 3.27, the bigger the value of k is, the sooner the ESO responds, and based on the definition of the 2% setting time, we can get

$$T_t \approx \frac{4}{k} \quad (3.30)$$

where T_t is well-defined as the time taken for z_3 to track f . In general, the tracking time T_t of ESO would be smaller than the required setting time t_s of the system. Once k , the key parameter of ESO, is specified, we calculate ω_0 using rule of thumb as

$$\omega_0 = 4\omega_c \quad (3.31)$$

Then the ESO parameters $\beta_1, \beta_2, \beta_3$ can be calculated by using equation 3.26. For this research project, ESO is used in the ADRC to control the wind turbine energy system.

3.6.2.6 ADRC Design for the Converter

Any physical system that could be non-linear to some extent can be described as

$$y^{(n)} + f(t) = b_0 u \quad (3.32)$$

Assuming $n = 2$, a state-variable implementation of the system described by equation 3.32 can be given as

$$\begin{bmatrix} \dot{x}_1 \\ \dot{x}_2 \\ \dot{x}_3 \end{bmatrix} = \begin{bmatrix} 0 & 1 & 0 \\ 0 & 0 & 1 \\ 0 & 0 & 0 \end{bmatrix} \begin{bmatrix} x_1 \\ x_2 \\ x_3 \end{bmatrix} + \begin{bmatrix} 0 \\ b_0 \\ 0 \end{bmatrix} u + \begin{bmatrix} 0 \\ 0 \\ 1 \end{bmatrix} \dot{f}(t) \quad (3.33)$$

Where the 3rd state variable x_3 represents unknown disturbances/noises contained in $f(t)$. ADRC can actively reject $f(t)$ given $x_3 \cong f(t)$. Since x_3 is an extra-state, it must be estimated for the proper implementation of ADRC. The ESO performs the state estimation including the extra state with the observer dynamics described as

$$\begin{bmatrix} \hat{x}_1 \\ \hat{x}_2 \\ \hat{x}_3 \end{bmatrix} = \begin{bmatrix} 0 & 1 & 0 \\ 0 & 0 & 1 \\ 0 & 0 & 0 \end{bmatrix} \begin{bmatrix} x_1 \\ x_2 \\ x_3 \end{bmatrix} + \begin{bmatrix} 0 \\ b_0 \\ 0 \end{bmatrix} u + \begin{bmatrix} l_1 \\ l_2 \\ l_3 \end{bmatrix} (y - \hat{x}_1) \quad (3.34)$$

Equation 3.34 can be simplified and expressed as

$$\begin{bmatrix} \hat{x}_1 \\ \hat{x}_2 \\ \hat{x}_3 \end{bmatrix} = \begin{bmatrix} -l_1 & 1 & 0 \\ -l_2 & 0 & 1 \\ -l_3 & 0 & 0 \end{bmatrix} \begin{bmatrix} x_1 \\ x_2 \\ x_3 \end{bmatrix} + \begin{bmatrix} 0 \\ b_0 \\ 0 \end{bmatrix} u + \begin{bmatrix} l_1 \\ l_2 \\ l_3 \end{bmatrix} y \quad (3.35)$$

Equation 3.33 can be used to design the observe parameters. while defining a control law

$$u = \frac{1}{b_0} [k_p(r - x_1) - k_i x_2 + f(t)] \quad (3.36)$$

Inserting Equation 3.36 into 3.30 yields

$$y'' + k_i y' + k_p y = k_p r \quad (3.37)$$

Equation 3.35 can be used to obtain the ADRC parameters. On the other hand, parameters for ADRC, k_p and k_i and of ESO, l_1 , l_2 and l_3 can be computed using arbitrary pole-placement theory[84]. The ADRC controller will force the process/plant to track the desired control command and from the definition of ADRC's required differential equation based on equation 3.17 and 3.30,

$$v_o'' + f(t) = \frac{V_o}{LC} u \quad (3.38)$$

For the design of the ADRC control system, only average values for the output voltage, the filtering parameters L and C are required. The ADRC parameters and the observer parameters were calculated for a percentage overshoot of less than 5% and settling time of 2ms the damping ratio of the closed loop system will be 0.69, and the undamped natural frequency (using 2% settling-time criteria (Ogata 2010), $ts=4/\zeta\omega_n$) of 2898.6 rad/s. Thus, the dominant pair of poles will be

$$s_{1,2} = -\zeta\omega_n \pm j\omega_n\sqrt{1-\zeta^2} = -2000 \pm j2098$$

Now, the characteristic equation of the desired system will become $s^2 - (s_1 + s_2)s + (\text{Re}^2(s_{1,2}) + \text{Im}^2(s_{1,2})) = s^2 + 4000s + 8401604 = 0$. Comparing this equation with Eq. (13), the ADRC parameters and the observer parameters are found to be $k_p = 8.402 \times 10^6$, $k_i = 4000$. The ESO poles should further be pushed into negative complex plane, toward negative infinity. This will make quick estimation of required states. A simple criterion for the location of ESO poles is $s_{1,2,3} = (2 \sim 10) \times \text{Re}(s_{1,2}^{ADRC})$. It should be noted all ESO poles will be placed on negative real axis, to make the ESO response overdamped. Underdamped ESO can produce undesired overshoot in the estimated states. Overdamped ESO will give no overshoots in estimated states. In this work, $S^{ESO} = 4 \times \text{Re}(s_{1,2}^{ADRC}) = 8 \times 10^3$. The desired characteristic equation of the ESO becomes $s^3 + 2.4 \times 10^4 s^2 + 1.92 \times 10^8 s + 5.12 \times 10^{11}$. Thus, ESO parameters are found to be $l_1 = 2.4 \times 10^4$, $l_2 = 1.92 \times 10^8$ and $l_3 = 5.12 \times 10^{11}$. The wind turbine model is presented next.

3.6.3 Maximum Power Point Tracking Control

The concept of optimal power-point tracking is presented in this section along with the description of some conventional methods, followed by the method used in this research work project.

3.6.4 Optimal Tip Speed Ratio

The optimal tip speed corresponding to maximum power extraction is derived by defining the time taken for the upset wind to restore itself to the time taken for a rotor blade of rotational recurrence w to move into the position of its predecessor. At the point when the blades turn too quickly, they will be continuously going through turbulent wind. This can only be true if the cutting blades are continuously going through an area they previously went through. If the blades turn too slowly, then most of the wind will blow through the rotor without being caught by the blades. Therefore, it is required to allow enough time lapse between two blades going through a similar area so that new wind can enter. When the blades are moving too moderately, they will not catch all the wind they could, and if they are moving too fast, then the blades will be turning through violent wind[55].

For a wind turbine with three blades, it has been empirically observed that $\lambda_{opt} \approx 5.24 - 5.45$, but for the proposed system $\lambda_{opt} = 5.45$. The value of the tip speed, λ , is set by equation (3.39) and given as

$$\lambda = \frac{w_m R}{v} \quad \text{OR} \quad \lambda_{opt} = \frac{R}{v} w_{ref} \quad (3.39)$$

Where w_m is the angular speed of the wind turbine generator, R is the radio of the wind turbine's swept area, and v is the wind speed applicable to the system. We can now find the wanted value of the generator's angular speed for any assumed wind speed to continue the λ_{opt} and obtain the maximum power from the system. The measurement of the exact wind speed is difficult, so it is better to calculate the maximum power without determining the wind speed as follows,

$$P_{mppt} = \frac{1}{2} \rho \pi R^2 \left(\frac{w_{ref} R}{\lambda_{opt}} \right)^3 C_{Pmx} \quad (3.40)$$

From the wind turbine's model, $C_{Pmx} = 0.48$, $\lambda_{opt} = 4.2$, and $R = 87.5\text{m}$. Assuming these values are constant, the reference value of the turbine's rotational speed is expressed as

$$w_{ref} = v \frac{\lambda_{opt}}{R} = v \frac{4.2}{87.5} = 0.0481v \quad (3.41)$$

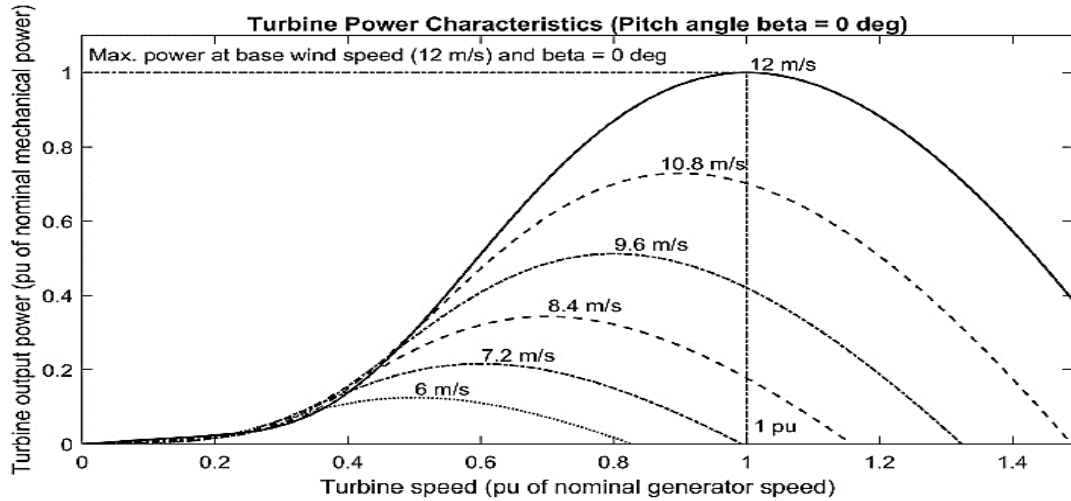


Figure 3.8: Turbine Power Characteristic with Maximum Power Point Tracking[81]

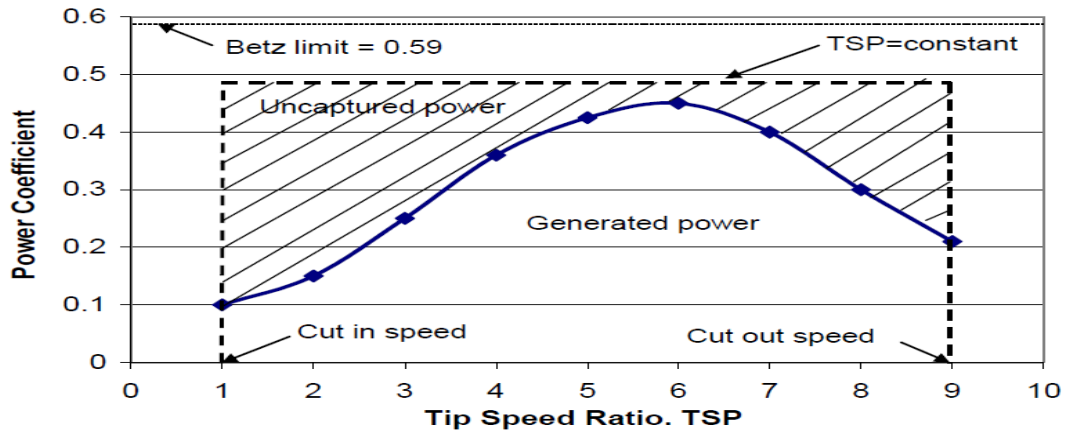


Figure 3.9: Power coefficient as a function of the tip speed ratio [55]

3.6.5 Tip Speed Ratio (TSR) MPPT

The optimal TSR for any given wind turbine is constant regardless of wind speed. When TSR is at optimum, the captured energy increases. TSR MPPT technique keeps energy change in a system constant by comparing the actual energy to the reference of the controller, thus changing the generator speed to avoid damage. Figure 3.9 shows TSR control technique. This technique is basic as the wind speed is easily and continuously estimated.

3.7 Control of Grid Side Converter

The main objective for the grid-side converter control is to regulator the active and reactive power fed into the electrical grid. The equation for the active and reactive power can be expresses as

$$P_g = \frac{3}{2}(v_{dg}i_{dg} + v_{qg}i_{qg}) \quad (3.42)$$

$$Q_g = \frac{3}{2}(v_{qg}i_{dg} + v_{dg}i_{qg}) \quad (3.43)$$

The d-axis and q-axis components of the grid currents and voltages are coupled in cross product fashion in the active power term which makes the active power and receptive power hard to control and diminishes the dynamic presentation of the grid side converter control. The PWM regulator delivers the gate pulse to the load side inverter. The corresponding gain for the voltage controller is 8, while the gain for integral controller is 400.

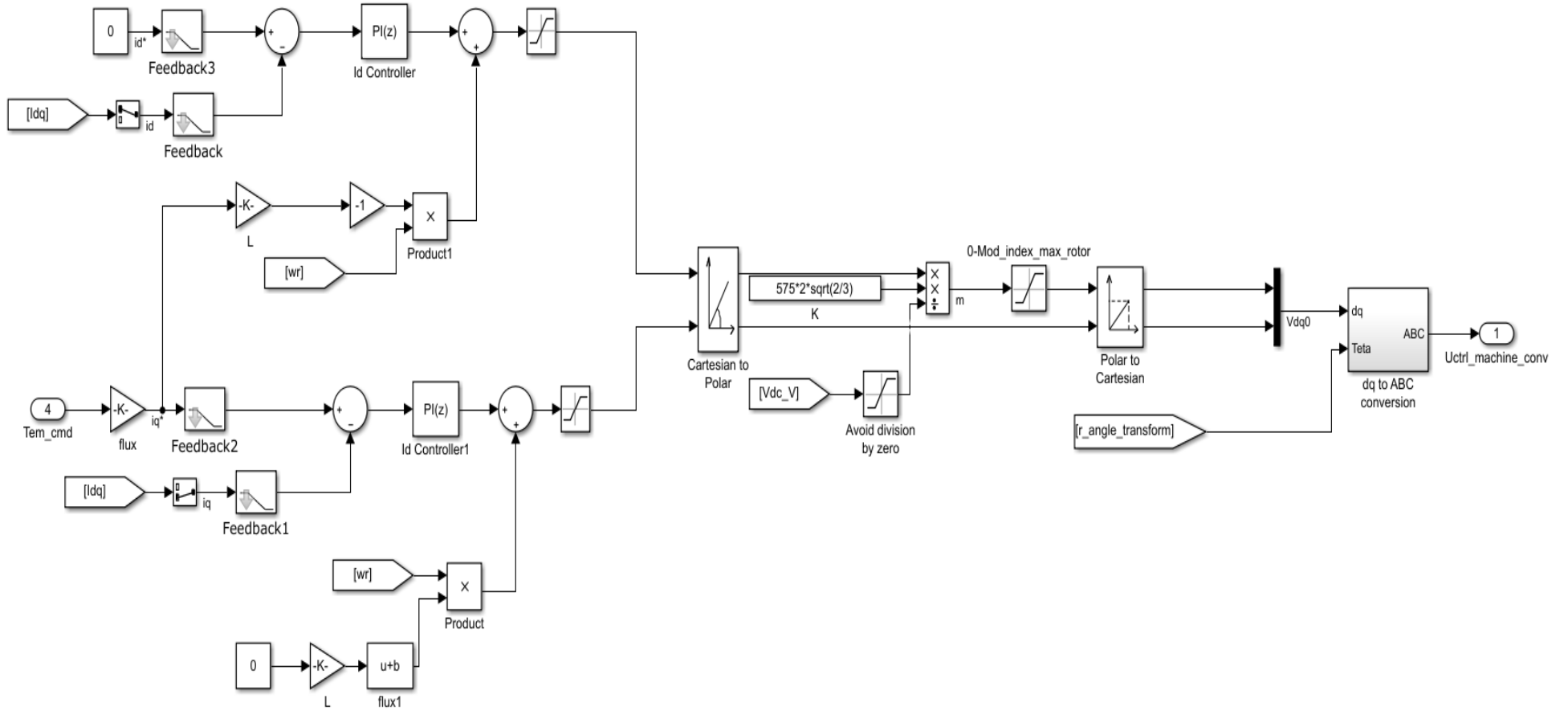


Figure 3.10. The machine side converter controller

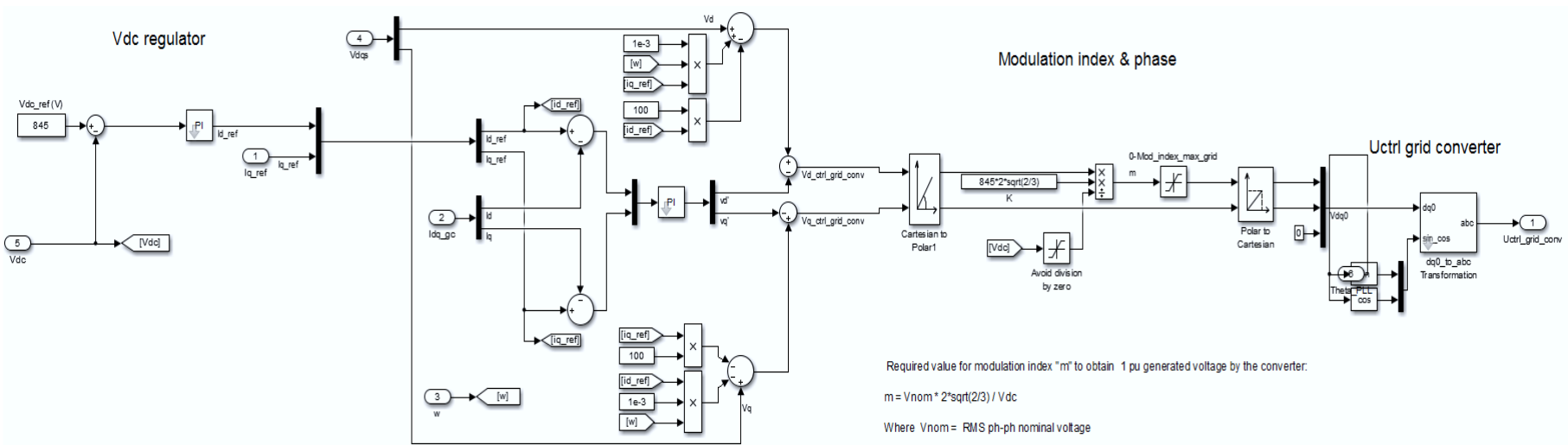


Figure 3.11. Current regulator for the grid side converter controller

3.8 Analysis testing

As shown below in Figure 4.2, the simulation was carried out with MATLAB/SIMULINK in order to validate the control strategy studied in this work. The system consists of several blocks, for example wind Source, wind turbine, PMGS, machine side converter, grid side converter, pitch control, MPPT, grid with its parameters, and controllers based on the ADRC and PI approach. All parameters are given in Appendix. To extract the maximum wind energy of the wind speed, an MPPT strategy is adopted. In order to maintain the DC-link voltage constant, a control of the grid side converter is necessary. This technique is based on the control of direct and quadratic grid currents and ensures also an exchange of active and reactive powers between the stator of the PMSG and the grid. To attain the unity power factor, it's necessary to regulate the grid reactive power to its desired value.

3.8.1 Test of robustness

In order to investigate the robustness of the proposed ADRC control, two cases were selected in which we have changed the internal parameter of the PMSG. In the first one, an increase of the 50% of the stator resistance nominal value is applied. To verify the validity and performance of the converter design and controller, the runtime for the simulation model is set to 0.1. The set-point voltage for the controller was set to 800V as shown in figure 4.8. Thus, even in the presence of loading, the ADRC controller has successfully tracked the available power while regulating the DC voltage. The controller regulated the output voltage at the desired voltage level and tracked the wind turbine output power. The results obtained with ADRC controller indicate improvement in system performance. The results of a comparison between ADRC and PI controllers. It can be noticed that the characteristics have been regulated to its reference value. ADRC controllers present excellent performances with good efficiency, smaller overshoot in the reactive power of grid and DC bus voltage, fast response, smaller overshoot in the reactive power of grid and DC bus voltage, fast response.

3.9 Validation

Since the performance of wind turbines is significantly affected by the used control strategy, considering new control strategies that can improve the controller performance of the WECS and motivation to use, adapt. To validate the theoretical study and the effectiveness of the presented control strategy (ADRC), the implementation of PMSG WECS based on ADRC controller is simulated under MATLAB/Simulink environment. The simulation parameters are given in appendix. The model is validated by simulation results presented by Laghrifat *et al.*, [37]. The model achieved 98.65% efficiency compared to that presented by Laghrifat *et al.*, which achieved an efficiency of 88%. The modeling and simulation of the PMSG wind energy conversion system with active disturbance rejection control is carried out in this thesis. Obtained results indicate system robustness, high performance, good regulation and stability against internal and external disturbances compared to the system in [37], which has high kernel ESO function suggesting inaccurate system model and which makes it difficult to estimate the total disturbances. For performance results for our PMSG simulation model were compared to the performance measurement of the PMSG in [56], which is based on the sliding mode control (SMC) system design for variable speed wind systems. This approach which can be augmented by advanced optimization techniques with several control mechanisms to enhance the performance. Furthermore, the results validate the robustness of the proposed control technique over other controller in terms of stability, precision and robustness against internal disturbances.

3.10 Summary

This chapter presented the mathematical modelling of the wind turbine and ADRC controller, design of boost converter, inverter modeling and control, optimal tip speed ratio, and power output from the System, design and implementation of the MATLAB/ Simulink simulation models for the wind turbine system, ADRC controller and converter .

CHAPTER 4

Results and Discussion

4.1 Introduction

This chapter covers the discussion of the simulation results for the developed MATLAB/Simulink wind turbine model based on the ADRC controller. The advantages and disadvantages of the modeled system versus the actual system implementation are also addressed. Relevant graphs showing key simulation results and the efficiency for the overall wind turbine system based on the ADRC controller are also presented.

4.2 System Implementation

Based on the established mathematical model for the wind turbine and controller, an equivalent Simulink model is constructed and implemented in MATLAB/Simulink environment. Existing Simulink libraries are used to build the model sub-systems and optimal system parameters are used for simulation to mimic the actual physical system.

4.2.1 Wind Turbine Model Settings

Figure 4.1 shows the wind turbine subsystem model. The model transduces the wind energy to mechanical rotational energy. The core model inputs include wind speed (m/s), pitch angle and the generator speed which is used for pitch control mechanism. The system efficiency c_p , is given as $P_w = \frac{1}{2} c_p(\lambda, \beta) \rho A v^3$. The system output torque from the turbine is determined by P_w/ω_r (where ω_r is generator speed). All calculations are given in pu units. The wind turbine model in Simulink library offers the option to enter most of the settings specified for an actual system such as power, wind speed etc. The model has wind speed as the input and produces torque as the output. The unit used for torque is pu. The operating principle for the wind turbine model can be understood by use of Figure 4.1. Figure 4.2 shows the block diagram representation of the complete system in Simulink environment consisting of the wind turbine, converters and ADRC controller. The model was derived using equations 3.36 – 3.38 which describe power generation of a wind turbine

However, the model produces torque as the output as opposed to the output equations which define the output as power. The power produced by the wind turbine is the product of torque and speed.

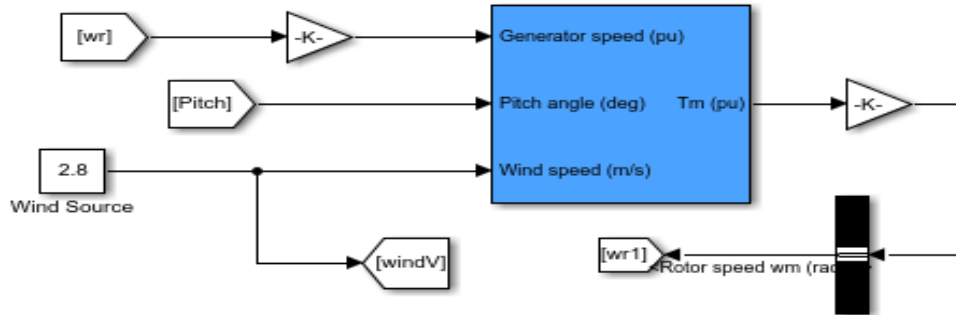


Figure 4.1. Wind turbine model.

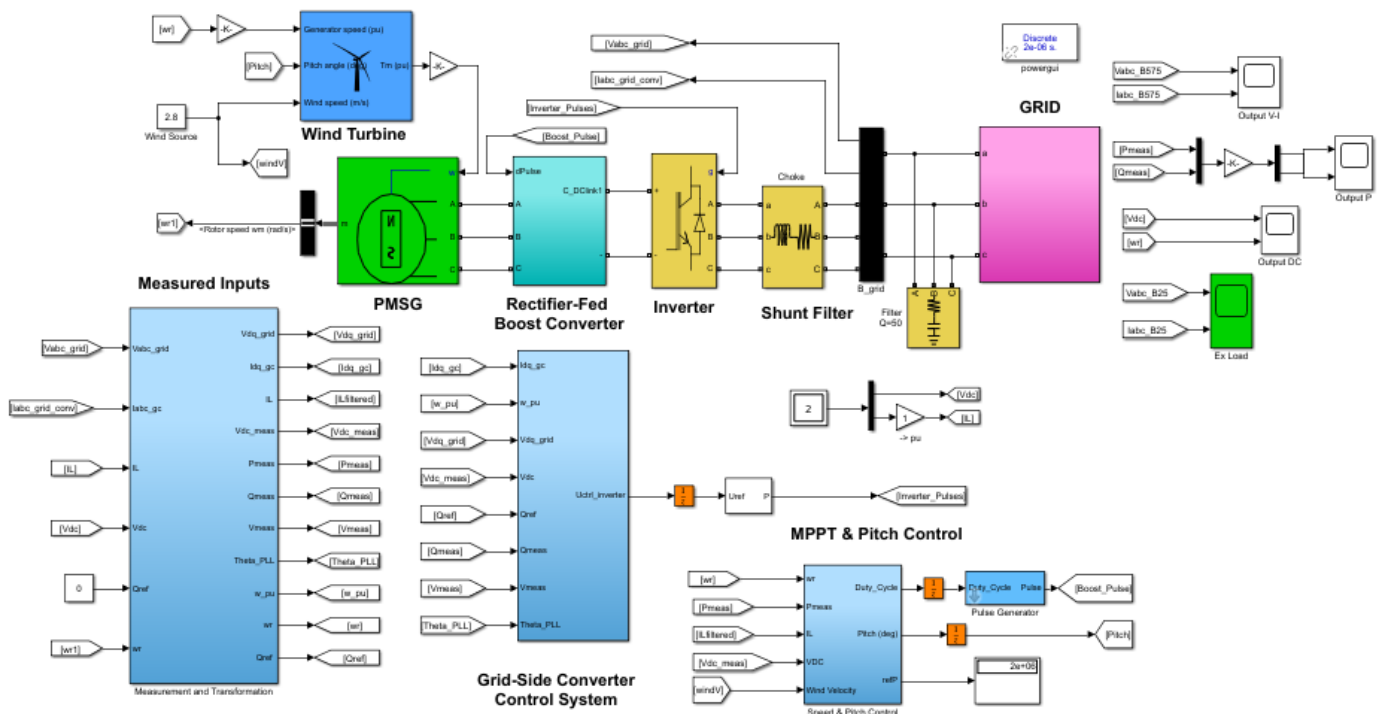


Figure 4.2. Block diagram representation of the wind turbine system and ADRC controller

4.2.1.1 Measurement Inputs Block

Figure 4.6 shows the subsystem for the Simulink measurement input block. The subsystem has two major purposes. Firstly, it filters any noise in measured signals and secondly it performs the transformations necessary for a 3-phase system to allow implementation of control actions. Performed transformations include rotational reference (a-b-c) frame and stationary reference (d-q-0) frame. The 3-phase input voltage and current measured at the interface of 3-phase inverter and the grid are converted to dq0-frame and used to control the switching of inverter devices. The inductor current from boost converter and the dc voltage at the interface of boost converter are filtered and used to control operation of the boost converter switching devices. Q_{ref} is the constant reference input Q-power. The last input is speed, also filtered, and is used to make some control and transformation signals. The output signals include the dq0 voltage and current, inductor current, dc voltage, the R and Q-powers, 3-phase voltage computed using transformations, speed and reference Q-power.

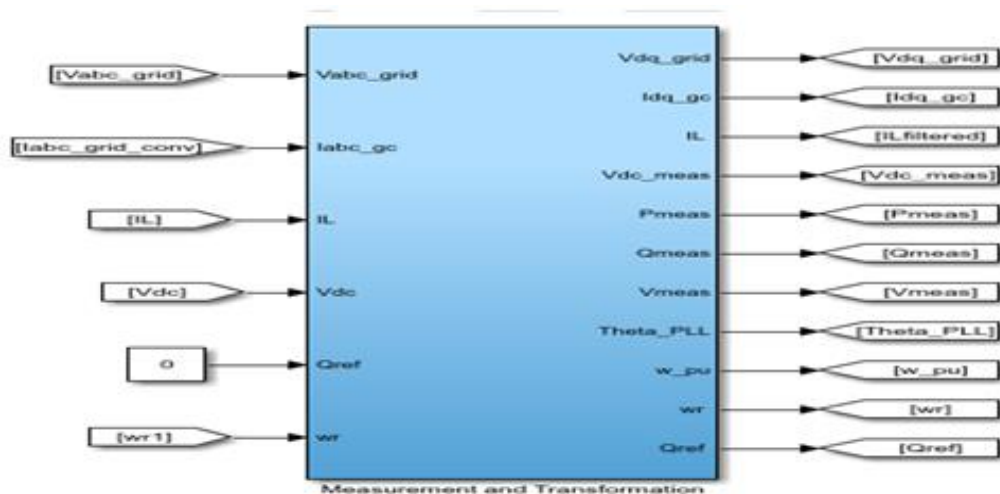


Figure 4.6. Measurements and transformations block.

4.2.1.2 Back-to-Back Converter

Figure 4.7 shows the back-to-back converter. As shown in the Figure, the input to the rectifier is the output from the PMSG which is regulated by the boost converter, and the output of the inverter is connected to the grid. The output of the boost converter is converted into 3-phase

regulated voltage/power by the three-phase converter. The inverter requires fixed dc voltage irrespective of the switching action occurring within the inverter. Thus, the switching control must cater for all anomalies. Such complex switching requirements, need a robust controller such as the ADRC. The ADRC controller not only offers the best control action, but it also mitigates for nonlinear behavior. The ADRC control action is aided by ESO which estimates the system's states along with an extra state. The extra state represents noise, disturbances, and any nonlinear behavior. The system's own states are used to form the feedback control, while the extra state is directly reduced to stop the transmission of its effect in the control action.

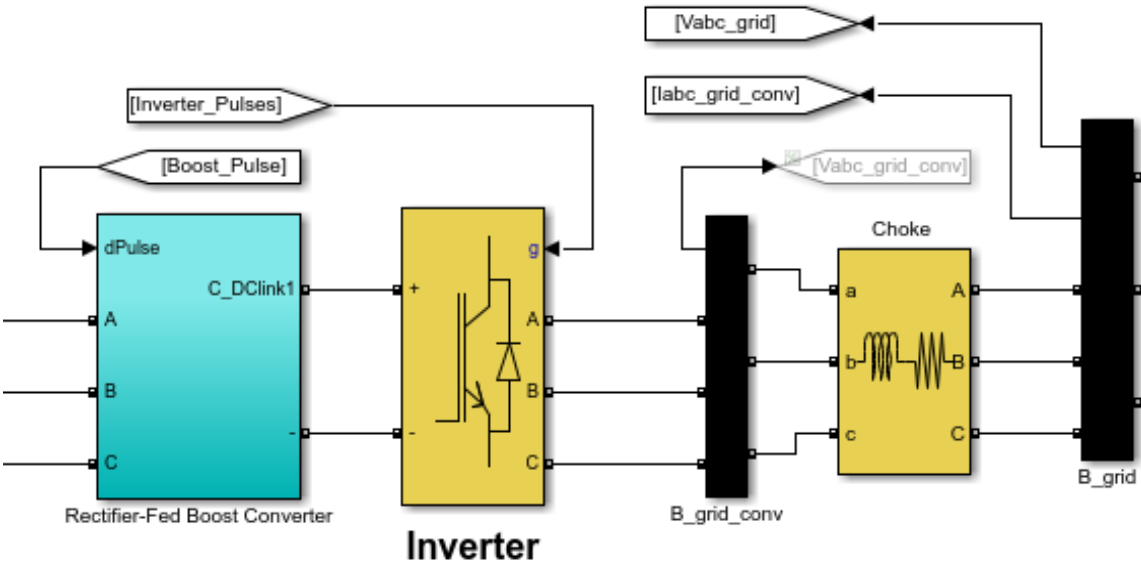


Figure 4.7. Back-to-Back Converter.

4.2.1.3 System load

Figure 4.8 shows the WECS load. The voltage is first stepped-up before transmission and feeding to the load.

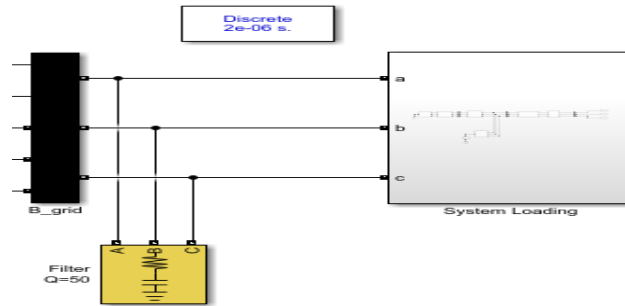


Figure 4.8. WECS Load.

4.2.1.4 Speed Regulator and Pitch control

Figure 4.9 shows the speed regulator and pitch control block. It provides control and generates the switching pulses for the boost converter. The pitch angle is generated based on the three operation modes of the turbine indicated on the turbine characteristic curve. The first operation mode is the MPPT mode, which occurs when the wind speed lies between cut-in speed and rated speed. The pitch angle is zero for this mode. The second operation mode is the constant power mode, which occurs when the wind speed exceeds the rated speed. During this mode the pitch angle is proportional to the wind speed and turbine output power remains constant. The third mode of operation occurs when the wind speed exceeds the maximum allowable limit, and the turbine is locked during this mode to save it from damage.

Speed Regulator & Pitch Control

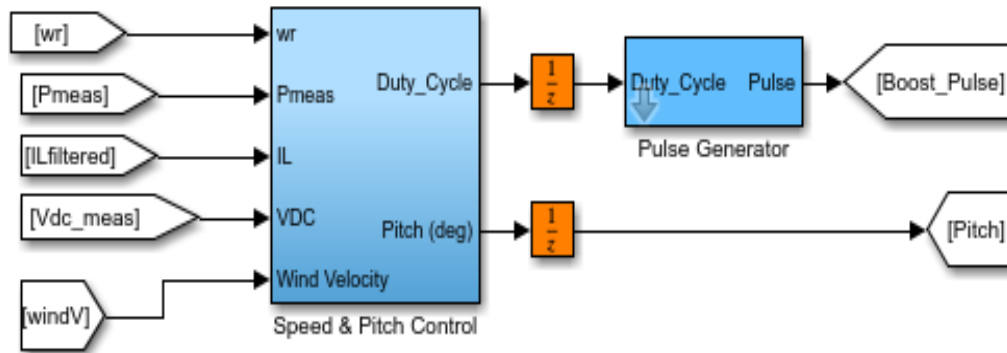


Figure 4.9. Speed regulator and pitch Control

4.2.1.5 Generator Settings

Figure 4.10 shows the PMSG model. The generator converts the rotational mechanical energy or torque of the wind turbine to electrical energy. The generator can operate on variable rotational speed to produce variable output voltage and frequency. The PMSG is configured to operate as 3-Phase machine producing 3-Phase sinusoidal back-EMF. These settings are selected because in practical machines PMs are distributed on the rotor such that the flux is distributed sinusoidally along the rotor surface. However, the power circuit parameters are set to default values, while the number of pole-pairs is set to 24 due to low generator input speed of about 5 rad/sec. This results in huge Back-EMF constants.

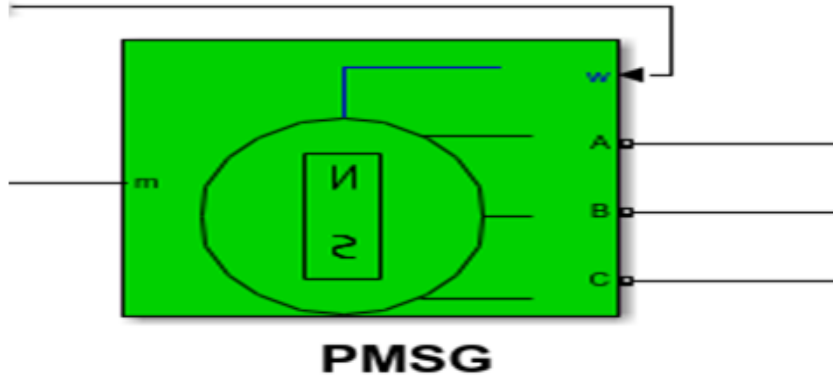


Figure 4.10. Permanent Magnet Synchronous Generator.

4.2.2 Generator Side Converter Settings

The generator side converter consists of a cascade of 3-phase diode rectifier and boost converter. The diodes for the 3-phase rectifier circuit are set to operate as ideal components with nominal forward voltage drops. The component values for the boost converter are calculated using the converter equations in chapter 3 and given in table 3.1

4.2.3 Grid-Side Converter

The grid-side converter consists of 3-leg converter formed by IGBTs that have diode for blocking reverse current. The output section of the converter consists of an RL circuit and shunt filter. The converter is implemented with its own controller and together with shunt filter produces the required 3-phase power and voltage. The inverter control is complex, and it is implemented using PI controllers. Q_{ref} and nominal dc voltage are the set-points for the inverter. The PI controller uses these set points to produce the reference d-axis and q-axis current and compares them with the grid current. The error signal is used to generate the d-axis and q-axis voltage and the inverter switching pulses are generated by comparing the two voltages. These control actions

produce the desired 3-phase sinusoidal voltages. The inverter is connected to the conventional grid with conventional power sources and loads.

4.3 Discussion of Simulation Results

Simulation results are obtained by running the developed MATLAB/Simulink model over distinct periods. The model is run for a total simulation time of 2 seconds at a nominal wind speed of 4 m/s for the first 1 second, then a disturbance is introduced at 1 second to reduce the speed to 3 m/s. For the given speeds, the model is designed to yield an output power of 2 MW. But according to Betz's law, the estimated maximum energy production based on the system design parameters could reach 1.186 MW [83]. The captured graphs indicate key waveforms for the system dynamic response, system response to transients and steady state performance. To illustrate the performance advantages of the proposed ADRC controller over the conventional PI controller, a comparison of the active and reactive power results for the system as well as the output voltage of the boost converter is carried out for the two control algorithms.

4.3.1 Performance of Generator-Side Converter

Figure 4.11 shows the waveforms for the output voltage of the boost converter and shaft speed of the PMSG with the ADRC controller and PI controller. The generator-side converter controller is designed to have minimal overshoot and settling time for improved regulation performance. To verify the validity and performance of the converter design and controller, the runtime for the simulation model is set to 0.1 and 0.2 seconds respectively. The controller regulated the output voltage at the desired voltage level and tracked the wind turbine output power. Results indicate a settling time of 0.03 seconds and an overshoot of 5% for the output voltage. A comparative analysis for the results obtained with ADRC controller indicate improvement in system performance as opposed to those obtained with the conventional PI controller shown in Figure 4.11.

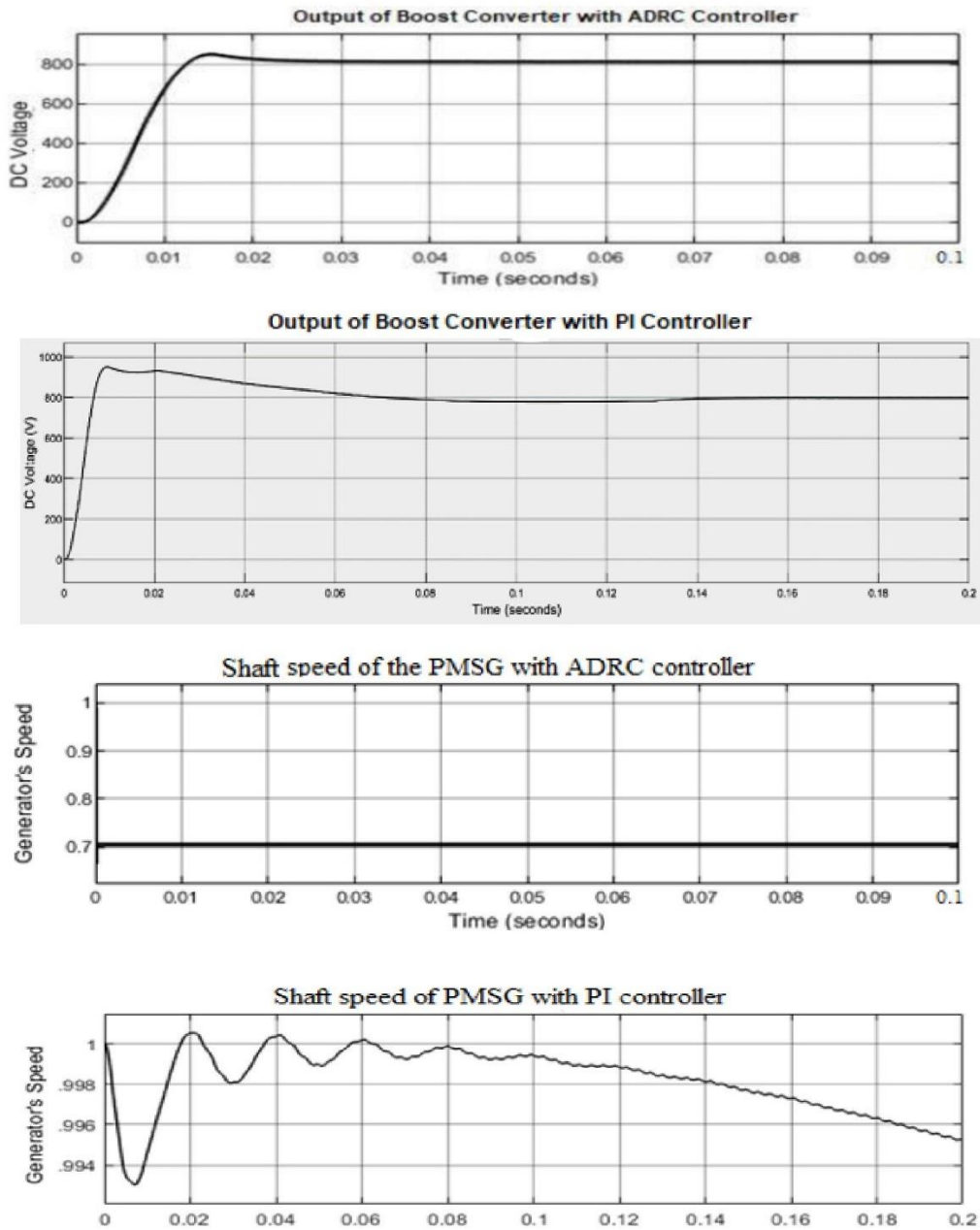


Figure 4.11. Output voltage of boost converter and shaft speed of the PMSG with ADRC controller and PI Controller.

Figure 4.12 shows the comparison of apparent power output versus real power output for the system with ADRC controller. At start up the system has high apparent power, but this reduces

to nearly zero as the system real power output reaches steady state at around 0.5 second with an output an of output of 1.17 MW.

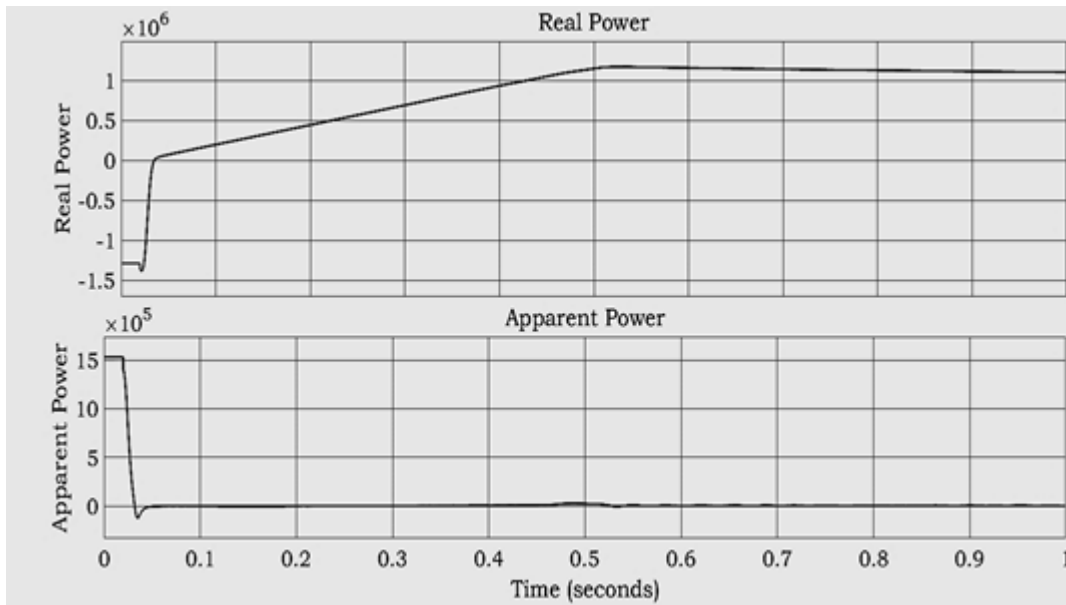


Figure 4.12. Comparison of system apparent power output versus real power output with ADRC controller

Based on figure 4.12 the results provided show clearly the feasibility and the effectiveness of the proposed controller techniques. It presents a good characteristic, excellent output from the ADRC control comparing with PI command especially in terms of robustness and reference tracking.

4.4 Performance of Grid Side Converter

The performance of the grid side converter is evaluated under different loads. The transient and steady state response of the system are analyzed under different loads to establish its performance. The output of the designed wind turbine system is connected to a 32 kV grid system. It is assumed that the grid also receives power supply from conventional power sources. A load disturbance was added to the simulation models. Figure 4.11 and 4.12 shows output waveforms for the system with ADRC control, while Figure 4.12 and Figure 4.13 shows the output waveforms for the system with PI control. The results show that the ADRC controller achieves output

regulation for the converter output voltage and current and responds promptly to disturbances without losing output regulation. On the other hand, results for the PI controller show that PI control is inadequate to produce the desired system performance specification e.g., in Figure 4.12 the system output power approaches its steady state design value of 1.187 MW with ADRC control, while in PI controller produces a high steady-state error and the power stability is very poor due to the generate of sinusoidal power has almost been drastic, also the starting dynamics are unacceptable as indicated in Figure 4.13 below.

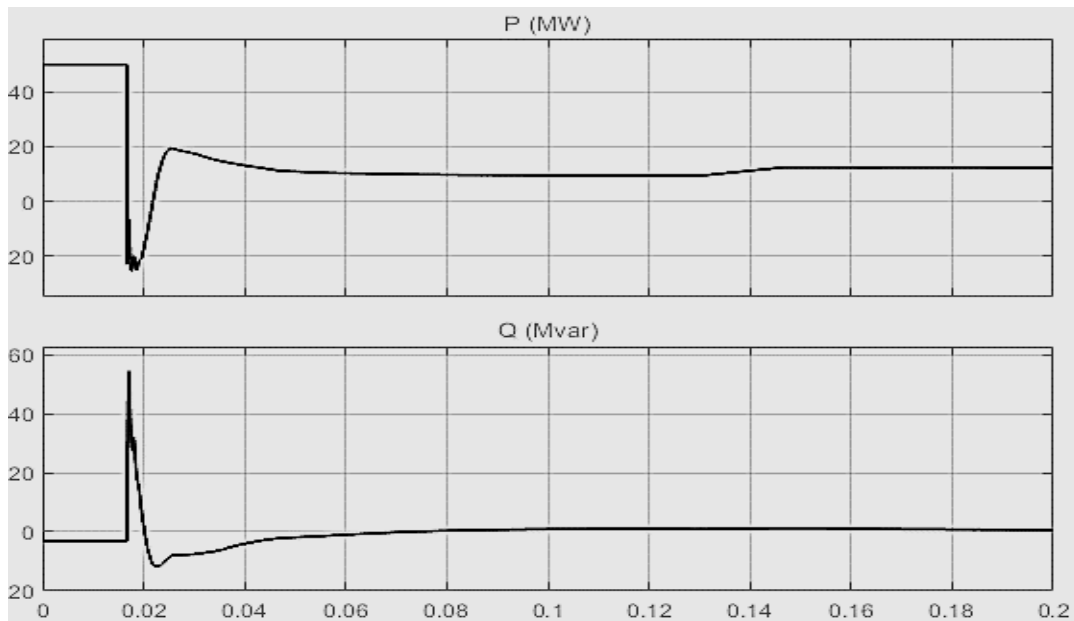


Figure 4.13. Comparison of system apparent power output versus real power output with PI controller

Figure 4.14 shows the unfiltered 3-phase output voltage and current (pu) measured at the inverter output, and Figure 4.15 shows the filtered 3-phase voltage and current measured at the load. Load regulation refers to the ability to maintain a constant voltage output from a power supply despite changes or variability in the input load. A comparative analysis of the two graphs shows that the LC filter was effective in smoothening the inverter output voltage and current and frequency stability was also achieved. Figure 4.16 shows results for the output voltage and current at the load with the PI controller. The results with PI controller indicate poor load regulation in

comparison to results with ADRC controller, this implies the ADRC control is superior to PI control.

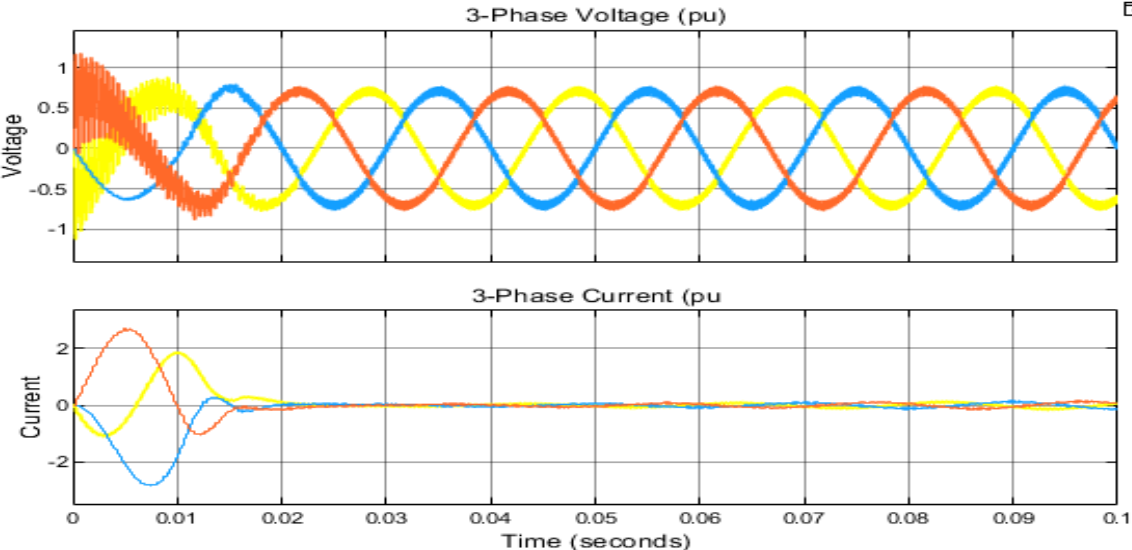


Figure 4.14. Unfiltered 3-phase output voltage and current (pu) at inverter output

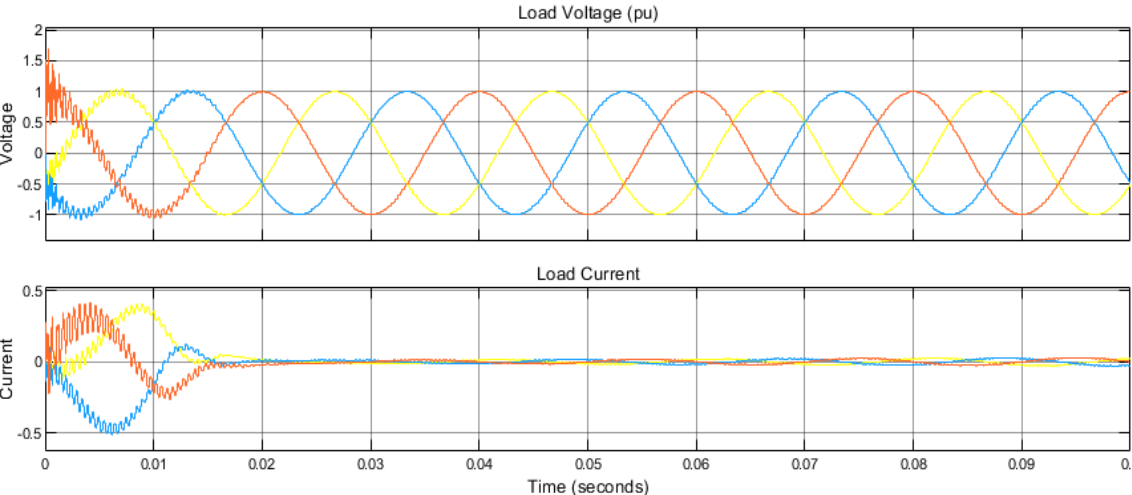


Figure 4.15. Filtered 3-phase output voltage and current (pu) at the load with ADRC controller.

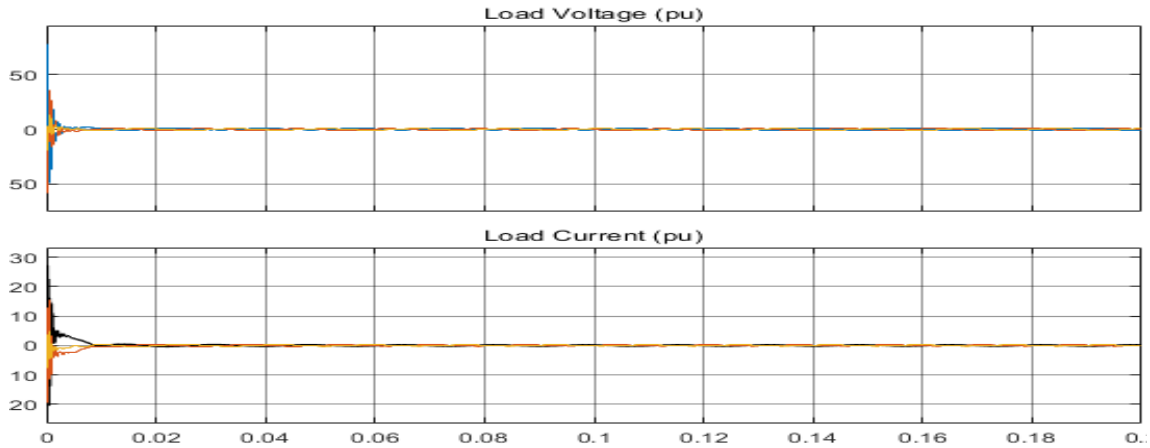


Figure 4.16. System Load voltage and current (pu) with PI controller

Table. 4.1 Comparison table of PI, PD and PID

Controller	Rise Time	Settling Time	Percentage Overshoot
PI	18.181 msec	27.521 msec	17.003%
PD	16.602 msec	22.551 msec	22.353%
PID	12.213 msec	30.250 msec	18.572%
ADRC	4.187 msec	7.252 msec	5.46%

Table 4.1 represent the comparison between the performances of PID controllers and the ADRC can be seen in the above table. If the PID controllers are compared with each other, PI looks better in terms of percentage overshoot, but is slower than PD or PID in terms of rise-time and settling time. ADRC has outperformed all the PID controllers in terms of speed and relative overshoot. Thus, if the ADRC is adopted in rea-time systems, it will be making the system performance better.

4.4.1 Results Summary

This chapter presented the discussion of the simulation results for a PMSG based WECS for two controllers viz. ADRC controller and PI controller. The obtained simulation results show that

the ADRC controller has better response to disturbance sensitivities, it is robust therefore less prone to the parametric variations of the PMSG than compared to the PI controller which has slower transient responses and other undesired behaviors. These results correlate to the projected performance of the controllers as indicated in the literature review. Furthermore, results for the proposed ADRC controller show that the system achieved the expected performance with the maximum simulated output power of 1.17 MW compared to the Betz theoretical value of 1.186MW. The system achieved an overall efficiency of about 98.65% with excellent performance in terms of stability, precision and robustness against internal disturbances.

4.5 Research Project Contributions

The modeling, design and simulation of a PMSG based WECS with ADRC control has been presented. The modeling and design of the developed PMSG of WECS and ADRC controller model has been validated with simulations results. Obtained results indicate higher system efficiency for ADRC controller in comparison to most existing controllers and high system performance, system robustness, high performance, good regulation and stability against internal and external disturbances compared to the system by Laghridat [37]. The results also show improvement in system performance with proposed controller, which is validated by constant DC voltage at the interface of the generator-side and grid-side converters and achieves maximum power compared to the controller presented in [66]. Lower power coefficient and lower turbine power with a speed ratio below optimum were also observed from the simulation results. The developed model achieved around 98.65 % efficiency, an improvement of about 10 % in comparison to the ADRC control based PMSG WECS presented by [37]. which achieved 88 % efficiency. However, the overall performance evaluation of PMSG could be improved by studying the maximum power point tracking (MPPT) and the control of the pitch angle for improving PMSG performance. Performance results for the proposed PMSG simulation model were compared to the performance of the PMSG in[56], which is based on sliding mode control (SMC) system design for variable speed wind systems. It was observed that the proposed model has higher efficiency than the system.

CHAPTER 5

Conclusion and Future Recommendations

5.1 Conclusion

The main objective of the research project was to improve the performance and modelling of robust controller for the wind energy conversion system (WECS) based on permanent magnet synchronous generator (PMSG). Most wind energy conversion systems are classified as fixed-speed systems. Until the arrival of PMSGs recently, there were very few to no wind turbines that could be used for energy conversion of variable wind speed to the equivalent electrical energy. PMSGs are based on synchronous machines and are the most common generator for wind power conversion systems. Several types of generators for wind energy conversion systems have been presented in this work including their pros and cons. The study also presented various power electronic converters and inverters that can convert variable wind generated power into constant electrical power in accordance with grid standards. It was also observed from the simulation results that although the use of PMSG simplifies the wind energy conversion system, there are challenges pertaining to overall system efficiency and power regulation with conventional controllers such as PI controller which could be resolved by use of better controllers. Various controllers are proposed in literature which promise good system performance and this research work proposed use of the ADRC controller which does not require detailed modelling of the system to be controlled. Furthermore, the performance analysis of the WECS with the proposed ADRC controller has been compared with other controllers and the results show that the WECS with ADRC controller performances better than most current industry standard controllers. The controller also effectively regulated the output voltage of the generator-side converter, thus producing a constant dc link voltage which is then converted to AC power by the inverter. The overall system efficiency based on proposed controller under various loading conditions approached 98.65 %.

5.2 Future Recommendations

The performance of ADRC is largely influenced by correct tuning of the observer and frequency response of the controller. On the other hand, the type of torsional plant sensors and actuators determines frequency response of the controller and observer. Normally, larger controller bandwidth yields very poor performance rendering the system impractical. While larger observer bandwidth is associated with noise and compromised controller performance. Therefore, continued study on fine tuning of the frequency response for the controller and observer must be carried out in the future. Implementation of ADRC relies on controller gain and system relative order. The future study could also explore alternative methods to implement ADRC without knowledge of the controller gain and system relative order.

References

- [1] A. Razmjoo, L. Gakenia Kaigutha, M. A. Vaziri Rad, M. Marzband, A. Davarpanah, and M. Denai, "A Technical analysis investigating energy sustainability utilizing reliable renewable energy sources to reduce CO₂ emissions in a high potential area," *Renew. Energy*, vol. 164, pp. 46–57, Feb. 2021, doi: 10.1016/j.renene.2020.09.042.
- [2] A. A. Hassan, M. El Habrouk, and S. Deghedie, "Renewable Energy for Robots and Robots for Renewable Energy-A Review," *Robotica*, vol. 38, no. 9, pp. 1576–1604, 2020.
- [3] Gitano-Briggs, Horizon, and S. M. Muyeen. "Small wind turbine power controllers." In *Wind power*, pp. 165-188. Vukovar, Croatia: Intech, 2010.
- [4] L. Arturo Soriano, W. Yu, and J. D. J. Rubio, "Modeling and control of wind turbine," *Mathematical Problems in Engineering*. 2013, doi: 10.1155/2013/982597.
- [5] S. Asiaban et al., "Wind and Solar Intermittency and the Associated Integration Challenges: A Comprehensive Review Including the Status in the Belgian Power System," *Energies*, vol. 14, no. 9, p. 2630, May 2021, doi: 10.3390/en14092630.
- [6] M. Cheah-Mane, J. Liang, and N. Jenkins, "Permanent magnet synchronous generator for wind turbines: Modelling, control and Inertial Frequency Response," in 2014 49th International Universities Power Engineering Conference (UPEC), Sep, pp. 1–6, 2014, doi: 10.1109/UPEC.2014.6934799.
- [7] A. D. Hansen, F. Iov, F. Blaabjerg, and L. H. Hansen, "Review of contemporary wind turbine concepts and their market penetration," *Wind Eng.*, vol. 28, no. 3, pp. 247–263, 2004.
- [8] Wu, Y.K., Chang, S.M. and Mandal, P, . Grid-connected wind power plants: a survey on the integration requirements in modern grid codes. *IEEE Transactions on Industry Applications*, 55(6), pp.5584-5593, 2019.
- [9] R. Tiwari and N. R. Babu, "Fuzzy logic based MPPT for permanent magnet synchronous generator in wind energy conversion system," 2016, doi: 10.1016/j.ifacol.2016.03.097.

- [10] E. G. Shehata, "A comparative study of current control schemes for a direct-driven PMSG wind energy generation system," *Electr. Power Syst. Res.*, vol. 143, pp. 197–205, Feb. 2017, doi: 10.1016/j.epsr.2016.10.039.
- [11] S. Wang, W. Tan, and D. Li, "Design of linear ADRC for load frequency control of power systems with wind turbine," in *2016 14th International Conference on Control, Automation, Robotics and Vision (ICARCV)*, Nov. 2016, pp. 1–5, doi: 10.1109/ICARCV.2016.7838795
- [12] Shourangiz-Haghighi, A., Diazd, M., Zhang, Y., Li, J., Yuan, Y., Faraji, R., & Guerrero, J. M. Developing more efficient wind turbines: A survey of control challenges and opportunities. *IEEE Industrial Electronics Magazine*, 14(4), 53-64. (2020).
- [13] Bryson, Arthur E., and Yu-Chi Ho. *Applied optimal control: optimization, estimation, and control*. Routledge, 2018.
- [14] Wang, L., Su, J., & Xiang, G. Robust motion control system design with scheduled disturbance observer. *IEEE Transactions on Industrial Electronics*, 63(10), 6519-6529. 2016.
- [15] Fadali, M. S. "On the stability of Han's ADRC." In *2014 American Control Conference*, pp. 3597-3601. IEEE, 2014.
- [16] Muliadi, J., & Kusumoputro, B. (2018). Neural network control system of UAV altitude dynamics and its comparison with the PID control system. *Journal of Advanced Transportation*, 2018.
- [17] Levine, W. (2018). *The Control Handbook* (2nd ed., p. 944). Hoboken: CRC Press.
- [18] Wang, L., Su, J., & Xiang, G. Robust motion control system design with scheduled disturbance observer. *IEEE Transactions on Industrial Electronics*, 63(10), 6519-6529. 2016.
- [19] H. Polinder, "Overview of and trends in wind turbine generator systems," in *2011 IEEE Power and Energy Society General Meeting*, Jul., pp. 1–8, 2011, doi: 10.1109/PES.2011.6039342.

- [20] N. S. Kumar and S. V. Devi, "Design of power electronic transformer based variable speed wind energy conversion system," 2016 International Conference on Circuit, Power and Computing Technologies (ICCPCT), , pp. 1-7, 2016, doi: 10.1109/ICCPCT.2016.7530337
- [21] G. Ofualagba and E. U. Ubeku, "Wind energy conversion system- wind turbine modeling," 2008 IEEE Power and Energy Society General Meeting - Conversion and Delivery of Electrical Energy in the 21st Century, 2008, pp. 1-8, doi: 10.1109/PES.2008.4596699.
- [22] L. Trilla, F. D. Bianchi, and O. Gomis-Bellmunt, "Linear parameter-varying control of permanent magnet synchronous generators for wind power systems," IET Power Electron., vol. 7, no. 3, pp. 692–704, 2014.
- [23] M. Moh Saad, N. Asmuin, and M. Ó. Óskarsdóttir, "A General Description and Comparison of Horizontal Axis Wind Turbines and Vertical Axis Wind Turbines," University of Iceland, 2014.
- [24] M. Tsili and S. Papathanassiou, "A review of grid code technical requirements for wind farms," IET Renew. Power Gener., vol. 3, no. 3, p. 308, 2009, doi: 10.1049/iet-rpg.2008.0070.
- [25] Anibal de Almeida, Steve Greenberg, in Encyclopedia of Energy, 2004.
- [26] M. A. Dranca, M. Chirca, S. Breban and D. Fodorean, "Comparative Design Analysis of Two Modular Permanent Magnet Synchronous Generators," 2021 7th International Symposium on Electrical and Electronics Engineering (ISEEE),pp.1-5. 2021. doi: 10.1109/ISEEE53383.2021.9628402
- [27] P. Tavner, Offshore Wind Turbines: Reliability, Availability and Maintenance, Stevenage, U.K.: IET, 2012.
- [28] X. Yuan, F. Wang, R. Burgos, Y. Li, and D. Boroyevich, "Dc-link voltage control of full power converter for wind generator operating in weak grid systems," Conf. Proc. - IEEE Appl. Power Electron. Conf. Expo. - APEC, pp. 761–767, 2009.
- [29] X. Wei, M. Cheng, W. Wang, P. Han and R. Luo, "Direct Voltage Control of Dual-Stator Brushless Doubly Fed Induction Generator for Stand-Alone Wind Energy Conversion

- Systems," in IEEE Transactions on Magnetics, vol. 52, no. 7, pp. 1-4, July 2016, Art no. 8203804, doi: 10.1109/TMAG.2016.2526049
- [30] V. Yaramasu, B. Wu, P. C. Sen, S. Kouro and M. Narimani, "High-power wind energy conversion systems: State-of-the-art and emerging technologies," in Proceedings of the IEEE, vol. 103, no. 5, pp. 740-788, May 2015, doi: 10.1109/JPROC.2014.2378692.
- [31] R. Cardenas, R. Pena, S. Alepuz, and G. Asher, "Overview of Control Systems for the Operation of DFIGs in Wind Energy Applications," IEEE Trans. Ind. Electron., vol. 60, no. 7, pp. 2776–2798, Jul. 2013, doi: 10.1109/TIE.2013.2243372.
- [32] P. J. Tavner, S. Faulstich, B. Hahn, and G. J. W. van Bussel, "Reliability and availability of wind turbine electrical and electronic components," EPE J., vol. 20, no. 4, pp. 1–25, 2011.
- [33] S. S. Gjerde and T. M. Undeland, "Fault tolerance of a 10 MW, 100 kV transformerless offshore wind turbine concept with a modular converter system," in Proc. EPE/PEMC, Sep., pp. LS7c.3-1–LS7c.3-8. 2012.
- [34] J. A. Ferreira, "The multilevel modular DC converter," IEEE Trans. Power Electron., vol. 28, no. 10, pp. 4460–4465, Oct. 2013.
- [35] P. K. Olsen, S. Gjerde, R. M. Nilssen, J. Hoelto, and S. Hvidsten, "A transformerless generator-converter concept making feasible a 100 kV light weight offshore wind turbine: Part I—The generator," in Proc. IEEE ECCE, Sep, pp. 247–252. 2012.
- [36] N. K. Jena, H. Pradhan, A. Choudhury, K. B. Mohanty, and K. Sanyal, "A Novel SMC Based Vector Control Strategy Used for Decoupled Control of PMSG based Variable Speed Wind Turbine System". International Conference on Circuit, Power and Computing Technologies (ICCPCT), IEEE, pp.1-6, 2017.
- [37] Laghridat, H., Essadki, A. and Nasser, T, . Comparative analysis between PI and linear-ADRC control of a grid connected variable speed wind energy conversion system based on a squirrel cage induction generator. Mathematical Problems in Engineering, 2019.
- [38] BENAOUINATE, L., KHAFALLAH, M., VOYER, D., MESBAHI, A. and Bouragba, T, . Nonlinear Control Based on Fuzzy Logic for a Wind Energy Conversion System Connected to the Grid. technology, 4, p.7 , 2020.

- [39] Zhang, S., Tseng, K.J., Vilathgamuwa, D.M., Nguyen, T.D. and Wang, X.Y, Design of a robust grid interface system for PMSG-based wind turbine generators. *IEEE transactions on industrial electronics*, 58(1), pp.316-328, 2011.
- [40] Rahmanian, E., Akbari, H. and Sheisi, G.H, . Maximum power point tracking in grid connected wind plant by using intelligent controller and switched reluctance generator. *IEEE Transactions on Sustainable Energy*, 8(3), pp.1313-1320, 2017.
- [41] S. M. Mozaya, "New Control Strategy for Permanent Magnet Synchronous Generator (PMSG) Wind Turbine," 2020.
- [42] J. Manwell, M. J.G. and L. Rogers A, *Wind Energy Explained - Theory, Design and Application*, New York: John Wiley & Sons, LTD, 2002.
- [43] I. Paraschivoiu, *Wind Turbine Design - with Emphasis on Darrieus Concept*, Québec: Presses internationales Polytechnique, 2009.
- [44] D. A. Spera, *Wind Turbine Technology - Fundamental Concepts of Wind Turbine Engineering Second Edition*, New York: ASME, 2009.
- [45] Fandi, G., Igbinoia, F.O., Ahmad, I., Svec, J. and Muller, Z., June. Modeling and Simulation of a gearless variable speed wind turbine system with PMSG. In 2017 IEEE PES PowerAfrica (pp. 59-64), 2017.
- [46] X. Zhang, W. Wei, and L. Ni, "DC Voltage Control of AC/DC Hybrid Distribution Network with Low-Speed Distributed Wind Energy Conversion Systems," in 2018 2nd IEEE Conference on Energy Internet and Energy System Integration (EI2), Oct. 2018, pp. 1–6, doi: 10.1109/EI2.2018.8582221.
- [47] Letcher, T.M., *Wind energy engineering: a handbook for onshore and offshore wind turbines*. Academic Press, 2017.
- [48] X. L. Zhang, " Optimizing Maximum Power Point Tracking of Wind Turbines with Consideration of Turbulence Effects," Nanjing University of Science & Technology, March. 2014.

- [49] Y. S. Kim, I. Y. Chung, and S. Il Moon, "Tuning of the PI controller parameters of a PMSG wind turbine to improve control performance under various wind speeds," *Energies*, vol. 8, no. 2, pp. 1406–1425, 2015.
- [50] M. Singh, E. Muljadi, J. Jonkman, and V. Gevorgian, "Simulation for Wind Turbine Generators With FAST and MATLAB-Simulink Modules," *Natl. Renew. Energy Labortory*, no. April, pp. 1–125, 2014.
- [51] W. Tong, *Wind Power Generation and Wind Turbine Design*, Southampon: WIT Press, 2010.
- [52] Y. Sawle, S. C. Gupta, and A. K. Bohre, "PV-wind hybrid system: A review with case study," *Cogent Eng.*, vol. 3, no. 1, pp. 1–31, 2016
- [53] K. Ma, *TOPICS IN WIND Power Electronics for the Next Generation Wind*. 2013.
- [54] N. Huang, "Simulation of Power Control of a Wind Turbine Permanent Magnet Synchronous Generator System," no. 2013, pp. 1–97, 2013.
- [55] M. Ragheb, "Optimal Rotor Tip Speed Ratio," p. 10, 2014.
- [56] Y. Mastanamma and D. Subbarayudu, "Permanent magnet synchronous generator for wind energy conversion systems (WECS): A review," *Int. J. Recent Technol. Eng.*, vol. 7, no. ICETESM18, pp. 217–221, 2019.
- [57] F. Delfino, F. Pampararo, R. Procopio, and M. Rossi, "A feedback linearization control scheme for the integration of wind energy conversion systems into distribution grids," *IEEE Syst. J.*, vol. 6, no. 1, pp. 85–93, 2012
- [58] Y. Errami, M. Ouassaid, and M. Maaroufi, "Control of a PMSG based wind energy generation system for power maximization and grid fault conditions," *Energy Procedia*, vol. 42, pp. 220–229, 2013.
- [59] L. T. Romero, "Power converter optimal control for wind energy conversion systems," 2013.
- [60] Samaria, A., Sharma, H.K. and Gidwani, L. *Modelling and Simulation of wind turbine using pmsg. Wind energy*, p.2, 2015.

- [61] N. Huang, "Simulation of Power Control of a Wind Turbine Permanent Magnet Synchronous Generator System," no. 2013, pp. 1–97, 2013.
- [62] W. Zhang, S. A. Gadsden, and S. R. Habibi, "Nonlinear estimation of stator winding resistance in a brushless DC motor," *Proc. Am. Control Conf.*, vol. 7, pp. 4699–4704, 2013.
- [63] M. Ran, J. Li, and L. Xie, "A new extended state observer for uncertain nonlinear systems," *Automatica*, vol. 131, p. 109772, Sep. 2021, doi: 10.1016/j.automatica.2021.109772.
- [64] Tan, K.T., Sivaneasan, B., Peng, X.Y. and So, P.L., Control and operation of a dc grid-based wind power generation system in a microgrid. *IEEE Transactions on Energy Conversion*, 31(2), pp.496-505, 2015.
- [65] Gokkus, G. and Kulaksiz, A. A. (2020) 'Design and implementation of a wind turbine emulator using an induction motor and direct current machine', *International Journal of Renewable Energy Research*, 10(3), pp. 1427–1438.
- [66] O. Elbeji, M. Ben Hamed, and L. Sbita, "PMSG Wind Energy Conversion System: Modeling and Control," *Int. J. Mod. Nonlinear Theory Appl.*, vol. 03, no. 03, pp. 88–97, 2014.
- [67] Chavero-Navarrete, E., Trejo-Perea, M., Jáuregui-Correa, J. C., Carrillo-Serrano, R. V., & Ríos-Moreno, J. G. (2019). Expert control systems for maximum power point tracking in a wind turbine with PMSG: State of the art. *Applied Sciences*, 9(12), 2469.
- [68] Li, Y. S., Wu, P. Y., & Ho, M. T. (2020, November). Dead-Time Compensation for Permanent Magnet Synchronous Motor Drives. In *2020 International Automatic Control Conference (CACCS)* (pp. 1-6). IEEE.
- [69] Jiao, X., Yang, Q., Zhu, C., Fu, L., & Chen, Q. (2019, June). Effective wind speed estimation and prediction based feedforward feedback pitch control for wind turbines. In *2019 12th Asian Control Conference (ASCC)* (pp. 799-804). IEEE.
- [70] Jon, R., Wang, Z., Luo, C. and Jong, M. Adaptive robust speed control based on recurrent elman neural network for sensorless PMSM servo drives. *Neurocomputing*, 227, pp.131-141. 2017.

- [71] Shengquan, L., Juan, L., Yongwei, T., Yanqiu, S., & Wei, C. Model-based model predictive control for a direct-driven permanent magnet synchronous generator with internal and external disturbances. *Transactions of the Institute of Measurement and Control*, 42(3), 586-597. 2020.
- [72] Gao, F., Wu, M., She, J. and Cao, W. Disturbance rejection in nonlinear systems based on equivalent-input-disturbance approach. *Applied Mathematics and Computation*, 282, pp.244-253. 2016.
- [73] Danapalasingam, Kumeresan A., Anders la Cour-Harbo, and Morten Bisgaard. "Disturbance effects in nonlinear control systems and feedforward control strategy." In *2009 IEEE International Conference on Control and Automation*, pp. 1974-1979. IEEE, 2009.
- [74] Moradmand, Anahita, Mehrdad Dorostian, and Bahram Shafai. "Energy scheduling for residential distributed energy resources with uncertainties using model-based predictive control." *International Journal of Electrical Power & Energy Systems* 132: 107074. 2021.
- [75] Huang, W., Du, J., Hua, W., Lu, W., Bi, K., Zhu, Y. and Fan, Q.,. Current-based open-circuit fault diagnosis for PMSM drives with model predictive control. *IEEE Transactions on Power Electronics*, 36(9), pp.10695-10704. 2021.
- [76] Song, D., Yang, J., Dong, M. and Joo, Y.H. Model predictive control with finite control set for variable-speed wind turbines. *Energy*, 126, pp.564-572. 2017.
- [77] Mahmoud, M.S. and Oyededeji, M.O. Adaptive and predictive control strategies for wind turbine systems: A survey. *IEEE/CAA Journal of Automatica Sinica*, 6(2), pp.364-378. 2019.
- [78] S. A.R., M. C. Pandey, N. Sunil, S. N.S., V. Mugundhan, and R. K. Velamati, "Numerical study of effect of pitch angle on performance characteristics of a HAWT," *Eng. Sci. Technol. an Int. J.*, vol. 19, no. 1, pp. 632–641, Mar. 2016, doi: 10.1016/j.jestch.2015.09.010.
- [79] Malaysia." Asia Wind Energy Association 2021. Accessed December 30, 2021. <https://www.asiawind.org/research-data/market-overview/malaysia/>.

- [80] Yang, Y., et al. (2014). Low-power wind energy conversion system with variable structure control for DC grids. 2014 IEEE 5th International Symposium on Power Electronics for Distributed Generation Systems (PEDG), IEEE.
- [81] Masters, G. M. (2013). Renewable and efficient electric power systems, John Wiley & Sons.
- [82] Haliade-X Offshore Wind Turbine.” World's Most Powerful Offshore Wind Platform: Haliade-X | GE Renewable Energy. Accessed December 30, 2021. <https://www.ge.com/renewableenergy/wind-energy/offshore-wind/haliade-x-offshore-turbine>.
- [83] Thongam, J.S. and Ouhrouche, M.,. MPPT control methods in wind energy conversion systems. *Fundamental and advanced topics in wind power*, 15, pp.339-360. 2011.
- [84] Moothedath, S., Chaporkar, P. and Belur, M.N. Minimum cost feedback selection for arbitrary pole placement in structured systems. *IEEE Transactions on Automatic Control*, 63(11), pp.3881-3888. 2018.

LIST OF PUBLICATIONS

The research work in this thesis has been presented in formal proceedings and published in the following articles:

A. JOURNAL PUBLICATION

Sadeq, S., Ovinis, M., & Karuppanan, S. (2022). Modeling and Simulation of PMSG Wind Energy Conversion System Using Active Disturbance Rejection Control. *Journal of Advanced Research in Fluid Mechanics and Thermal Sciences*, 92(1), 105-122.

APPENDIX A

A.1 Common parameters

```
%% Universal and Common Parameters
Tsample = 2e-6;           % Sampling Rate
Pnom = 2e6;               % Nominal system power
Pmec = 2e6/0.8;          % Nominal Turbine power
Vnom = 415;               % RMS Voltage (3-Phase)
Fnom = 50;                % Grid voltage frequency
nomVdc = 800;             % Nominal DC Voltage
invL = 0.15;              % Inverter Inductor
invR = 0.15/50;          % Inverter Resistance
genV = 600;               % Generator Voltage
snubTc = 50e-6;          % Snub capacitor time-constant
Ron = 10e-3;              % On-Resistance
filterFO = 10000;        % Filter Cutoff Frequency
filterZta = 0.707;       % Filter Damping ratio
```

A.2 Wind turbine parameters

```
%% Wind-Turbine
nomMechPower = 2e6;      % Nominal Mechanical Power
pmsgBasePower = 2e6/0.8; % Base Power of the Electrical Generator
baseWindSpeed = 2.8;     % Base wind speed (m/s)
mPatBaseSpeed = 1;       % Maximum power at the base wind speed
genBaseSpeed = 0.035/1.25; % Base Rotational Speed
pitchAngle = 0;          % Pitch Angle
wtSpeedNom = 0.035;
Tnom = Pnom/wtSpeedNom;
```

A.3 Generator side converter parameters

```
%% Generator Side Converter Parameters
Rboost = 0.01;            % Parasitic Resistance of Inductor
LBoost = 100e-6;         % Boost Inductors
CBoost = 78125e-6;       % Boost Capacitor
```

A.4 Boost converter controller parameters

```
% BOOST CONVERTER CONTROLLER PARAMETERS
Tspeed = 5; % Speed controller time-constant
KPspeed = 5; % Proportional gain for speed regulator
KIspeed = 1; % Integral gain for speed regulator
KpBoostCurReg = 0.025; % Proportional gain for Boost current regulator
KiBoostCurReg = 100; % Integral gain for Boost current regulator
pitchGain = 15; % Pitch gain
maxPitch = 20; % Maximum pitch angle (deg)
pitchRate = 10; % Pitch Rate = d(pitch)/d(Wind Speed)
KpCompensation = 1.5; % Pitch Compensator proportional gain
KiCompensation = 6; % Pitch Compensator integral gain
swFreqBoost = 2000; % Switching Frequency for Boost Converter
pitchTC = 0.01; % Pitch Time-constant
```

A.5 Grid side converter

```
%% Grid-Side Converter
kpDC = 1.1; % Proportional gain for DC regulator
kiDC = 27.5; % Integral Gain for DC regulator
ImaxGridConv = 500; % Maximum grid converter
kiVARreg = 0.05; % VAR regulator
varRegulatorUL = 1.1; % VAR regulator output upper limit
varRegulatorLL = 0.9; % VAR regulator output lower limit
kiVoltageReg = 2; % Integral gain for voltage regulator
Iq_ref_limit_time_constant = 0.3; % Q-regulator time constant
maxModIdx = 1.1; % Inverter Modulation Index
pwmFreq = 3000; % Inverter PWM Frequency
varFilterC = 100e-6; % VAR Filter capacitor
varFilterQ = 50; % VAR Filter Q
kpGCCurReg = 1; % Grid-side current regulator P-gain
kiGCCurReg = 50; % Grid-side current regulator I-gain
CurrentRegOutputLimit = 1100; % Current regulator current limit
```

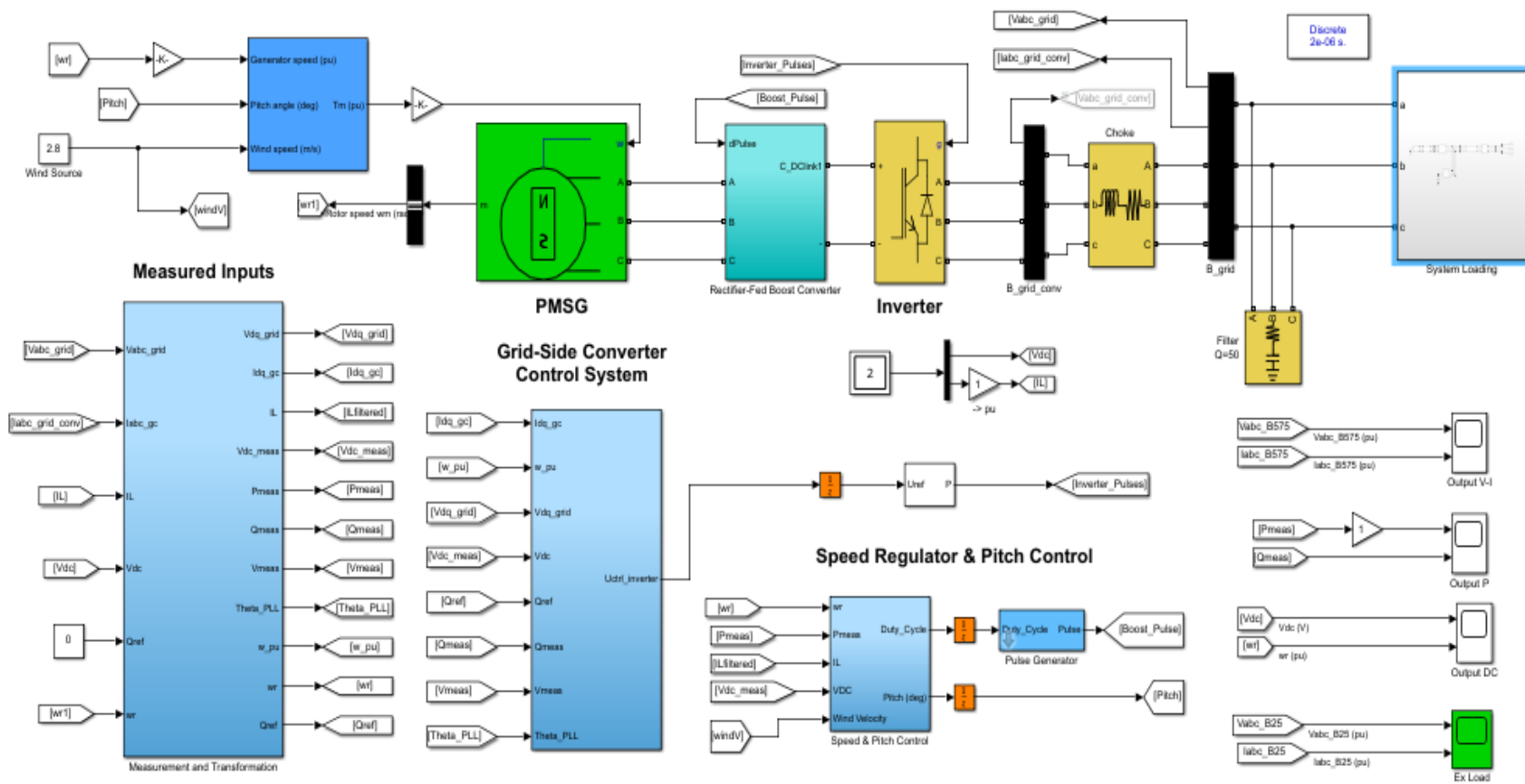
A.6 transfer function

```
%% Boost Controller Design
% TRANSFER FUNCTION
eqRout = 1;
D = 1 - 600/800;
CparasiticR = 0;
avgVI = 600;
bcGain = -avgVI/(1-D);
factor = (LBoost*CBoost)/(1-D)^2;
bcGain = bcGain/factor;
num = [LBoost/(eqRout*(1-D)^2), -1];
den = [1, LBoost/(eqRout*(1-D))/factor, 1/factor];
boostTF = tf(bcGain*num, den);
```

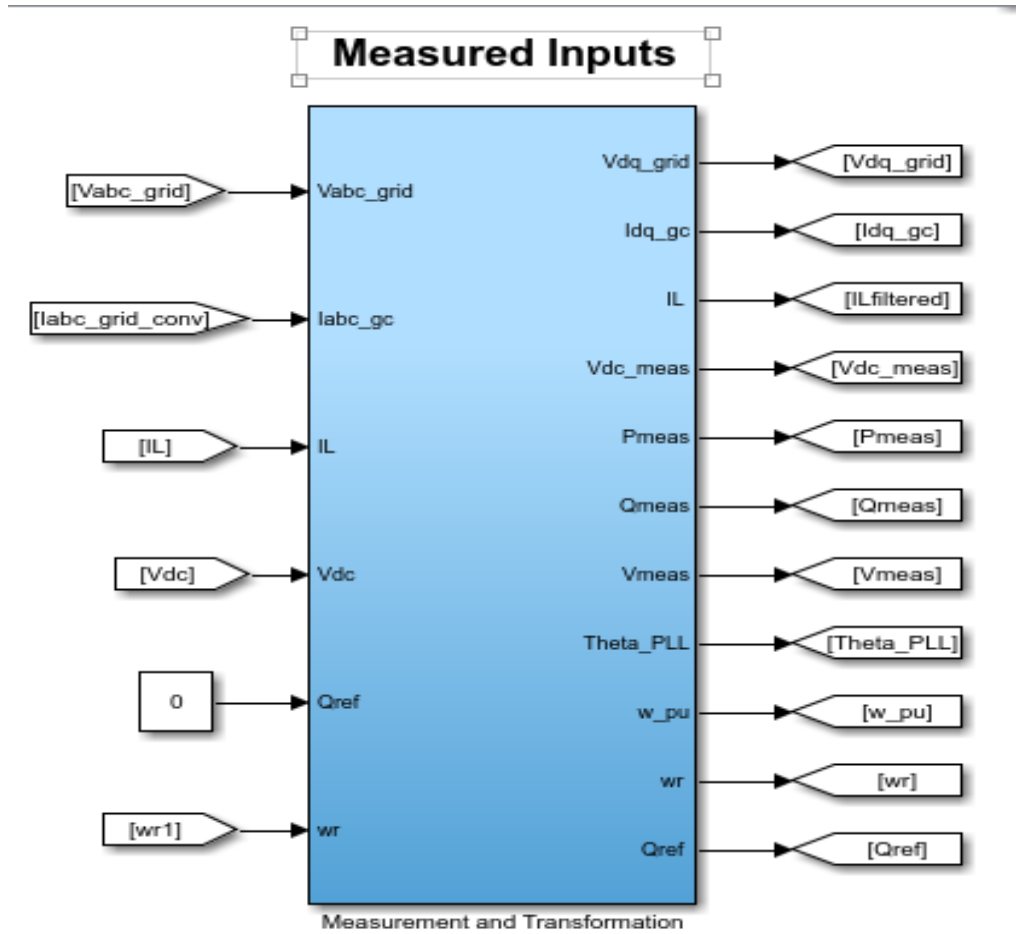
A.7 ADRC parameters

```
% ADRC PARAMETERS
A1 = [0.9970, 0, 0; -1.4993, 1, 0; -250, -0.0005, 1];
B1 = [0.0001; 115.1998; -0.0288];
LC = [0.003; 1.4993; 250];
b0 = 5.76e7;

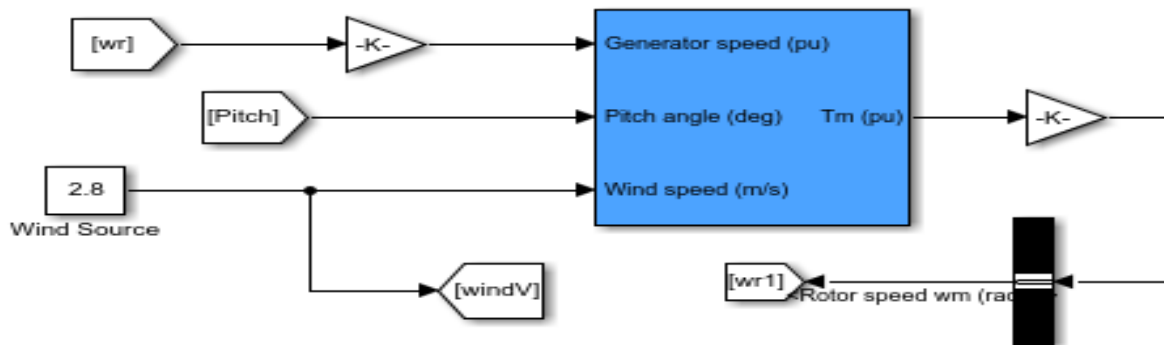
adrcGains = [750000, 15500];
```



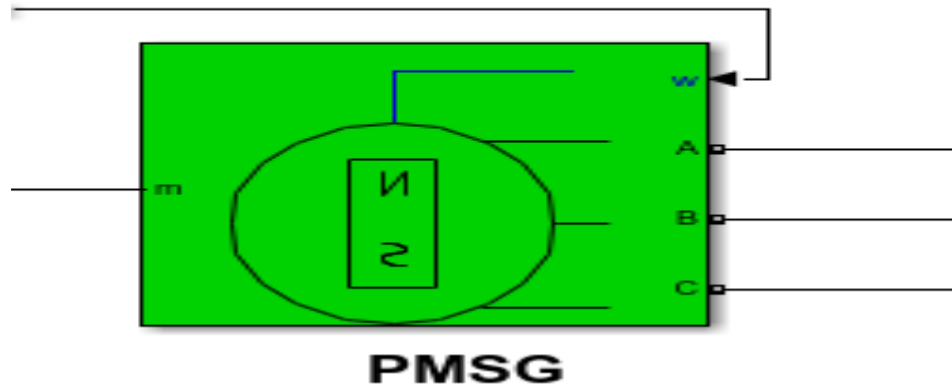
A.8 Measurement input



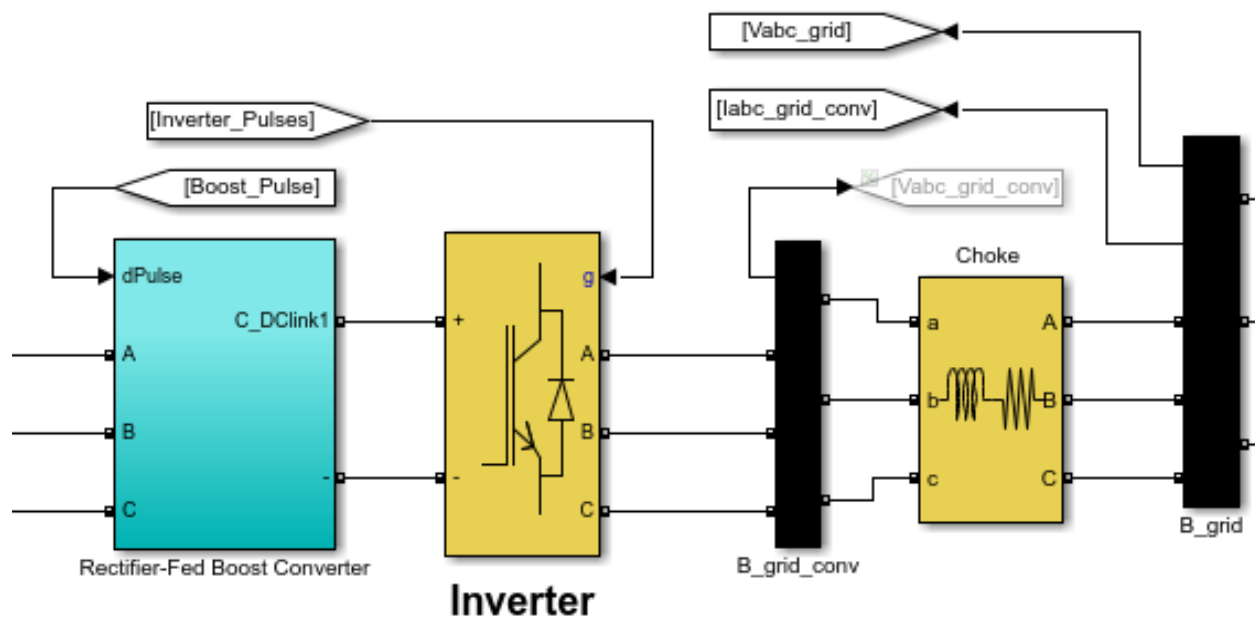
A.9 Block diagram for wind turbine



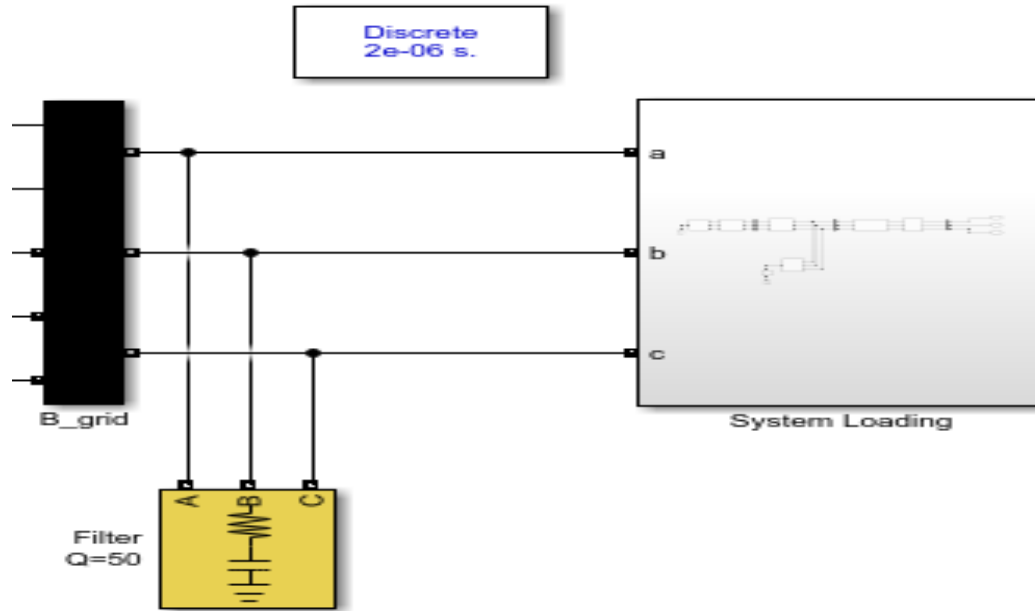
A.10 PMSG block



A.11 Rectifier-Fed Boost Converter and inverter block

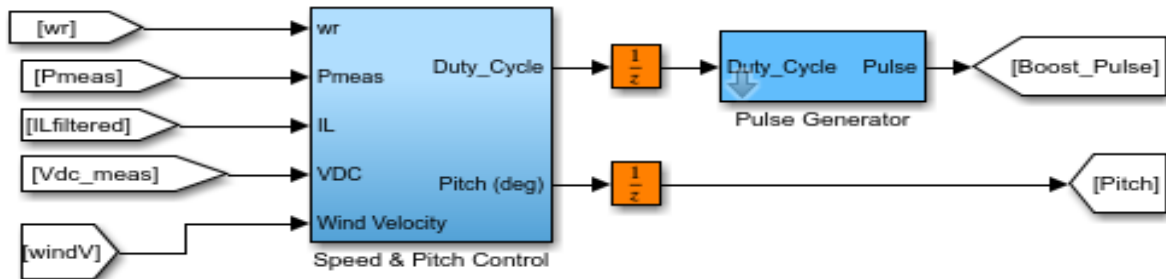


A.12 System loading

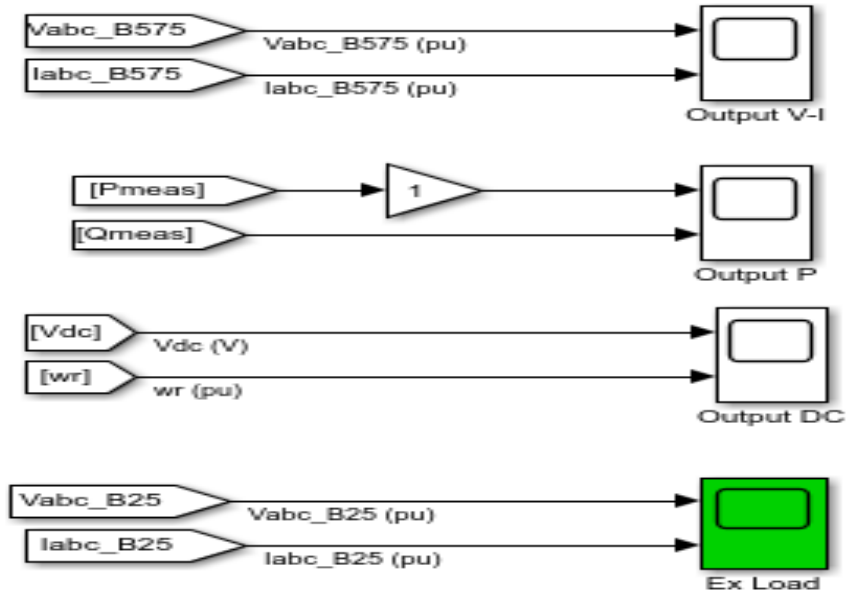


A.13 pitch control

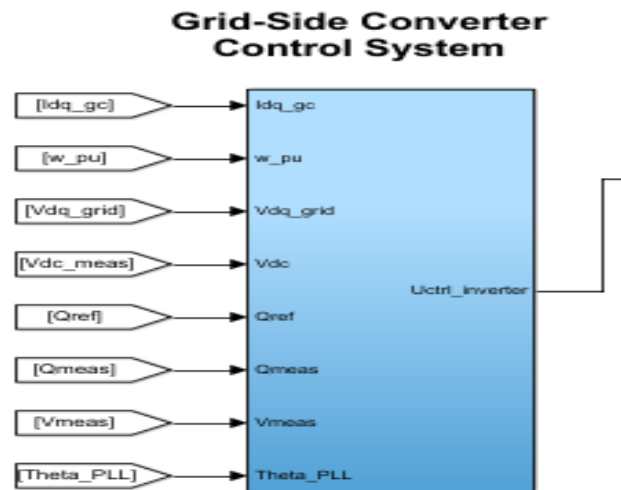
Speed Regulator & Pitch Control



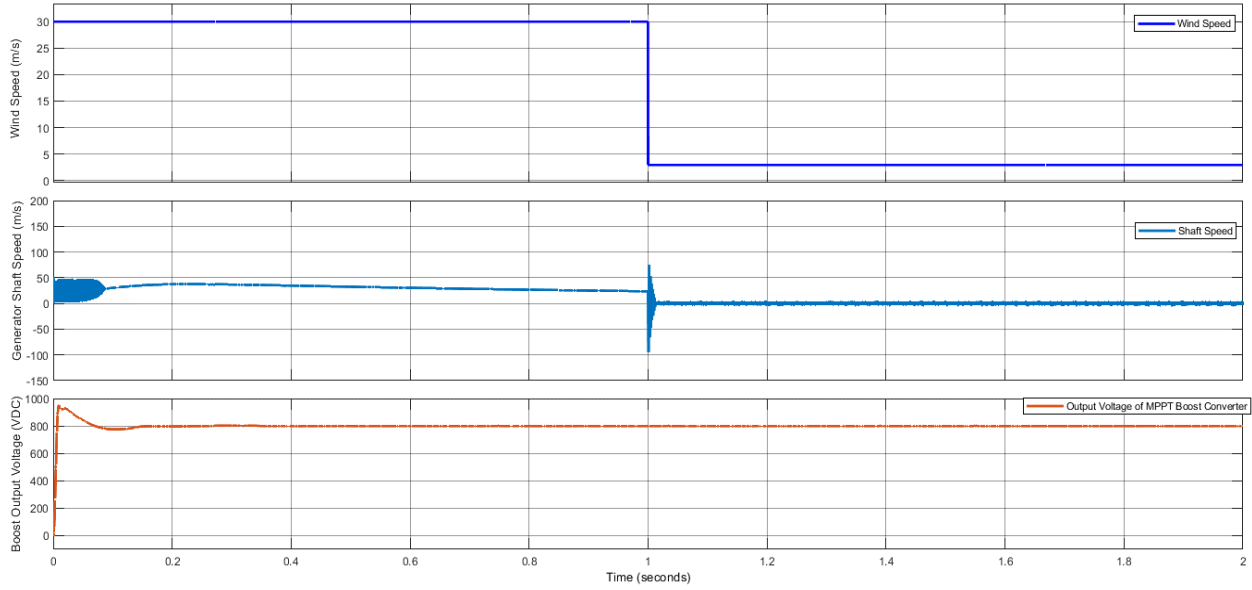
A.14 Output



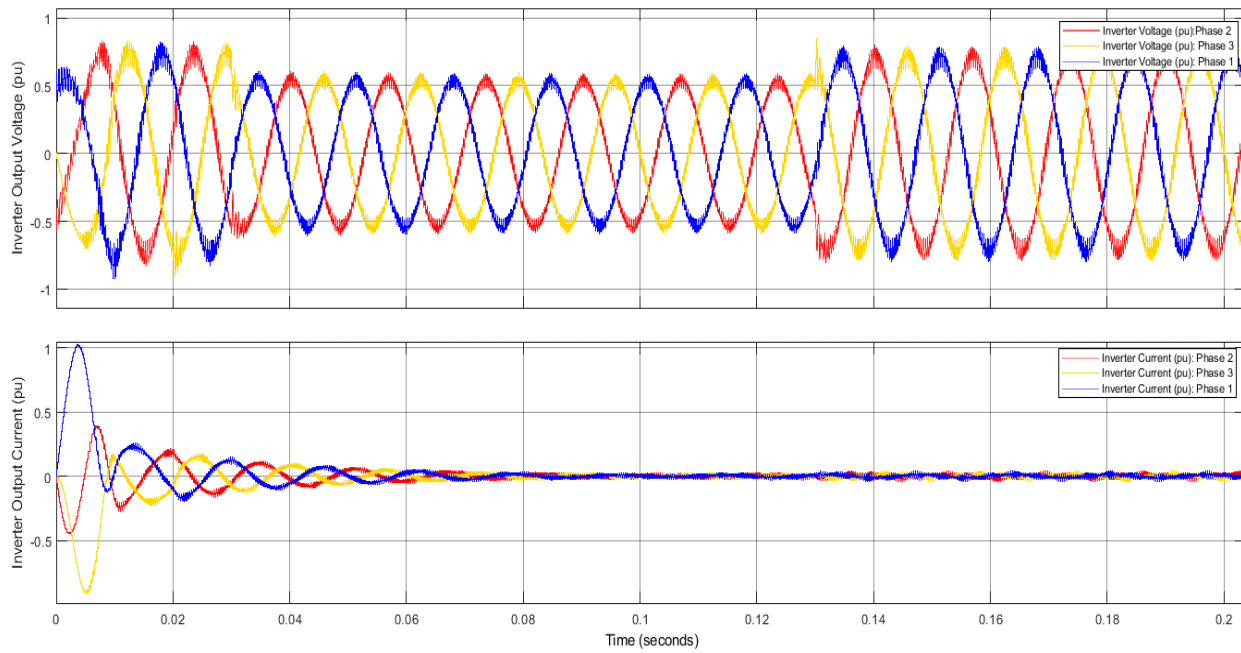
A.15 Grid side converter control system



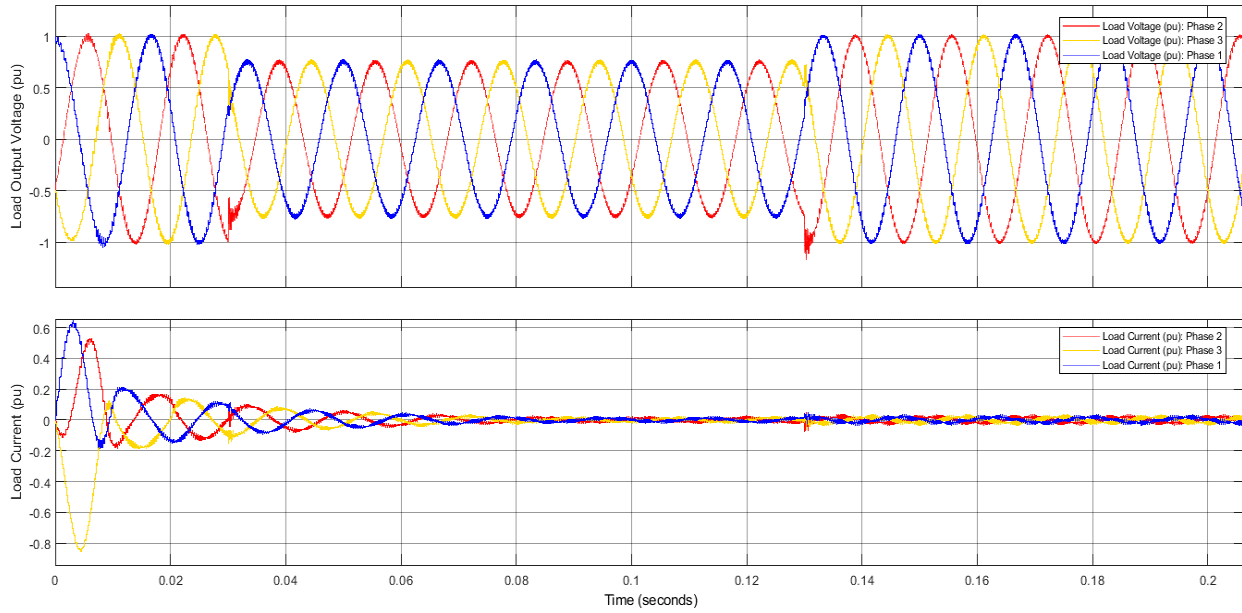
A.16 Shaft Speed and Boost Output Voltage versus actual Wind Speed with ADRC controller.



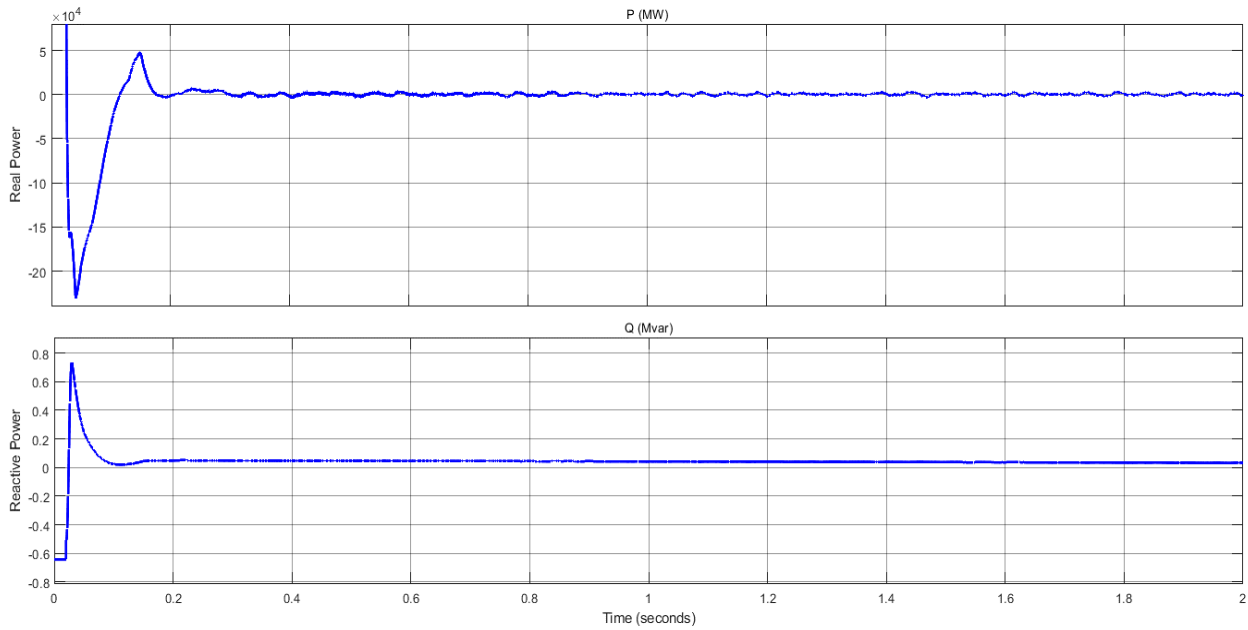
A.17 Inverter 3-Phase Output Voltage (pu) and Current (pu) fed to the Grid.



A.18 Load Voltage (pu) and Current (pu) with ADRC controller.



A.19 Comparison of System Real Power versus Reactive Power with ADRC Controller.



A.20 Turnitin report

MODELING AND SIMULATION OF PMSG WIND ENERGY CONVERSION SYSTEM USING ACTIVE DISTURBANCE REJECTION CONTROL

ORIGINALITY REPORT

20% SIMILARITY INDEX	13% INTERNET SOURCES	15% PUBLICATIONS	7% STUDENT PAPERS
--------------------------------	--------------------------------	----------------------------	-----------------------------

PRIMARY SOURCES

1	repositorio.ufmg.br Internet Source	1%
2	Submitted to Marquette University Student Paper	1%
3	www.mdpi.com Internet Source	1%
4	www.scribd.com Internet Source	1%
5	tci-thaiio.org	1